

DETERIORATION OF NEMRUT SANDSTONE AND DEVELOPMENT OF ITS  
CONSERVATION TREATMENTS

A THESIS SUBMITTED TO THE GRADUATE SCHOOL OF NATURAL AND APPLIED  
SCIENCES  
OF  
MIDDLE EAST TECHNICAL UNIVERSITY

BY

KIRAZ GÖZE AKOĞLU

IN PARTIAL FULFILLMENT OF THE REQUIREMENTS  
FOR  
THE DEGREE OF DOCTOR OF PHILOSOPHY, IN RESTORATION  
IN  
ARCHITECTURE

September, 2011

Approval of the thesis:

**DETERIORATION OF NEMRUT SANDSTONE AND DEVELOPMENT OF ITS  
CONSERVATION TREATMENTS**

submitted by **Kiraz Göze Akođlu** in partial fulfillment of the requirements for the degree of **Doctor of Philosophy in Architecture Department, in Restoration, Middle East Technical University** by,

Prof. Dr. Canan Özgen \_\_\_\_\_  
Dean, Graduate School of **Natural and Applied Sciences**

Prof. Dr. Güven Arif Sargin \_\_\_\_\_  
Head of Department, **Architecture**

Prof. Dr. Emine N. Caner-Saltık \_\_\_\_\_  
Supervisor, **Architecture Dept., METU**

**Examining Committee Members:**

Prof. Dr. Asuman Türkmenođlu \_\_\_\_\_  
Geological Engineering Dept., METU

Prof. Dr. Emine N. Caner-Saltık \_\_\_\_\_  
Architecture Dept., METU

Prof. Dr. Tamer Topal \_\_\_\_\_  
Geological Engineering Dept., METU

Assoc. Prof. Dr. S. Sarp Tunçoku \_\_\_\_\_  
Architectural Restoration Dept., IYTE

Asist. Prof. Dr. Güliz Bilgin-Altınöz \_\_\_\_\_  
Architecture Dept., METU

**Date:** 05.09.2011

**I hereby declare that all information in this document has been obtained and presented in accordance with academic rules and ethical conduct. I also declare that, as required by these rules and conduct, I have fully cited and referenced all material and results that are not original to this work.**

Name, Last name : Kiraz Göze Akođlu

Signature :

## **ABSTRACT**

### **DETERIORATION OF NEMRUT SANDSTONE AND DEVELOPMENT OF ITS CONSERVATION TREATMENTS**

Akođlu, Kiraz Gze

Ph.D., Department of Architecture, Restotariion  
Supervisor: Prof. Dr. Emine N. Caner-Saltık

September, 2011, 166 pages

In this study, it was aimed to develop conservation methodologies for the historic sandstones using the case of Nemrut Mount Monument to help their survival in open air conditions. The main conservation approach of this study was holistic as well as aiming at minimum intervention targeted to the problem areas.

The most important weathering forms of Nemrut Sandstones were material loss due to loss of scales and granular disintegration as well as detachments by scales, back weathering due to loss of scales, cracking, granular disintegration, rounding/notching and discoloration/biological deposition.

Deterioration mechanisms of sandstones were studied on deteriorated and relatively sound sandstones by nondestructive methods of UPV and QIRT, and by microstructural analyses using thin section, XRD and SEM-EDX analyses. In addition, the changes in physical and physcomechanical properties such as, color, bulk density, effective porosity, hydric, hygric and thermal dilatation and CEC of clays were determined.

Sandstone deterioration was caused by swelling of clay minerals distributed in their matrix and clay accumulations between the detaching scales. Considerable thermal dilatation characteristics was also an important decay factor. Iron oxides caused discoloration at the surfaces, their phase changes was thought to be important in decay.

The use of surfactant DAA, to control clay swelling was found to decrease the hydric dilatation by 40%. The consolidation treatments with nanosilica and silicate dispersions namely Funcosil KSE500STE, SytonX3, KSE300 and KSE100 have improved physicommechanical properties as followed by UPV measurements and decreased hydric dilatation. Their long term behaviour needed to be further investigated.

Keywords: sandstone deterioration, clay swelling, dilatation, surfactants, nanodispersive silica solutions.

## ÖZ

### NEMRUT KUMTAŞLARININ BOZULMALARI VE KORUMA İŞLEMLERİNİN GELİŞTİRİLMESİ

Akođlu, Kiraz Göze

Ph.D., Mimarlık Bölümü, Restotasyon

Danışman: Prof. Dr. Emine N. Caner-Saltık

Eylül, 2011, 166 sayfa

Bu çalışmada, tarihi kumtaşlarının açık hava şartlarında koruma yöntemlerinin geliştirilmesi amaçlanmıştır. Kumtaşlarının bozulma mekanizmalarını inceleyerek bunları kontrol altına alacak yöntemlerin geliştirilmesi çalışmaları Nemrut Dağı Anıtı'ndaki kumtaşlarının detaylı incelenmesiyle yapılmıştır. Taş koruma yöntemlerini geliştirirken sorunun bütüncül bir yaklaşımla incelenmesine ve tarihi malzemenin özgünlüğünün devamı açısından en az ve en gerekli müdahalelerin oluşturulmasına çalışılmıştır.

Nemrut kumtaşlarında görülen en önemli bozulma şekilleri tabaklanma ve taneleşme ile malzeme kayıpları, tabakalanma sonrası geri yüzeyler, yuvarlaklaşmalar, çatlaklar, taneleşme ve renk değişimleri, biyolojik birikimler olarak sıralanabilir.

Bozulmuş ve daha az bozulmuş kumtaşlarının bozulmuşluk derecesi arazide UPV ve QIRT ile tahribatsız olarak, mikro yapılarındaki değişimler ise ince kesit analizleri, XRD ve SEM-EDX analizleri ile yapılmıştır. Ayrıca, renk değişimi, gözeneklilik, birim hacim ağırlığı, su, nem ve ısı ile diatasyon özellikleri gibi fiziksel ve fizikomekanik özelliklerdeki değişimler ve killerin iyon değiştirme kapasiteleri belirlenmiştir.

Kumtaşlarının yapısında bulunan kil minerallerinin ve ayrılmakta olan tabakalar arasında biriken killerin ıslanma-kuruma döngüleri sırasındaki hareketliliğinin ve ısı genleşmenin bozulmalarda en önemli etkenler olduğu görülmüştür.

Ayrıca yapılarında bulunan demiroksitlerin de faz deęişimleri ile bozulmada etkili olabilecekleri ve yüzeylerde oluşan renk deęişimlerine neden oldukları düşünölmektedir.

Killerin ıslanma-kuruma döngülerinden etkilenmelerini kontrol etmek amacıyla denenen yüzey aktif maddelerden DAA'nın etkili olduęu ve su ile dilatasyonu %40 civarında azalttığı saptanmıştır.

Nanosilika ve silikat içeren çözeltilerden, Funcosil KSE500STE, SytonX3, KSE300 ve KSE100 ile yapılan sağlamlaştırma işlemlerinin fizikomekanik özelliklerde iyileşme sağladığı da UPV ve dilatasyon ölçümleri ile takip edilmiştir. Koruma işlemlerinin uzun dönemdeki başarıları takip edilmelidir.

Anahtar Kelimeler: kumtaşı bozulmaları, kil genişmesi, dilatasyon, yüzey aktif malzeme, nanotaneli silika çözeltiler.

## ACKNOWLEDGEMENTS

First and foremost, I would like to express my sincere thanks and appreciation to my supervisor Prof. Dr. Emine Caner-Saltık for her understanding, special guidance and wisdom throughout my Restoration Education and this study. Any positive outcome of this study is the consequence of her guidance and my productive discussions with her.

I am indebted to Assist. Prof. Dr. Ayşe Tavukçuoğlu for her collaboration in IR Thermography image taking and processing at the heights of Nemrut Mount and in the laboratory, without her valuable comments on those aspects this study would have been incomplete.

I must offer my heartfelt thanks to Dr. Jean Didier-Mertz from LRMH – “Laboratoire Recherches de Monuments Historiques” for his contribution and the valuable discussions. I must not forget Estel Colas to mention here with my appreciation, without her valuable help in LRMH, that part of work would have not been completed easily.

It is a very big pleasure for me to thank to Paulette Hugon from LRMH – “Laboratoire Recherches de Monuments Historiques” for her contributions in SEM-EDX analyses.

I am also indebted to Assoc Prof. Neriman Şahin Güçhan to her valuable criticism and positive attitude in our collaboration in CNCDP – “Commagene Nemrut Conservation and Development Program”.

Prof. Dr. Tamer Topal and Assist Prof. Dr. Güliz Bilgin-Altınöz who are also the members of my thesis supervising committee, provided their significant guidance with their insightful suggestions throughout this study. Prof. Dr. Asuman Türkmenoğlu and Assoc. Prof Dr. Sarp Tunçoku contributed and offered very profound criticisms and comments on the thesis defense.

I would like to thank all my friends who were always supportive during this long struggling period. Ozan Bilge always provided his support, and friendship together with his technical expertise. I would also like to mention my gratefulness to my friends in the Faculty of Architecture with whom we shared similar problems, Onur Yüncü, Zeynep Tuna-Yüncü, Çağla Caner-Yüksel, Günseli Filiz Demirkol, Pelin Yoncacı, Aydın Öztoprak, Leyla Etyemez, Pınar Aykaç and Mert Rifaioğlu.

My special thanks go to my younger friends in the Materials Conservation Laboratory A. Şenay Dinçer, Duygu Ergenç and O. Mete Işikoğlu who also shared their enthusiasm and friendship at the heights of Nemrut Mount and during long hours of work in the laboratory.

Finally, I am grateful to my family, who have always supported, understood, and believed in me. My gratitude for the support of my father A. Ersin Akoğlu, my mother Birim Akoğlu and my sister Özge Akoğlu can never be enough.

## TABLE OF CONTENTS

ABSTRACT .....	iv
ÖZ .....	vi
ACKNOWLEDGEMENTS .....	viii
TABLE OF CONTENTS .....	x
LIST OF FIGURES .....	xii
LIST OF TABLES .....	xix
LIST OF ABBREVIATIONS.....	xxi
CHAPTER	
1.INTRODUCTION .....	1
1.1 Nemrut Mount Monument.....	4
1.2 Aim and Scope of the Study .....	10
2. WEATHERING OF SANDSTONES AND ITS CONTROL .....	13
2.1 Clay Swelling and Its Control by Surfactants.....	21
2.2 Consolidation Treatments.....	25
2.2.1 Consolidation Treatments with Silicates.....	26
2.2.2 Evaluation of the Stone Consolidation Treatments .....	33
3.EXPERIMENTAL METHODS .....	37
3.1 Mapping of Visual Weathering Forms.....	37
3.1.1 Main Visual Decay Forms .....	38
3.2 Determination of Physical and Physicomechanical Properties.....	39
3.2.1 Bulk Density and Effective Porosity .....	40
3.2.2 Mercury Intrusion Porosimetry.....	41
3.2.3 Dilatation measurements.....	43
3.2.4 Drying Rate Measurements at Site .....	44
3.2.5 Ultrasonic Velocity Measurements .....	45
3.2.6 Infrared Thermography Analyses.....	47
3.2.7 Color Measurements.....	48
3.2.8 Artificial Salt Crystallization Tests .....	49

3.3 Determination of Micro-Structural Properties .....	49
3.3.1 Thin Section Analyses by Optical Microscopy.....	50
3.3.2 X-Ray Diffraction (XRD) Analyses .....	50
3.3.3 Cation Exchange Capacity (CEC) Measurements .....	54
3.3.4 Scanning Electron Microscopy (SEM) Coupled with Energy Dispersive X- Ray (EDX) Analyzer .....	56
3.4 Application of Surfactants.....	56
3.5 Application of Consolidants .....	57
4.EXPERIMENTAL RESULTS.....	58
4.1 Mapping of Visual Weathering Forms.....	58
4.2 Physical and Physicomechanical Characteristics .....	61
4.2.1 Results of UPV Measurements.....	61
4.2.2 Quantitative IR Thermography (QIRT) Results.....	77
4.2.3 Color Measurements.....	80
4.3.4 Results of Effective Porosity and Bulk Density Experiments .....	86
4.2.5 Mercury Intrusion Porosimetry.....	91
4.2.6 Dilatation Measurement Tests.....	96
4.2.7 Drying Rate Measurements at Site .....	101
4.3 Determination of Micro-Structural Properties .....	102
4.3.1 Thin Section Analyses by Optical Microscopy and Image Analyses.....	102
4.3.2 X Ray Diffraction (XRD) Analyses.....	112
4.3.3 CEC Determination by UV-Vis Spectrometry .....	118
4.3.4 Scanning Electron Microscopy (SEM) Coupled with Energy Dispersive X- Rays (EDX) Analyses .....	119
5.DISCUSSION.....	129
5.1 Characteristics of Nemrut Mount Sandstones.....	129
5.1.1 Micro-Structural Characteristics of Nemrut Mount Sandstones .....	129
5.1.2 Physical and Physicomechanical Properties of Nemrut Sandstones ....	131
5.2 Factors Affecting the Deterioration of Nemrut Mount Sandstones .....	133
5.2.1 Weathering forms and state of deterioration .....	134

5.2.2 The change in the microstructure of sandstones by weathering .....	137
5.3 The Conservation Treatments Targeted to the Control of Deterioration ...	141
6.CONCLUSIONS .....	146
REFERENCES .....	151
CURRICULUM VITAE.....	166

## LIST OF FIGURES

Figure 1.1 Map showing Adiyaman Province and Nemrut Mount. ....	5
Figure 1.2 Nemrut Mount Tumulus (The photo was processed on the aerial photo of the tumulus provided by GAP administration, for CNCDP in 2007 ODTÜ-CNCDP Archive, 2007). ....	6
Figure 1.3 General view of East Terrace on a rainy day in Nemrut Mount Monument .....	7
Figure 1.4 A view from West Terrace in Nemrut Mount Monument .....	7
Figure 4.1 Mapping of visual weathering forms of a relief (DTKM058) in the East Terrace (CNCDP, Final Report, 2011) (left) and its photo (right). ....	59
Figure 4.2 Mapping of visual weathering forms of West face of Lion Statue (DTKM066) at East Terrace (CNCDP Final Report, 2011) (left) and its photo (right)	59
Figure 4.3 The old PVA applications got florescent and became visible under UV light.....	60
Figure 4.4 $UPV_{(a,b,c)}$ values for each sandstone cube before salt crystallization tests. ....	64
Figure 4.5 Percentage change in the $UPV_{(a,b,c)}$ values for each sandstone cube after 5th cycle of salt crystallization in comparison to their fresh state. ....	64
Figure 4.6 Percentage change in the $UPV_{(a,b,c)}$ values for each sandstone cube after 10th cycle of salt crystallization in comparison to their fresh state. ....	65
Figure 4.7 Percentage change in the $UPV_{(a,b,c)}$ values for each sandstone cube after 15th cycle of salt crystallization in comparison to their fresh state. ....	65
Figure 4.8 Indirect and direct UPV values of undeteriorated and deteriorated sandstone cubes taken parallel and perpendicular to bedding planes at dry state (33% RH). ....	66
Figure 4.9 Indirect and direct UPV values of water saturated undeteriorated and deteriorated sandstone cubes taken parallel and perpendicular to bedding planes. ....	67

Figure 4.10 Indirect and direct UPV values of a sandstone sample taken from the site (Figure 4.11) in situ, dry and water saturated states.....	68
Figure 4.11 Sandstone cubes that were soaked into water. ....	69
Figure 4.12 Indirect UPV measurement taken from different points of a deteriorated sandstone block (above) in East Terrace, and graphic representation of the UPV values for each point pairs, red: very deteriorated parts, pink: detrriorated parts.....	70
Figure 4.13 Indirect UPV measurement taken from a sandstone showing granular disintegration (above) at East Terrace, and graphic representation of the UPV values for each point pairs, red: very deteriorated parts.....	71
Figure 4.14 Indirect UPV measurements from sandstone treated with epoxy by the old conservation team (East Terrace), and graphic representation of the UPV values for each point pairs, red: very deteriorated parts, pink: detrriorated parts, white: sound.....	72
Figure 4.15 UPV measurements from different points on Sandstone Lion Statue at East Terrace; the measurement points (above); and UPV values of those points pairs; red: very deteriorated parts, pink: detrriorated parts, white: sound. ....	73
Figure 4.16 Indirect and direct UPV values of sandstone cubes before and after consolidation treatments.....	74
Figure 4.17 Indirect and direct UPV values of sandstones blocks before and after consolidation treatments; direct (long) measurements are parallel to the bedding and the direct (short) being perpendicular to bedding. ....	75
Figure 4.18 Indirect UPV values of the points of UPV measurements of untreated and treated Layers of sandstone on North Terrace, the areas C and D are treated with Syton X30, areas F and G are treated with Funcosil KSE 500 (above). ....	76
Figure 4.19 Photograph of Lion Statue at East Terrace (left), single IR image of the statue showing the relatively hot surfaces and the cold surfaces of the statue (above left), differential IR image in cooling period (above right). ....	77

Figure 4.20 Differential IR image and UPV measurements of the detaching scales. The degree of deterioration of detaching parts can be determined by the changes in UPV measurements that are taken parallel to the surface. ....	78
Figure 4.21 Treated and non-treated layers of sandstone in North Terrace. The UPV and Differential IR images showing that the consolidation treatments done with Funcosil KSE500STE and SytonX30 improve the sandstones' UPV and thermal inertia characteristics. ....	79
Figure 4.22 CIELAB color values of sandstone cubes from Nemrut Quarry .....	81
Figure 4.23 Sandstone cubes from 5 <sup>th</sup> , 10 <sup>th</sup> and 15 <sup>th</sup> cycle of salt crystallization....	81
Figure 4.24 $\Delta E$ values of artificially weathered sandstone samples after 10 <sup>th</sup> cycle of salt crystallization.....	83
Figure 4.26 $\Delta E$ values of artificially weathered sandstone samples after 15 <sup>th</sup> cycle of salt crystallization.....	84
Figure 4.27 $\Delta E$ , $\Delta L^*$ , $\Delta a$ , $\Delta b$ values of artificially weathered sandstone samples after 15 <sup>th</sup> cycle of salt crystallization. ....	84
Figure 4.28 Color values of non-treated and treated sandstone cubes with Syton X30 and Funcosil KSE500STE. ....	85
Figure 4.29 $\Delta E$ values of fine and medium grained sandstones treated with Syton X30 and Funcosil KSE500STE. ....	85
Figure 4.30 Color values of non-treated and treated sandstone cubes with KSE100 and KSE300. ....	86
Figure 4.31 Bulk density and total porosity of sandstone cubes from Nemrut Sandstone Quarry.....	87
Figure 4.32 Percentage change in the bulk density and porosity values with salt crystallization cycles.....	89
Figure 4.33 Pore size distribution of medium and fine grained sandstones from quarry. ....	93
Figure 4.34 Pore size distribution of weathered sandstone samples from site. ....	93
Figure 4.35 Pore size distribution of exterior surface of a scale from site. ....	94

Figure 4.36 Pore size distribution of interior surface of a scale from site.....	94
Figure 4.37 Pore size distribution of artificially weathered sample from 10th cycle of salt crystallization.....	95
Figure 4.38 Pore size distribution of artificially weathered sample from 18th cycle of salt crystallization.....	95
Figure 4.39 Hygric Dilatation measurement of medium and fine grained sandstones; 94A: hygric dilatation of medium grained sandstone perpendicular to bedding; 94B: hygric dilatation of medium grained sandstone parallel to bedding; 91A: Hygric dilatation of fine grained sandstone perpendicular to bedding, 91B: Hygric dilatation of fine grained sandstone parallel to bedding. ....	97
Figure 4.40 Thermal Dilatation measurement of medium and fine grained sandstones; 94A: thermal dilatation of coarse grained sandstone perpendicular to bedding; 94B: thermal dilatation of medium grained sandstone parallel to bedding; 91A: thermal dilatation of fine grained sandstone perpendicular to bedding, 91B: thermal dilatation of fine grained sandstone parallel to bedding.....	98
Figure 4.41 Hydric Dilatation measurement of medium and fine grained sandstones perpendicular to bedding. ....	99
Figure 4.42 Hydric Dilatation measurement of sample Sandstone _D before treatment with HDTMA, as well as treatment with HDTMA and wetting after the treatment. ....	99
Figure 4.43 Hydric dilatation measurement of sandstone after treatment with antihydro and ethylenediamine.....	100
Figure 4.44 Hydric dilatation measurement of medium and fine grained sandstones after treatment with SytonX30. ....	100
Figure 4.45 Hydric dilatation measurement of medium and fine grained sandstones after treated with FuncosilkSE500STE. ....	101
Figure 4.46 Drying rate of saturated sandstone cubes at site. ....	102
Figure 4.47 Thin section photomicrograph of a fresh sandstone sample (crossed nicols). Showing the presence of quartz, plagioclase feldspar, granite, igneous rock	

fragments, alkali feldspar, biotite, orthoclase, calcedony, quartzite, calcite, Limestone particles .....	103
Figure 4.48. Thin section photomicrographs of fresh sandstone, fine grained (left), cross nicols; medium grained (right) crossed nicols. ....	104
Figure 4.49. Thin section photomicrograph of a fresh sandstone sample, crossed nicols X10 (left) and single nicol X63 (right), showing opaque minerals as iron oxides and some amorphous phases around them observed as small spheres. ..	104
Figure 4.50. Thin section photomicrograph of naturally weathered sample crossed nicols (left) and single nicol (right). Cracks in the microstructure and clay accumulations on the surfaces of cracks are observed. ....	105
Figure 4.51. Thin section views from naturally weathered samples. Micro-cracks are observed in the microstructure. ....	105
Figure 4.52. Thin section photomicrograph of naturally weathered sample crossed nicols (left) and single nicol (right). A crack of ~300 $\mu$ m size, accumulation of micritic calcite and clay minerals on one of its surfaces.....	106
Figure 4.53. Chlorite and iron oxide minerals in deteriorated fine grained sandstone can be seen in the single nicol (left), cross nicols (right). ....	106
Figure 4.54. Aggregates of colloidal iron oxide in the matrix of deteriorated sandstone around the iron oxide minerals, single nicol. ....	107
Figure 4.55. Thin section photomicrograph of fine grained deteriorated sandstone, crossed nicols, deterioration of feldspar minerals (left) and calcite in the matrix (right).....	107
Figure 4.56. Thin section photomicrograph of deteriorated sandstone from north terrace crossed nicols (right), single nicol (left).....	107
Figure 4.57 Thin section photomicrograph of deteriorated sandstone from north terrace (crossed nicols), a closer look into the microcrack of about 470 $\mu$ m, detached minerals can be seen in the crack. ....	108
Figure 4.58. Thin section photomicrograph of naturally weathered sample (NS1) crossed nicols (left) and single nicol (right). A crack network can be seen. ....	108

Figure 4.59. Thin section photomicrograph of deteriorated sandstone from east terrace, presence of opaque minerals, single nicol (left), crossed nicols (right)...	109
Figure 4.60. Thin section photomicrographs of artificially deteriorated sandstone presence opaque minerals single nicols (left) cross nicols (right). .....	109
Figure 4.61 Image analysis of medium grained sandstone. The average diameter was found to be 333 $\mu$ m. ....	110
Figure 4.62. Frequency distribution of medium grained sandstone, it was found to be poorly sorted.....	110
Figure 4.63. Image analysis of fine grained sandstone. The average diameter was found to be 176 $\mu$ m .....	111
Figure 4.64. Frequency distribution of fine grained sandstone, it was found to be poorly sorted.....	111
Figure 4.65 XRD trace of fine grained powdered sandstone from Nemrut Quarry, C: Calcite, Q: Quartz, Al: Albite, An: Anorthite, Ch: Chlorite.....	113
Figure 4.66 XRD trace of medium grained powdered sandstone from Nemrut Quarry, C: Calcite, Q: Quartz, Al: Albite, An: Anorthite, Ch: Chlorite .....	113
Figure 4.67 XRD trace of HCl Treated powdered sandstone from Nemrut Quarry, C: Calcite Q: Quartz, Al: Albite, An: Anorthite, Ch: Chlorite.....	114
Figure 4.68 XRD trace of powdered deteriorated sandstone before clay extraction , C: Calcite Q: Quartz, Al: Albite, An: Anorthite, Ch: Chlorite.....	114
Figure 4.69. XRD trace of magnetically collected iron oxides during clay extraction procedure. He: Hematite, Goe: Goethite, Mag: Magnetite/Maghemite, Q: Quartz, Al: Albite .....	115
Figure 4.70. XRD trace of air dried, ethylene glycolated and heated clay extraction from nondeteriorated sandstone, Ch(Fe): Chlorite Ferric, Ha: Halloysite.....	115
Figure 4.71. XRD trace of air dried and ethylene glycolated clay extraction from deteriorated sandstone Ch(Fe): Chlorite Ferric, Ha: Halloysite .....	116
Figure 4.72. XRD trace of of air dried, ethylene glycolated and heated accumulation between two scales of a naturally deteriorated sandstone sample, Sm: Smectite, Ch: Chlorite, Il: Illite; Ka: Kaolinite.....	116

Figure 4.73 Standard curve of methylene blue concentration versus absorption at 632 nm.....	118
Figure 4.74 Macro view of deteriorated sandstone sample (left), SEM image of interior face of deteriorated sandstone sample (right).....	120
Figure 4.75 Elemental (Ca, Al, K, Fe, Mn, Mg, Si, Na) mapping of surface of deteriorated sandstone sample.....	121
Figure 4.76 SEM view from surface of deteriorated sandstone sample (on top) and EDX analyses from points (1, 2, 3,4) shown on the image.....	122
Figure 4.77 SEM view from surface of deteriorated sandstone sample (on top) and EDX analyses from points (1, 2, 3,4) shown on the image.....	123
Figure 4.78 Macro view of interior face of relatively nondeteriorated deteriorated sandstone sample (top), SEM image of interior face of deteriorated sandstone sample (bottom).....	124
Figure 4.79 Elemental (Ca, Al, K, Fe, Mn, Mg, Si, Na) mapping of interior face of deteriorated sandstone sample shown in Figure 4.77. ....	125
Figure 4.80 SEM image of interior face of deteriorated sandstone piece (on top, and EDX analyses from points (1, 2, 3, 4) shown in image. ....	126
Figure 4.81 SEM image of interior face of deteriorated sandstone piece on top, and EDX analyses from the points (1, 2, 3, 4) shown in image.....	127
Figure 4.82 SEM image of interior face of deteriorated sandstone piece on top, and EDX analyses from the points (1, 2, 3, 5) shown in image.....	128

## LIST OF TABLES

Table 3.1 The changes in basal reflections of clays by treatments.....	54
Table 4.1 Average UPv values of sandstone cubes at different salt crystallization cycles. ....	66
Table 4.2 Indirect and direct UPV values of undeteriorated and deteriorated sandstone cubes taken parallel and perpendicular to bedding planes at dry state (33% RH). ....	67
Table 4.3 Indirect and direct UPV values of water saturated undeteriorated and deteriorated sandstone cubes taken parallel and perpendicular to bedding planes. ....	68
Table 4.4 Indirect and direct UPV values of a sandstone sample taken from the site (Figure 4.11) in situ, dry and water saturated states.....	69
Table 4.5 Indirect and direct UPV values of sandstone cubes before and after consolidation treatments.....	74
Table 4.6 Indirect and direct UPV values of sandstones blocks before and after consolidation treatments; direct (long) measurements are parallel to the bedding and the direct (short) being perpendicular to bedding. ....	75
Table 4.7 CIE La*b* values of sandstone cubes before subjected to salt crystallization cycles.....	82
Table 4.8 Bulk Density and Porosity values of sandstone cubes before salt crystallization test. ....	88
Table 4.9 Porosity change (%) of each sandstone cube after the 5 <sup>th</sup> cycle of salt crystallization test.....	89
Table 4.10 Porosity change (%) of each sandstone cube after the 10 <sup>th</sup> cycle of salt crystallization test.....	90
Table 4.11 Porosity change (%) of each sandstone cube after the 15 <sup>th</sup> cycle of salt crystallization test.....	91
Table 4.12 Observed “d values” of minerals in XRD traces .....	117

Table 4.13 Determination of Cation Exchange Capacity by UV-Vis Spectrometry.....	118
--	-----

## LIST OF ABBREVIATIONS

CEC	Cation Exchange Capacity
CNCDP	Commagene Nemrut Conservation and Development Programme
DAA	Ethylenediaminedihydrochloride
NDAASC	Nemrut Mount Academic Advisory Steering Committee
HDTMA	Hexadecylmethylamonium
LVDT	Linear-Variable Differential Transformer
PVA	Polivinyll acetate
QIRT	Quantitative IR Thermography
UCS	Uniaxial Compressive Strength
UPV	Ultrasonic Pulse Velocity
UV	Ultra Violet
XRD	X-Ray Diffraction
SEM –EDX	Scanning Electron Microscopy coupled with Energy Dispersive X-Rays

## **CHAPTER 1**

### **INTRODUCTION**

Conservation is defined as all activities involved in the protection and retention of heritage resources. It includes the studies on protection, development, administration, maintenance and interpretation of heritage resources, whether they are objects, buildings or structures, or environments (Nara Document, 1994).

A monument is not only a document of historical material but also a witness of historical construction techniques and technologies. Therefore, conservation should secure the material substance itself as well as the remains of its production technique. The conservation treatment should meet those demands (Sasse and Snethlage, 1996).

Conservation of historic stone structures is founded on the agreements that were concluded in several international charters. The technical and scientific issues of conservation are generally reported as the specialized subjects of the conservation. The need for the technical charters is frequently emphasized by the scientists involved in the conservation of historic structures (Tabasso, 1993).

Throughout its development, the role of science in conservation has been changed. Science in conservation aims to find methods not only for improving the appearance of works of art but also find methods which render them stable and resistant to further deterioration (Tennent, 1992).

According to Tennent (1992) conservation science is very similar to the medical sciences in their holistic approach in diagnostic and treatment methods' development.

However, conservation research is in its early state. In comparison to medical research

it is at its early twentieth century. In the nineties, conservation scientists have put forward that conservation innovations should not be treatment based where the fundamental understanding of the processes involved comes behind. Development of treatment methods can only be achieved by deep understanding of technology of the substrate material; analyses of deterioration and its mechanisms, analysis of treatment chemicals and the treated substrate. The need for standards in conservation is also vital. In this context the conservation scientists can contribute to develop specifications and validation of standards, test methods for evaluation of conservation materials, methods of analysis, methods for assessing appropriate treatments, or maintenance and monitoring programs (Tennent, 1992).

Stone conservation studies have started during the last century, however, due to the lack of well established methodologies, stone conservation studies has long been unsuccessful (Tabasso, 1993; Sasse and Snetlage, 1997; Wendler, 1992; Schaffer, 1949; Toracco, 1976). Today, the researchers in the field are in agreement that the methodology should be a holistic one. The holistic approach means the organic or functional relations between parts and the whole are to be emphasized. In other words, looking at the whole system rather than just concentrating on individual components.

Ideally **the scientists** will be able to develop new, simple, low-cost approaches to treatment and/or preventive conservation. As a consequence, a shift from conventional attitudes is necessary. Constraints of time, health and safety, contractual obligations, etc., are important factors which often dominate a conservation plan. In those circumstances, the presence of conservation scientist as an integral part of the team can help to set the best compromise which ensures the well-being of buildings and monuments (Tennent, 1992).

Stone conservation treatments involve mainly three types of interventions concerning the material: Removal of damaging products, depositions on the surface or in the

porous body, indicated as "*Cleaning*"; re-establishment or amelioration of the cohesion and adhesion among the mineral components, indicated as "*Consolidation*"; reduction of the probability and the rate of deterioration processes, indicated as "*Protection*". The requirements of any of the above interventions are rather specific (Tabasso, 1993).

Commonly accepted approach in stone conservation treatments is to do **minimum intervention** that is to try to keep the interventions at the minimum level; only to do what is **strictly necessary** and to try and to ensure the **long term compatibility and durability** of the treatments (Tabasso, 1993, Sasse and Snethlage, 1997).

Diagnosis is the first step in the sequence of any conservation studies. Knowledge on the deterioration in terms of the detailed mechanisms and the rate of stone decay is an important stage in the attempts to conserve and protect historic monuments. There are many deterioration processes determined by a large number of variables that may affect stone, in the stone itself and in the environment. A progress in conservation practice may be expected only when the action to be taken will be selected on the basis of a presumed deterioration process (Toracca, 1982).

Diagnostic studies answer two main questions that have vital importance in material conservation strategies: 1) Assessment of the state of deterioration of the material, from a macro scale (building scale, e.g. visual decay forms) to micro scale (e.g., petrophysical changes), a. Types of deterioration, b. Depth and degree of deterioration, c. Distribution of deterioration 2) The mechanisms and causes of deterioration.

The degree of weathering and decrease in durability are usually expressed by the changes in some important physical and physico-mechanical properties such as bulk density, effective porosity, ultrasonic velocity, color change and dilatation characteristics.

It must be kept in mind that acceleration of the decay processes is not exempt from problems, because it is practically difficult to know how and up to what extent acceleration factors affect the true reactions and decay phenomena (Theoulakis and Tzamalis, 2000).

Application of treatments without diagnosis is widespread still today; often some scientific data are thrown in just to give a reputable appearance to the operation, but correlation to deterioration factors or to action of the conservative processes is seldom attempted. The result is that several processes have been used for over 100 years and no agreement yet exists on their reliability (Toracca, 1982).

To sum up, it is necessary to have reliable and reproducible methods of recording the present conditions of artefacts and buildings in order to assess the rate at which they are changing. Furthermore, the establishment of standard procedures for evaluating the condition of buildings and artifacts, as well as for recording the results of these studies, is necessary to observe the rate of deterioration and to develop a proper conservation strategy. It is necessary to observe the rate of deterioration and to develop a proper conservation strategy. It is accepted that the alteration of a culturally significant building by a conservation treatment is preferable to its loss by demolition due to lack of conservation (Saniford et al., 1992).

## **1.1 Nemrut Mount Monument**

Nemrut Mount Monument is located near Kahta-Adiyaman in South East Anatolia (Figure 1.1). The site is one of Turkey's nine UNESCO World Heritage Sites (UNESCO-WHL). Although Nemrut Mount Monument has survived to the present day in a moderately preserved state; there are number of stone deterioration problems seen on its limestones and sandstones.



**Figure 1.1** Map showing Adiyaman Province and Nemrut Mount.

The tumulus was built by Antiochos I (69-31 BC) of Commagene on top of Nemrut Mount (2026 m) including the tumulus and three terraces as east, west and north. The tumulus itself is made of crushed limestone pieces piled up in conical shape. The east and west terraces are similar consisting of rows of limestone and sandstone statues. On both terraces, in addition to the giant statues, there are two rows of sandstone stele, mounted on pedestals with an altar in front of each stele. The rows on the east terrace are located on two opposite sides, while on the narrower west terrace they are aligned with the two edges perpendicular to each other. On the west terrace there is an additional row of steles of the handshake scenes (dexiosis) among them the stela with a lion horoscope is very famous since it is believed to be indicating the construction date of the cult area. These steles represent the particular significance of Nemrut. In contrast, the east terrace contains a square platform that has been

defined as an altar; while the north terrace is rectangular in shape, and hosts a series of sandstone pedestals. In the north terrace the steles lying near the pedestals have no reliefs or inscriptions (Figure 1.2).

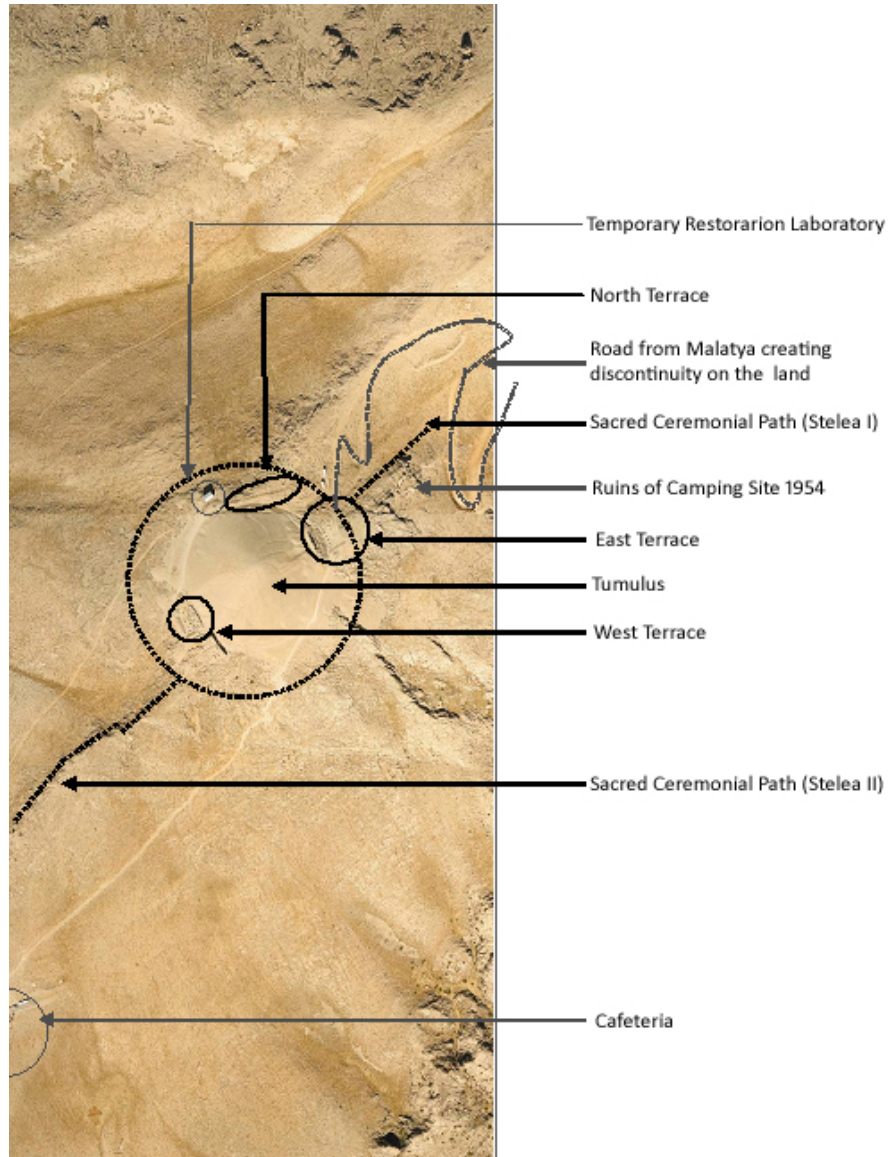


**Figure 1.2** Nemrut Mount Tumulus (The photo was processed on the aerial photo of the tumulus provided by GAP administration, for CNCDP in 2007 ODTÜ-CNCDP Archive, 2007).



**Figure 1.3** General view of East Terrace on a rainy day in Nemrut Mount Monument



**Figure 1.4** A view from West Terrace in Nemrut Mount Monument

The sandstone formations in the lower parts of the Nemrut Mount Monument site located at the Malatya gate, about 1750m east – northeast direction were decided to be the quarries that were possibly used in making the sandstone statues and steles at the site of the Nemrut Mount Monument based on their comparison of the colors, textures and weathering forms (Topal and Ertaş., 2011).

Those sandstone formations and their quarries were placed in “Lice Formation” of the Lower Miocene stage according to the fossils they contained (Perinçek and Kozlu, 1983; Topal and Ertaş, 2011). In Eastern Anatolia, the general lithology of “Lice Formation” was given as limestones, sandstones, siltstones and marls (Akdeniz, 2003). The sandstones in Lice Formation was defined as poorly sorted feldspathic litharenites. The sandstones were observed in an area of about 0.46 km<sup>2</sup>. In the sandstones, the layers are observed and the separation by layering was widespread. The sandstones used in the site are grey, fine to medium layered having low to average strength (Topal and Ertaş, 2011). Separation by layering was also observed for the statues and stele of sandstones at the site (Topal and Ertaş, 2011). Those sandstones from the quarries were found to have low to average strength  $UCS_{dry}=41.63$  (Mpa),  $UCS_{wet}= 25.25$  (Mpa) (Topal and Ertaş, 2011).

Nemrut Mount Monument was regarded as an asset to be protected by its technical, architectural and sculptural features for the future generations by UNESCO in 1987. Moreover, its spectacular physical and historical context gave Nemrut Mount Monument an important contextual symbolic meaning that it conveyed information about religious beliefs personal feelings and meanings.

A number of teams have studied Nemrut Mount Monument since its discovery in 1881 (Şahin-Güçhan, 2011a). The past studies mainly aimed at understanding the area and discovering the Tomb of King Antiochus I. In 2003, team of Bridjer, Moormann and Crijin made a few site interventions. Some wrong and/or harmful interventions were also done in Nemrut Mount Monument by previous teams. Among those wrong

interventions; repairs with cement mortars and epoxy resins could be observed at the site, moreover, some consolidation interventions with polyvinyl acetate were also reported by Sanders (1996). Sanders (1996) reported that polyvinyl acetate (PVA) solutions in acetone were used on the animal statues around the altar and on some fragile sandstone pieces either by spraying or using brushes.

Following those interventions, with the request from Adana Regional Council for Conservation of Cultural and Natural Heritage, Nemrut Mount Academic Advisory Steering Committee (NDAASC) was constituted by Ministry of Culture and Tourism in May 2005 (Şahin- Güçhan, 2011a). NDAASC was composed of Turkish experts who are known by the international conservation organizations, they defined the difficulties of the conservation decisions and interventions concerning the Nemrut Mount Monument and its surroundings and the definitions of the conservation projects according to the mentioned difficulties. Those difficulties and principles can be found elsewhere (Şahin- Güçhan, 2011a, b, Şahin-Güçhan, 2010).

The conservation of the Nemrut Mount Monument and its Surroundings has been issued to a Conservation Programme rather than a project because of its specific site problems, in 2006 after a four-month preliminary study, METU developed the CNCDP (Commagene Nemrut Conservation and Development Programme) ([www.nemrut.org.tr](http://www.nemrut.org.tr)). The primary goal of the CNCDP in the signed protocol was quoted below:

“to conserve, the Nemrut Mount Monument enlisted under the UNESCO World Cultural Heritage and the region withholding the monuments within the limits of the Nemrut Dağ National Park, the names of which are designated by a protocol that belong to the Commagene Civilization, along the principles of the contemporary conservation principles, together with its architectural, archaeological, historic, economic, social, cultural, natural, and ecological

assets as a whole and ensure its interpretation, presentation, and sustainability.”

The projects developed were based on the results of the studies of the CNCDP team consisting of academics from different disciplines and the requirements of the legislations. The studies included the documentation of the Nemrut Mount Monument area, the series of analysis and projects regarding the seismic assessments, structure of monuments, material analyses to determine the most appropriate methods and materials for the restoration and the urgent actions needed in the area (Şahin Güçhan, 2011).

A part of this study covers the conservation intervention needs of the sandstones of Nemrut Mount Monument in CNCDP under the subproject titled as “The Nemrut Mount Tumulus and Monuments project encompassing studies on materials, on structural conditions, geological surveys, and development of conservation proposals”. The definition and explanation of the sub-projects and project phases can be found elsewhere (Şahin-Güçhan, 2011a, 2011b, Şahin Güçhan, et al., 2010; Osmay et al., 2010).

## **1.2 Aim and Scope of the Study**

The **aim of this study** is mainly to develop conservation methodologies for the historic sandstones using the case of Nemrut Mount Monument, to keep them at their place, i.e. at the heights of Nemrut Mount **with a holistic approach by applying minimum interventions**.

The conservation intervention should not harm the cultural asset’s authenticity which is expressed as “truthfully and credibly expresses through a variety of attributes” in the Operational Guidelines of World Heritage Convention in 1982 (Alberts and Hazen,

2010). Thus not to harm the authenticity one should not make unacceptable changes on the "form and design, materials and substance, use and function, traditions and techniques, location and setting, spirit and feeling, and other internal and external factors" as it is stated in Nara Document (1994).

The conservation intervention should not damage the integrity of the cultural asset. "The general meaning of the word '**integrity**' refers to material wholeness, completeness, and unimpaired condition", hence the material decay changes the integrity of the cultural asset. On the other hand, integrity of a cultural asset can be disturbed by some conservation interventions such as transportation of the cultural asset from its original context.

Keeping those restrictions in mind, the conservation interventions for the sandstones of Nemrut Mount Monument should assure them to be kept at their place with minimum change in visual and aesthetic aspects and should assure their durability at the heights of Nemrut Mount. As widely accepted, the conservation interventions should be minimum and if possible reversible or at least repeatable. Moreover, the applications are preferred to be low cost and easy to apply as much as possible.

Thus, to achieve those aims, a comprehension of sandstone deterioration mechanisms, development of conservation methods for slowing down or if possible stopping those mechanisms and in particular development of consolidation treatments as a method of conservation, were the main tasks of the study.

This study included the examination of sandstone deterioration by studying the sandstones of the Nemrut Mount Monument to determine the most effective deterioration mechanisms that affect the historic sandstones and the development of conservation methods aiming to slow down those mechanisms of the deterioration and developing the consolidation measures for the weak sandstones with silica and silicate dispersive.

This work was composed of 6 chapters; first one being the introduction where the aim and scope of the study was explained, second chapter compiled a review on the weathering of sandstones and their control, third chapter was on the experimental methods used in this study both for understanding the deterioration mechanisms and evaluation of the consolidation treatments, the fourth chapter was the summary of the experimental results; fifth chapter was discussion where the experimental results were discussed, and the final and the sixth chapter was the conclusions derived from the study.

## CHAPTER 2

### WEATHERING OF SANDSTONES AND ITS CONTROL

Weathering is a group of processes i.e., physical, chemical and biological processes, that alter the physical and chemical state of rocks in atmospheric conditions. Those processes may work solely, sequentially or simultaneously. In weathering studies the emphasis should be given to relationships between processes, weathering forms, rock properties and environmental conditions. A holistic weathering research that is including intrinsic (chemical, physical and physico-mechanical properties together with mineralogical and petrographical characteristics of stone) and extrinsic (environmental conditions, antropogenic factors) influences is vital for the better understanding of the decay and decay mechanisms.

Although stone is one of the most durable materials used to make human artifacts, and many buildings, weathering agents may cause rapid change in the initial petrophysical properties of rocks and thus limit their durability (Benavente et al., 2004, Drever, 1992). Rock may weather or disintegrate at different scales. The individual minerals that make up the rock can dissolve or alter, a rock may loose cohesiveness along the boundaries between the mineral grains or along cleavage planes within the minerals and separation may occur along planes whose spacing is much greater than the scale of individual grains. The stability of a rock is thus a consequence of both the nature of the minerals of which it is composed and of chemical processes and mechanical stresses it has experienced since it was originally formed (Drever, 1992).

There are four basic groups of reactions responsible for deterioration of stone. They are; i) purely physical degradation caused by the action of water, temperature

variations and abrasion; ii) physico-chemical mechanisms involving the recrystallization of soluble or semi-soluble salts, without associated chemical change; iii) chemical reactions initiated by normal constituents and pollutants of the atmosphere and ground water; iv) microbiological activity causing direct physical damage to the surface and promoting chemical attack via trace element concentration and waste product manufacture (Caner, 1978).

Weathering of sandstones was a relatively less studied subject when compared to the other types of building stones such as limestones and granites (Young and Young, 1992; Turkington et al., 2005; Jimenez-Gonzalez, et al., 2008). On the other hand, the studies on sandstone weathering are increased over the last decade (Felix, 1995; Wray, 1997; Mertz and Jeannette, 2002; Sancho et al.; 2002; Jager et al., 2003; Turkington et al.; 2003; Turkington et al., 2005; Götze et al.; 2007; Heinrichs and Fitzner, 2007; Jimenez-Gonzalez et al., 2008; Wangler et al., 2008; Sebastian et al., 2008; Peters, 2009; Weng et al., 2009; Soe et al., 2010).

Microstructural properties of stone play important role in its durability. Mineral grains of stone are in physical contact with one another. The fit between adjacent grains is not perfect, even in marble and granite, there exist microscopic and submicroscopic pores that play a key role in the durability of stones. Although the importance of grain boundaries and related microporosity is recognized, our understanding of their influence on deterioration process need to be better understood. Mineralogical composition and its change by deterioration, texture, pore morphology are the important characteristics that have to be studied before and after the conservation treatments of the stone.

Moisture that has a key role in many weathering processes has influences on sandstone deterioration (Goudie and Viles, 1997; Turkington, 2005; Mol et al., 2010). The surfaces of the stones can be protected from the rainfall. However for a total protection, the control from all sources of moisture is necessary e.g. rising damp or

high relative humidity (Mol et al., 2010). Although there are studies about low porosity being advantageous for the capillary movement (Meiklejohn, 1994, 1997; Mol et al., 2010), Mol et al. (2010) stated that the largest source of moisture was actually internal moisture transport along the bedding planes and large fractures. With the help of the ERT (electrical resistivity tomography) measurements they found the evidence of moisture movement within the sandstones of Clarens (Mol et al., 2010) although the porosity of the sandstone was found to be unfavorable for the capillary movement by Meiklejohn (1994, 1997).

When porous stones adsorb moisture or if they absorb liquid water in a natural environment, a dimensional change of their original size occurs. Water content increase in the porous media of natural rocks leads always an elongation, whereas decrease of water content results in a global contraction (Felix, 1995; Mertz and Jeanette, 2002). Cyclic hydric swelling and shrinkage by repeated wetting-drying phases lead to dimensional changes and induces a material fatigue and the weakness of the stone (Snethlage and Wendler, 1997). Furthermore, sandstones and many sedimentary rocks have clays in their composition and they swell when they are exposed to moisture. This mechanism results in stresses in the rock and causes damages (Mohan et al., 1993; Mertz et al., 2000; Scherer, et al., 2005; Wangler et al., 2008; Jimenez-Gonzalez et al., 2008). Not only wetting but also drying induces the deformation of the clay bearing stones since drying may cause a gradual reduction in volume that may result in tensile cracking and opening at the bedding planes (Soe et al., 2010; Jimenez-Gonzalez et al., 2008).

Freezing is another weathering phenomenon for rocks when the temperature gets below 0°C in the presence of water. The volumetric expansion of 9% during water to ice transformation results in the internal pressure in the rock. This pressure is thought to be the reason for rock's disintegration, new microfractures are developed and present ones are deepened and widened, if that pressure due to water expansion

reaches the tensile strength of rock. After thawing, water can migrate into the newly developed microfractures. Recurrent freeze-thaw cycles cause enlarging of the existing fractures and further weakening of the material (Yavuz et al., 2006). However as Hallet (2006) explained in his paper for rocks, the 9% water-to-ice expansion is not so significant under natural conditions if the rock is not totally saturated and frozen from all sides (Hallet, 2006). For soils Taber (1929) was one of the first authors who explained that pressure as;

“Pressure effects accompanying the freezing of soils are due to the growth of ice crystals and not change in volume. Pressure is developed in the direction of crystal growth, which is determined chiefly by the direction of cooling. Heaving is often greater than can be explained by expansion. It is due to the segregation of water as it freezes, more water being drawn up by molecular cohesion.” (Taber, 1929)

The evidence for this came from an experiment done with helium and argon (Dash et al., 2006). Those liquids are contracting liquids upon freezing, but they caused the expansion of soils and other porous materials (Dash et al., 2006). Murton et al. (2006) also showed the ice segregation fracturing wet chalk by experiment. The findings of Murton et al. (2006) was in accordance with the findings of Hallet (2006) that is freezing sandstone does not fracture at the nominal freezing temperature of water at 0°C (as would be expected if it resulted from the water to ice expansion). However, since the lower temperatures are essential for substantial pressure in microcracks to develop as segregated ice grows, it fractures at lower temperatures. Nonetheless, this temperature should not be so low, for that unfrozen water films let waterflow to the growing ice effectively (Hallet, 2006). For sandstones and similar rock types the temperature range is about -3 to -6°C for freezing (Hallet, 2006).

One of the important agents of decay is the crystallization of soluble salts within the pores of building materials. When the salt solutions are present in the stone material

they are generally not so dangerous if the pores are large and the salt solution is dilute. However with the changes in the temperature or with evaporation they tend to crystallize and they generate pressure on the pore walls. That crystallization pressure in porous materials is related to the structure of the pores, saturation of the salt solution and the action of the solvent to the material. Crystallization pressure is lower in the bigger pores so the low saturation of the solution (Benavente et al., 2004; Scherer, 2000). Soluble salts can crystallize on the surface (efflorescence) and in the porous media of stone (subflorescence). Subflorescence results in more decay than efflorescence. (Schaffer, 1949; Benavente et al., 2004; Scherer, 2000).

For sandstones, many scholars linked tafoni and alveolization to salt weathering (Wellman and Wilson, 1965; Evans, 1970; Bradley et al., 1978; Mustoe, 1982; Smith and McAlister, 1986; Young, 1986; Matsukura and Matsuoka, 1991, Turkington et al., 2005). Salt weathering is said to be the cause of rock disintegration, but how cavernous forms develop through salt weathering process is still not clear. Salt crystallization and hydration processes are disruptive for the sandstones but Young (1987) and Young and Young (1992) stated that tafoni are produced by solutional processes, which may be increased in the presence of salt solutions. Snethlage and Wendler (1997) proposed a model of grains' displacements relative to each other by dilatation and contraction under the influence of moisture and ionic solutions. This process provides open spaces in the grain structure for the precipitation of the salts. In the same paper authors stated the honeycombs as a special case of sanding and they listed the conditions to be met for honeycombs forming as:

- "Sufficient amount of highly soluble salts
- Primary inhomogeneities in the water transport behavior as a result of primary sedimentary structures

- Protection against intense rain (although alveolae are primarily found on sheltered areas, they can also occur on rain-exposed areas, the rain, however, must not be too strong so as to extract the salt from the stone).” (Snethlage and Wendler, 1997).

As a result of increasing population and industrialisation, environmental pollution problems are faced. The atmospheric/environmental pollution is effective on building stones used in either present day constructions or historical buildings and monuments. The main pollutants which affect the building materials are primarily sulphur dioxide (SO<sub>2</sub>), and nitrogen oxides (NO<sub>x</sub>). These pollutants composing very complex structure of the urban atmosphere are reactive and corrosive for the building materials as well as for the other various essentials of our lives (Böke, 1987; Caner et al., 1988).

The actors of biodeterioration of stones can be roughly divided in two groups as microbes (bacteria, fungi, algae and lichens) and higher organisms (mosses, plants, insects and mammals) (Koestler, et al., 1997). By their biological action, they cause stones' physical alteration in pore size, cracking, changes in water circulation and their thermo-hygric properties; in addition, mechanical pressure due to the shrinking and swelling of the colloidal biofilms might cause a further weakening of the mineral lattice (Warscheid et al., 2000; Kain et al., 2009). It is known that excessive moisture in the stone makes it suitable for microbiological growth (Warscheid et al., 2000; Kain et al., 2009). Microbial interactions are also strongly influenced by the details of the intergranular pore system. In the recent study of Jain et al. (2009) authors investigated the effect of humidity being more than 55% on the microbial activity in sandstones (Jain et al., 2009). Authors have concluded that fungi formation above the 55% humidity was very likely and they involved in dissolution of sandstone and use the existing minerals by microbial interaction (Jain et al., 2009). The other factors that affect the biological growth are climatic exposure, nutrient sources, pH and

petrological/mineralogical parameters, such as mineral composition, type of cement as well as porosity and permeability of the stone (Warscheid et al., 2000).

Deep penetration of moisture is suitable for microbial contamination to a depth of up to 3-5 cm when the stone has high-porosity values from around 14 vol % with an average pore radius between 1 and 10  $\mu\text{m}$  (Warscheid et al., 2000). The short water retention of large-pore sandstones promotes a temporary contamination of microorganisms, while the stones with longer water retention time offer more advantageous conditions for the stone colonizing micro-organisms (Warscheid et al., 2000).

Stone scales and crusts may act as a protective layer for the microflora from the influence of strong solar radiation and consequently high temperatures and detrimental UV-light and desiccation (Warscheid et al., 2000). The carbonate compounds in the stone, e.g., >3%  $\text{CaCO}_3$  as in the case of calcareous sandstones, may prepare a constant suitable pH-medium by buffering of biogenic metabolic products for the growth of bacteria (Warscheid, et al., 2000). Sandstones having significant amounts of feldspars, clays and ferruginous minerals, >5% by weight that have a tendency of weathering are particularly susceptible to the development of microorganisms since those minerals could be nutrient sources for the stone-inhabiting microflora (Warscheid et al., 2000).

Migration of iron in sandstones may cause discoloration of the stone and the formation of an iron rich crust layer that is non durable, thus affecting the durability of the stone (McAlister et al., 2003). Some of the minerals present in sandstones may contain  $\text{Fe}^{2+}$  that transforms to iron oxides, by weathering mechanisms. Fe oxides may accumulate as bands, discrete physical concretions or circular shapes (Busigny et al., 2006, MacAlister et al., 2003). The primary reactions during their formation are mainly hydrolytic and oxidative decomposition of  $\text{Fe}^{2+}$  silicates (McAlister et al., 2003). Those hydrous ferric oxides are amorphous and amphoteric, they have the capacity to offer

H<sup>+</sup> or OH<sup>-</sup> ions for cation or anion exchange as pH conditions change (McAlister et al., 2003). The pH in the range 5.0–8.0 controls the sorption behavior and each ion has a different pH range for adsorption (McAlister et al., 2003). Uncomplexed Fe<sup>2+</sup> oxidises to Fe<sup>3+</sup> much faster than complexed Fe<sup>2+</sup> and the time of those reactions depends on the temperature, pH, dissolved oxygen concentration as well as the presence of other soluble ions (McAlister et al., 2003). Stone can be attacked by autotrophic microflora that use the minerals for energy production since the stone itself is inorganic and heterotrophic species microflora that use carbon as source of energy because of the accumulations on the surface of the stone as the results of atmospheric pollution, pollen, bird droppings, etc. Carboxyl and hydroxyl functional groups present as part of the organic structure may interact iron oxides (McAlister et al., 2003). The mobility of many inorganic compounds is determined by redox reactions, e.g. redox reactions of nitrogen and sulphur that are biologically important materials.

Thermal shock damage is a result of differential thermal expansion and contraction of the mineralogical components and of the interior and exterior portions of a stone sample. Anisotropic thermal expansion can occur both within and between individual grains of such a sample. These processes lead to cumulative fatigue and formation of internal stresses, which can combine to generate tensile strain sufficient for microfracturing to occur (Hale et al., 2003).

At the beginning of the 1900's the sandstone weathering studies remained focused on physical breakdown with a particular interest in the role of sun as the cause of temperature changes on rock surfaces. It was accepted that although there was an unclear relationship between the solar radiation induced temperature changes and weathering, there was a connection. Lately, Kerr (1984) and McGreevy (1985) demonstrated that insolation may work through the separations of a particle from its matrix. Micro cracks can develop in the matrix by the change of quartz volume on thermal expansion and contraction (Jenkins and Smith, 1990).

The thermal characteristics of the rock is important for the surface temperatures and thermal gradients created by the radiation of sun (McGreevy, 1985) and may result in micro fracturing of surface grains (Yatsu, 1988) but they are not likely to be the only cause of sudden and serious rock breakdown (Warke and Smith , 1994). On the other hand, thermal cycling may have a considerable effect on the activity of other weathering mechanisms like salt crystallization, hydration, oxidation or solution. In the work of Paradise (2000), among the deterioration mechanisms in Petra sandstones the most effective one was found to be the insolation (sunlight) when accompanied with wetting-drying and heating-cooling cycles. In that study it was also found that the deterioration was more serious at the south-eastern and south-western places where the temperature was higher (>50°C) with the effect of solar radiation. Author has also found that this situation was more emphasized when the calcite amount was higher in the sandstones (Paradise, 2000).

## **2.1 Clay Swelling and Its Control by Surfactants**

Clay is a natural material with very fine texture and consists of fine mineral particles with sizes <2µm. Because of its fine size it has a large surface area (Carroll, 1970). Main clay minerals can be found in sandstones are smectite, chlorite, kaolinite, illite, and mixed-layer clays (Tucker, 2001). They can be both detrital and authigenic and not all the clay minerals can be identified by optical microscope especially the ones that are detrital (Tucker, 2001).

There are two types of swelling with clay minerals in the presence of water; intracrystalline swelling and interparticle or osmotic swelling. Osmotic or interparticle swelling is experienced by all types of clay. On the other hand the intracrystalline swelling is experienced only by so-called expandable/swelling clays. Clays that have only osmotic swelling are called as nonexpandable/nonswelling clays since the

swelling is much smaller compared to intracrystalline swelling (Rodriguez-Navarro et al., 1998, Jimenez-Gonzalez et al., 2008).

Smectites, mixed layer smectite-chlorite and smectite-illite are known to be swelling clays. Intracrystalline swelling results in an increase in  $d_{001}$  spacing when the clays are in contact with a polar liquid such as water or ethylene glycol. Chlorite –a nonswelling clay- is shown to develop swelling layers through weathering (Wangler et al., 2008).

The rocks containing clays thus experience swelling when they get wet, the amount of swelling is much more in the rocks having expandable or swelling clays (Jimenez-Gonzalez et al., 2008; Wangler et al., 2008). Thus, for rocks it is important to identify the swelling mode for the effective prevention of swelling.

As mentioned before, one of the two kinds of swelling, intracrystalline swelling is marked by discrete jumps in interlayer spacing about  $2.5\text{\AA}$ , which corresponds to one monolayer of water whereas when the swelling is osmotic, the interlayer spacing increases with increasing water activity (Wangler et al., 2008).

Sandstones have clays in their cement as the binding agent. This makes them very susceptible to deterioration, especially under wetting and drying cycles that result in swelling and shrinkage of clay minerals. If the stresses developed during the swelling of clays could overcome the wet compressive strength of the stone, it results in damage (Jimenez-Gonzalez et al., 2008).

In many studies, different types of sandstone weathering had been linked to the clays i.e., polygonal cracking (Williams and Robinson, 1989), tafoni (Martini, 1978), honeycombs (Gill et al., 1980), and spalling/multiple scaling as well as contour scaling (Robinson and Williams, 1994; Heinrichs, 2005). However, the physicochemical behavior of clay minerals especially their swelling and shrinkage under wetting and drying cycles in relation to the weathering of sandstone is still in need of investigations (Jimenez-Gonzalez et al., 2008).

In the field of sandstone deterioration, studies on swelling characteristics of clays are very valuable. Higher swelling strains are observed in rocks containing expandable clays than in rocks containing non-expandable clays. Timothy et al. (2008) have shown that Portland sandstone has chlorite and some other non-swelling clays. They also added that in chlorite, weathering may create the swelling layers among non-swelling layers. In a former study Jimenez-Gonzalez et al. (2004) also showed that having swelling clays in cementing phase affects the elastic and viscoelastic properties of the stone.

Damage during wetting could happen if those stresses overcome the wet compressive strength of the stone. On the other hand, shear forces that develop during wetting could be responsible for cracks opening parallel to the stone surface (Jimenez-Gonzalez et al., 2008). This can create a disruption between the dry and wet layers producing the buckling of the wet outer surface and resulting in scaling or contour scaling. For tensile strengths, the authors found that according to their calculations, damage should always happen during drying. However, for tensile stress to develop, the stone must first be sufficiently expanded, which will only occur if a block or ornamental piece is almost completely saturated. Since estimated capillary rise of the waterfront is not very high in the studied sandstones and that water penetrates only superficially to a depth of 2cm, that mode of failure therefore only seems probable for ornamental elements that are fully saturated. As would be expected, if drying stresses are causing the damage, the cracks are mud-cracking type on those ornamental features. Other factor that reduce the stresses is slow drying, which permits viscoelastic relaxation, in a humid environment (Jimenez-Gonzalez et al., 2008, Smith et al., 2005).

The damage from the swelling depends on the water penetration depth, swelling strain amount, and the elasticity of the stone (Jimenez-Gonzalez et al., 2008). It is also mentioned by scholars that not only drying but also swelling can cause damage to the

stone (Soe et al., 2010; Jimenez-Gonzalez et al., 2008; Turkington et al., 2005; Wendler, 1997). The compressive stresses are created when the wet surface of a dry stone expands, conversely, and the tensile stresses caused when the dry surface of a saturated stone contracts (Jimenez-Gonzalez et al., 2008).

The use of surfactants for the swelling inhibition of clay minerals in historic stones was proposed in several studies (Wendler et al., 1996; Wendler et al., 1991; Wangler et al., 2008; Jimenez-Gonzalez et al.; 2008). The DAA (diaminoalkane) as surfactants is known to reduce the swelling of the materials without affecting the overall hydric transport in the material (Wendler et al., 1996). Surfactants make preferential bonding to the surface of reactive minerals and this action prevents their hydration in the presence of water which is the reason for swelling (Wendler et al., 1996).

In their study, Jimenez-Gonzalez et al., (2008) used diaminoethane dihydrochloride ( $C_2H_8N_2 \cdot 2HCl$ ) as the swelling inhibitor. They found out that the swelling strain normal to the bedding plane was diminished about 50% but they estimated the swelling pressure decrease as 33% (Jimenez-Gonzalez et al., 2008). On the other hand, the viscoelastic relaxation would increase and it would contribute to an overall pressure reduction by 44% (Jimenez-Gonzalez et al., 2008).

Since the clays are used for many different industrial applications, suitable surfactants are designed for them for specific purposes (Bildiren et al., 2009; Xi et al.; 2010; Sanchez-Martin et al.; 2008; Wendler et al.; 1996; Jimenez-Gonzalez et al., 2008; Wangler et al.; 2008).

Organoclays have been extensively investigated for hydrophobic contaminants immobilization, hydrophobic characteristics or water purification (Xiet al.; 2010). Bildiren et al. (2009) and Xi et al.; (2010), investigated the hydrolic permeability of the organoclay composites that were created with different doses of an organic cation HDTMA (*hexadecylmethylamonium*)The authors have found out that with the increase

of the dosage, the impermeability characteristics of the organoclays were increased (Bildiren et al.; 2009; Xi et al.; 2010).

## **2.2 Consolidation Treatments**

Conservation involves series of treatments needed for the control of deterioration factors as well as the improvement of the state of deteriorated material. As mentioned previously, weathering processes cause loss of cohesion meaning decrease in strength and physicommechanical properties, starting from the surface of the stone. As a result, grains may sand off from the surface and/or flakes and scales of different thicknesses may start to detach from the surfaces. Very often, a changing strength profile towards the interiors of the stone can be observed.

Materials and methodologies used in consolidation must be effective and not dangerous, both in the short and long term. The evaluation of consolidation treatments for their long term behaviour are quite difficult. Methods are being developed for that purpose.

The role of consolidants in the conservation of stone is to restore the chemical and physical properties of weathered stone to those of more sound stone, while maintaining its natural features. Ethically, consolidants should be reversible and/or the surface should remain retreatable, and they should not interfere with further scientific analysis (O'Connor, 2000).

In most cases, it is not necessary to increase the load-bearing capacity of the stone on its surface zone. What is needed is to avoid the "sanding off" of grains or to prevent loosening of scales. As the internal stresses are very small, it is only necessary to consolidate the grain structure. Since this can be achieved with very "soft" impregnation materials, it is recommended using the term "consolidation" instead of

“strengthening” which is used in civil engineering for increasing the load-bearing capacity of weak concretes by polymer or microcement injection.

Consolidation of a porous material is achieved through deep impregnation by a suitable product, capable of improving the cohesion of the mineral constituents and the adhesion between the damaged portions and the sound core. As a result, the consolidated material will be more resistant both to external and internal stresses.

It is worth considering methodologies and criteria to evaluate the efficiency of products. Apart from specific requirements depending on the nature and condition of the object to be treated, all consolidation materials used for the stone conservation should be effective, not dangerous and compatible with the original substratum, long lasting and, as far as possible reversible or, even if not removable when aged, they should not prevent further, new treatments with the same or other products.

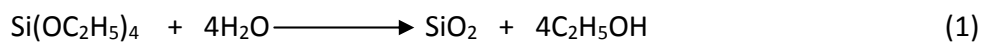
### **2.2.1 Consolidation Treatments with Silicates**

Use of silica solutions as stone consolidation agents dates back to more than a century (Barff, 1860; Church, 1862; Tate et al., 1861; Wright and Sommerdijk, 2001), and in the latest years, their use in the form of ethyl silicate and silicic acid esters have been widely extended, especially for deteriorated silicious stones (Moropoulou et al., 1997; Koblischek, 1995).

Silica ( $\text{SiO}_2$ ) can be found in nature in crystal (quartz, cristobalite), and amorphous phases (Opal-A, Opal-CT etc.). Its amorphous phases are hydrated. Hydrated silicon oxides behave as weak acids. They form salts which are called silicates. When these salts get into hydrolysis reaction they form silicic acid. The silicic acid formed in the hydrolysis reaction is responsible for the consolidation of the materials. When the acid is left alone, it forms a gel which undergoes a progressive contraction as it loses water

until it is transformed into silica (Toracca, 1982). If the silicic acid is formed inside a material that has hydroxy groups (OH) in its composition, such as brick, clay, wood and several types of stone; de-hydration takes place between the acid and the material by forming chemical bonds which improve the cohesion of the material (Toracca, 1982).

Through hydrolysis of ethylsilicate, an anorganic “polymer” is produced here from an inorganic ester (1).



The ethanol (ethyl-alcohol) which comes out as a by-product is not damaging either to the building material or the building structure (Koblischek, 1995). The hydrolysis of the silicic acid esters takes place slowly, so that the silicic acid ester can penetrate deeply into the stone to be strengthened; only in this way a uniform degree of strength can be achieved. Since the silicic acid ester is not so reactive (hydrolysis is slow), layers won't be formed at the upper levels that it has already passed through. The penetration should therefore be provided for up to a depth of 50 mm. The pre-condensed product has a well-balanced consolidation profile with a smooth inward course by slow hydrolysis (Koblischek, 1995).

To sum up, the main reasons for using ethyl silicates are related to its chemical compatibility with the stone and the polymerization rate that permits it to penetrate into deep parts of the material (Moropoulou et al., 1997).

On the other hand, the presence of the consolidant within the pores may lead to cracking owing to the tensile stresses, when shrinkage of the consolidant is constrained. This phenomenon also occurs in the case of the gels if their viscoelastic relaxation behaviour is not appropriate (Scherer, 1999; 1997). Therefore elastified ethyl silicates are developed to be used as consolidant.

Storemyr et al., (2001) reports that the ethyl silicates have low viscosity and are not able to bridge distances between minerals larger than 50-100  $\mu\text{m}$  so they are not able to fill most fissures. The problem can be overcome by using precondensed ethyl silicate and adding silica fume. Such a product (Funcosil VM857-STE) is able to bridge larger distances (Storemyr et al., 2001). In their study authors used several combinations of ethyl silicate products for example Funcosil 300E by adding Propyl Amino Silane (1-3 %) to use for consolidation of granular disintegration and microfissures; Funcosil VM857-500 STE alone for fissures and delamination. For thicker fissures and scales they have used Funcosil VM857-500 STE together with quartz and stone powder and pigments (Storemyr et al., 2001). However, the efficiency of their conservation treatments were not yet evaluated.

There are also colloidal dispersions of silica particles in the market for the restoration purposes. Several studies with colloidal silica dispersions give optimistic results. The particle size of the silica in the dispersion is very small, so the reactivity of the consolidant with the substratum is expected, with a deep penetration of the consolidant. Storemyr et al., (2001) have also used colloidal dispersions of silica together with fume silica aggregates in the laboratory and in the field. They have not yet evaluated the efficiency of the treatments.

In the study of Moropoulou et al., (1997) water based colloidal dispersions of silica was used to consolidate some sandstone types in the monuments of Rhodes. They found that aqueous colloidal dispersions of 20 % silica was superior to dispersions of ethyl silicate in alcohol as consolidant. Colloidal silica dispersions diminished the rate of hygric swelling and shrinking in the deteriorated stone in a compatible way. Capillary water was able to enter the pore space, and vapor diffusion was not inhibited (Moropoulou et al., 1997). However, in their study, authors mentioned that

there was need to further studies on the sol<sup>1</sup>-gel<sup>2</sup> transformation of the consolidants within the porous system of the original material under capillary pressure. That was expected to provide special characteristics to the gel systems, such as viscoelastic relaxation and the rigidity of the gel network (Moropoulou et al., 1997).

The study on the reactivity of the different types of the silicatic consolidants done by Zendri et al. (2006), showed that both the surface area of the consolidant and the system of the lattices of silica formed by the consolidant were important for the reactivity. Solidified silicate networks in the consolidated material were described as xerogels of Q<sup>1</sup>, Q<sup>2</sup>, Q<sup>3</sup> and Q<sup>4</sup> crystalline and amorphous phases by those authors<sup>3</sup>. The structures of xerogels were determined by NMR spectroscopy using <sup>29</sup>Si. The investigations on reactivity between different types of silica (ethyl silicate, colloidal silica and sodium silicate) and stone support were executed by mixing consolidants with calcite and quartz powder in the study of Zendri et al.(2006).

“In xerogel coming from colloidal silica prevails the presence of Q<sup>4</sup> systems related to tri-dimensional systems while in xerogels coming from ethyl silicate and sodium silicate prevail more planar “open” systems, much more available for a chemical interaction with calcium carbonate and quartz. The calcite reacts with xerogels involving significant structural modifications. In all cases the presence of Q<sup>3</sup> systems seems to influence on the reactivity of the silicatic consolidants towards the support.

---

<sup>1</sup> A sol is a dispersion of colloidal particles suspended in Brownian motion within a fluid matrix. Colloids are suspensions of particles of linear dimensions between 1nm (10A<sup>0</sup>) and 1 μm (10000 A<sup>0</sup>) (Wright and Sommerdijk, 2001).

<sup>2</sup> A gel is a structure very far from equilibrium. For example, the equilibrium state of silica under ambient conditions is crystalline quartz, whereas a silica gel is amorphous and has a surface area in the range of 100-1000m<sup>2</sup>/g, which contributes a large additional energy to the material (Scherer,1999) .

<sup>3</sup> In silicates the Si atoms are bound to four oxygen atoms and can be represented by a tetrahedron of which the corners link to other tetrahedra. In order to describe the substitution pattern around a specific silicon atom the Q<sup>n</sup> notation is used in which the Q represents a silicon atom surrounded by four oxygen atoms and n indicates the connectivity, i.e., the number of silicone atoms the Q unit is linked to. Hence, Q<sup>0</sup> denotes monomeric units, Q<sup>1</sup>, end groups, Q<sup>2</sup>, middle groups in chains (or rings), Q<sup>3</sup> branching points and Q<sup>4</sup> fully interconnected silicate groups (Wright and Sommerdijk, 2001).

The consolidant based on ethyl silicate proves more reactive than others and this effect could offer good reasons to suppose that ethyl silicate has a best re-aggregating effect on substrate. On the contrary, measures of cohesion on mortar samples treated with the three examined consolidants do not give great differences between the products and in particular, the ethyl silicate proves to have less cohesive effect on mortars than sodium silicate and colloidal silica. Instead, the porosity distribution of treated samples evidences a greater penetration capacity of the colloidal silica, characterized by little dimensions of the particles in comparison with sodium silicate and ethyl silicate" (Zendri et al., 2006).

Till now, consolidation of silicic stone with silicates was mentioned, however, normal or elastified ethyl silicates were also used as consolidant for the calcereous materials. Although there were unsuccessful applications of ethyl silicate for the calcereous materials, better results were found by Grissom et al., (1999). They have used ethyl silicates to improve the strength of the lime plasters (Grissom et al., 1999). They have found 300% increase in the strength measured by MOR (Modulus of Rupture) tests and no negative changes occurred on the consolidated material over the 11 years. Those plasters were displayed in a museum in Jordan with no climatic control where the conditions were far less severe than exterior exposure.

Silicates are also used as surface treatment agents for water proofing. The fundamental demand for a water repellent is, after its application, no change in the water vapor permeability.

In their study the Von Plehwe-Leisen et al., (1996) investigated the 20 years performance of some consolidation agents that were used on sandstones. Experiments included the 40 cubes of eight building stones of Cologne Cathedrale that were treated with different consolidants such as non-hydrophobic and hydrophobic silicic acid esters, silicone hydrophobation, aluminium stearates, organic resins, organic water repellents, silicate paint and different coatings. The mechanic

properties of the specimens consolidated with silicic acid esters (SAE) products revealed an increase (Von Plehwe-Leisen et al., 1996). The specimens that silicic acid water repellents were used after consolidation with silicic acid esters showed the minimum microbiological activity. However when the consolidants were used separately they were less successful concerning the microbial activity. Water uptake measurements of the samples showed that the capillary uptake for the ones with water repellent treatment were decreased, the best results were obtained both for hydrophobic and non-hydrophobic silicic acid esters; cubes only strengthened by application of silicic acid esters without water repellent showed a reduced absorption this could be linked to the reduced pore space by silica gel (Von Plehwe-Leisen et al., 1996).

During the hydrolysis of silicic acid ester, a relatively large amount of ethanol has to escape from the system. The consequence is a strong shrinkage and high tensile strength formation in the gel. During the hydrolysis of a silicic acid ester, silanols are developed as an intermediate stage. If the gel exists as silanol for a longer time, a larger amount of ethanol can be separately evaporated, the shrinkage of the gel is substantially diminished after the complete hydrolysis and dehydration. Tension is reduced and the consolidants are more uniform. The non-pre-condensed, high catalyzed products shows a rough increase of the consolidation towards the surface by rapid hydrolysis. The pre-condensed products on the other hand have a well-balanced consolidation profile with a smooth inward course by slow hydrolysis (Koblischek, 1995).

The effectiveness of silicon alkoxides as consolidants for weathered stone depends on the properties of both the sol and the silica gel phase. Rheology and surface tension of the sol affect the penetration depth of the consolidant into the stone, while physical properties of the gel determine the development of strength and its maintenance over time. The currently used ethyl silicate consolidants show excellent properties in

sol phase, but the gel phase physical properties such as thermal expansion coefficient and porosity do not match those of stone. Moreover gel phase is affected by cracking induced by residual stress during drying that limits the development of strength (Miliani, et al., 2007, Wright and Sommerdijk, 2001, Scherer, 1999, 1997).

Miliani et al. (2007) report that the particle modified consolidants (PMCs) obtained by adding colloidal oxides to the silicate consolidant are promising as stone consolidants because of reduced drying shrinkage of the gel network. They also noted that the  $\text{Al}_2\text{O}_3$ -PMC,  $\text{SiO}_2$ -PMC and  $\text{TiO}_2$ -PMC provide a remarkable protection against salt crystallization. It is also worth to note that  $\text{Al}_2\text{O}_3$ -PMC and  $\text{TiO}_2$ -PMC performed better than silica against the salt resistance tests (Miliani, et al., 2007).  $\text{TiO}_2$ -PMC caused an unacceptable color change because of the high refraction index while the others provide composites giving color changes near the threshold ( $\Delta E \leq 5$ ) (Miliani et al., 2007). The authors also state that the thermal coefficient of the PMCs are smaller than the unloaded ethyl silicate, which is closer to the stone's thermal coefficient and they concluded that this may be an advantage for reducing the risk of cracking during thermal cycles of treated stone (Miliani et al., 2007).

Control on the sol-gel synthesis of materials are dependent on the *i) ability to determine the sizes of the initial colloid particles ;ii) the ways in which chemical links are formed between different colloid particles and the subsequent development; iii) drying and densification of the resulting aggregates* (Wright and Sommerdijk, 2001).

The size of the silica particles in the solution has a great importance and the small sized silica particles are more advantageous for the sol-gel preparation. The small particles tend to dissolve, while the larger particles tend to grow (Ostwald ripening of precipitates). In the stone conservation point of view, it is better to have smaller particles in the solution since the deep penetration of the consolidant is more probable.

Silica and silica based materials are widely used in industrial , technological and domestic applications. There is a growing demand for improved silica types with specific properties such as mechanical strength, pore volume, pore-size distribution, specific surface area or surface reactivity. Accordingly, extensive work has been carried out to produce mesoporous silica and to reveal the complicated physical chemistry accompanying the simpler condensation reaction in which silica monomers are used to build the large polymeric structures typical for such porous silicas (Sun, et al., 2004). Those chemically produced silicas generally are produced under harsh conditions e.g. at high temperatures/pressures and/or strongly acidic or alkaline media.

### **2.2.2 Evaluation of the Stone Consolidation Treatments**

To evaluate the effectiveness of a conservation treatment, there is need to a set of selected properties to be described (Sasse and Snetlage, 1997, Wendler, 1997, Charola, 2001).

The suitability of a consolidant for the intended use can be investigated by using several tests. In order to decide on the method(s) to be used, stone deterioration should be well described in terms of the changes in physical and mechanical properties, microstructure and chemical composition. After the conservation treatments, treated and untreated parts of the material should be compatible and that compatibility is to be expressed in terms of measurable parameters (Sasse and Snetlage, 1997, Wendler, 1997, Charola, 2001).

In an evaluation system for stone conservation, it is first necessary to establish a reference level to which the measurements can be referred. The reference is always fixed to the properties of the unweathered stone, which can either be measured on the back side of sufficiently deep drill cores from the object or freshly quarried

samples. Generally, the aim of a treatment is to return the altered properties to their starting point, but not to make the stone better than its original state. In some cases negative properties need to be improved if any harmful consequences of those properties must be prevented. In such cases, the mechanical properties of a deteriorated stone can be elevated beyond those of the fresh stone. For protective purposes, the physical and chemical properties of stone must normally be changed to better durability.

Aim of consolidation treatment is to improve the properties of decayed stone to such an extent that a compatible relationship is formed with the decayed and the relatively non-decayed parts after the treatment. It is aimed to form a structure with similar physical and mechanical properties as well as chemical and mineralogical properties. In other words, deteriorated, less deteriorated and not deteriorated parts of the building stone should be connected to get a compatible and durable unit, since the compatibility of materials is directly related to their durability and finally to the durability of the historic structures to which they belong (Caner-Saltık, et al., 2005, Tunçoku et al., 2004).

The physical and mechanical properties before and after the consolidation treatment should be investigated by some measurable parameters. Physical and mechanical properties such as bulk density, effective porosity, ultrasonic velocity, color change and dilatation characteristics are among the important parameters to be measured. The parameters to be measured before the treatments also describe the state of deterioration of the material. To obtain references to those properties, geological equivalents of the stones used in the historic monuments can be investigated in the field and in the laboratory by subjecting them to some tests of physical and physicommechanical properties as well as some cyclic weathering tests. The measurements of the same parameters after the treatments are used to describe the

efficiency of the treatments. In addition, in-situ and laboratory non-destructive tests are helpful both to describe the efficiency of the treatments and their monitoring.

Consolidation treatments should not significantly change the color of the material. Colour measurements are currently carried out with colorimeters, typically on homogeneous surfaces using the parameters defined by CIELAB. The CIELAB chart is the basis for the colour representation and it expresses the colors in numbers by translating the qualitative perception of color that one has when looking at polished stone slab or at specimens treated with distinct products (Costa and Delgado Rodrigues, 1996).

The spectral reflectance curves of each measurement allow the determination of three parameters in the 'Lab' system (the three axis  $L^*$ ,  $a^*$  and  $b^*$ ), as proposed by CIE (ASTM E 308, 1993). It is also possible to compute color differences after the treatments ( $\Delta L^*$ ,  $\Delta a^*$ ,  $\Delta b^*$  and  $\Delta E$ ,  $\Delta C$ ), by using the initial color average of the untreated sample as reference and using color difference equations according CIE (ASTM D2244, 1993).

In monitoring studies of the treatments, color changes due to treatment products or ageing processes can be computed as mean values. Total color differences or relevant color coordinates before and after treatment may evidence the changes promoted by different products. Only a slight color change ( $\Delta E \leq 5$ ), and no darkening or gloss is required for a good consolidant (Sasse and Snethlage, 1997). The variations in color observed in treated/deteriorated stones can be taken as a parameter showing the ageing or decay in time.

Dilatation is an important property to evaluate the compatibility and durability of the consolidation treatments. After the treatments, dilatation should not be different than the untreated parts that are connected with the treated areas. Dilatation properties, especially "dilatation kinetics follow up measurements" have gained

importance in recent stone conservation research, on the evaluation of the consolidation treatments. The swelling and shrinkage of the stones during the cyclic atmospheric changes must neither be increased nor reduced excessively after the treatment (Wendler, 1997).

## CHAPTER 3

### EXPERIMENTAL METHODS

Before any conservation treatment stone deterioration has to be evaluated by the use of several analytical techniques that are performed in situ and in the laboratory. The changes in physical and physicochemical properties of stone and the changes in its mineral composition and texture have to be well defined in order to determine the expectations from the conservation treatments. Experimental work carried out in the field and in the laboratory were summarized below with the major headlines being “Mapping of Visual Weathering Forms”, “Determination of Physical and Physicochemical Properties”, “Determination of Microstructural Properties”, “Application of Surfactants” and “Application of Consolidants”.

#### 3.1 Mapping of Visual Weathering Forms

Mapping of weathering forms is a method, which allows the registration of type, extent and distribution of visual weathering damages. It offers a classification scheme of weathering forms. Mapping of weathering forms of natural stones at the monuments is the first step for understanding the deterioration causes and mechanisms (Fitzner, 1997). The mapping of visual decay forms has also a key role in determining the methods used for the other diagnostic studies. From that point Non-Destructive Techniques (NDT) such as IR-Thermography, and Ultrasonic Velocity measurements should be used to determine the depth and degree of deterioration together with the other qualitative and quantitative scientific methods.

### 3.1.1 Main Visual Decay Forms

According to Fitzner et al. ( 1995) there are four main groups of weathering forms as it was mentioned in Chapter 1, they are 1) Loss of stone material, 2) Detachment, 3) Fissures/deformations, and 4) Discoloration and Deposits, these main classes have many subclasses to explain the weathering forms visually. The important forms of weathering for the sandstones of this study that were decided to be demonstrated are listed below:

1. Material loss as breakouts,
2. Scales and back weathering due to Loss of Scales
3. Material loss as granular disintegration
4. Alveolar weathering
5. Fissures/cracks
6. Discoloration and biological depositions,

*Breakout:* The breakouts mostly due to partial or selective losses of stone material, here the forms of breakout are characterized by material losses as large compact pieces.

*Scales and Back Weathering Due to Loss of Scales:* The term scaling describes the detachment of large stone sheets or plates following the stone structure. The scales are those sheets or plates separated from the stone.

Back weathering is characterized by uniform loss of the stone material at the surface by loss of scales. Since it was difficult to differentiate the scale formations and the back weathering on the drawings they were mapped together, as those scales would be the future backweathering areas.

*Granular disintegration:* There are three weathering forms of granular disintegration depending on the size of the detaching stone elements. a) granular disintegration into grus (mainly for granites) b) granular disintegration into sand and c) granular disintegration into powder. In Nemrut sandstones granular disintegration areas, granular disintegration into sand grains of various sizes were mapped together.

*Alveolar Weathering:* This type of weathering is frequently encountered on sandstones. It is a type of relief in the form of small cells, sacs or sockets.

*Fissures/Cracks:* Fissures were visually similar to the cracks; they were mapped independent on their dimensions.

*Discoloration and biological deposition:* All kinds of changes of stone color were grouped together with the biological colonization. Biological deposits showed themselves as the coloration on the stone surfaces such as white, grey, yellow, orange, red and green etc. coloration etc. Since most of the time it is difficult to differentiate the source of the coloration those were combined in one class.

### **3.2 Determination of Physical and Physicomechanical Properties**

Physical and physicomechanical properties of stones are dependent on the type of the stone as well as the degree and type of their weathering. Bulk density, effective porosity, pore size distribution determination by mercury porosimetry, dilatation measurements, drying rate determination at site, ultrasonic pulse velocity (UPV) measurements, quantitative IR Thermography (QIRT) and color measurements by spectrophotometer were the tests carried out on deteriorated, non-deteriorated and treated sandstone samples.

Artificial salt crystallization tests were also done in MCL Materials Conservation Laboratory) on sandstone cubes of 5cm according to RILEM (1980) test techniques to follow the progressive changes in bulk density, effective porosity, pore size distribution, ultrasonic pulse velocity (UPV) and color as the salt crystallization cycles were repeated. The graphs showing those changes during salt crystallization cycles formed some reference data for the evaluation of changes caused by deterioration as well as after the treatments.

### **3.2.1 Bulk Density and Effective Porosity**

Bulk density and effective porosity measurements were done on 40 sandstone cubes in relatively nonweathered state, 15 sandstone cubes were used for the determination of bulk density and effective porosity at each salt crystallization period of 5 cycles e.g., 5<sup>th</sup>, 10<sup>th</sup> and 15<sup>th</sup> cycles.

The samples were left in the oven at 60°C to constant weight and their dry weights were recorded ( $M_1$ , g). Then they were immersed in distilled water for 24 hours and left under vacuum for about 30 minutes in order to let water into the finest pores. Each sample was then weighed as immersed in water and its Archimedes weight was recorded ( $M_2$ , g). The sample was wiped with a dampened tissue to take away the excess water on stone surfaces, its weight was recorded again ( $M_3$ , g). Bulk density and effective porosity properties were calculated with the aid of following equations and related definitions (RILEM, 1980).

$$\text{Real volume} = M_1 - M_2 \quad (1)$$

$$\text{Real Density} = [M_1 / (M_1 - M_2)] * 100 \quad (2)$$

$$\text{Apparent Volume} = M_3 - M_2 \quad (3)$$

$$\text{Bulk Density} = [M_1 / (M_3 - M_2)] * 100 \quad (4)$$

$$\text{Effective Porosity \%} = [1 - (\text{Bulk Density} / \text{Real Density})] * 100 \quad (5)$$

$$\text{WAC \%} = [(M_3 - M_1) / M_1] * 100 \quad (6)$$

where,

*Real volume* is found by subtracting the pore space accessible to water from the apparent volume.

*Real density* is the ratio of the mass to the real volume of the sample.

*Apparent volume* is the total volume of a sample, which includes the pore space.

*Bulk (apparent) density* is the ratio of the mass to the apparent volume of the sample.

*Effective Porosity* is the empty spaces or voids in a solid mass, expressed as percent volume of the solid mass.

*Water absorption capacity (WAC)* is the maximum amount of water, which a sample can absorb under cited conditions, expressed as weight percent of the sample.

### 3.2.2 Mercury Intrusion Porosimetry

In this study the mercury intrusion porosimetry method was used to understand the pore size distribution change with the deterioration of Nemrut sandstones. The Micromeritics AutoPore IV Mercury Porosimeter System of LRMH - France was used for the experiments. The sandstone samples studied by mercury porosimeter was fine and medium grained nonweathered samples, exterior and interior surfaces of a scale sample, sandstone sample showing granular disintegration and artificially weathered samples from 10<sup>th</sup> and 18<sup>th</sup> cycles of salt crystallization test.

A typical mercury intrusion test involves placing a sample into a container, evacuating the container to remove contaminant gases and vapors (usually water) and, while still evacuated, allowing mercury to fill the container. This creates an environment consisting of a solid, non-wetting liquid (mercury), and mercury vapor. Next, pressure is increased toward ambient while the volume of mercury entering larger openings in the sample bulk is monitored. When the pressure has returned to ambient, pores of diameters down about 12 mm have been filled. The sample container is then placed in a pressure vessel for the remainder of the test. A maximum pressure of about 60000 psi (414 MPa) is typical for commercial instruments and this pressure will force mercury into pores down about 0.003 mm in diameter. The volume of mercury that intrudes into the sample due to an increase in pressure from  $P_i$  to  $P_{i+1}$  is equal to the volume of the pores in the associated size range  $r_i$  and  $r_{i+1}$  sizes being determined by substituting pressure values into Washburn equation, which is :

$$D = -4\gamma\cos\theta/P \quad (7)$$

where,

$\gamma$  : surface tension

**D** : diameter

$\theta$  : liquid-solid contact angle

*Pore volume distribution by pore size:*

Rather than pumping the system immediately to maximum pressure as in the example of obtaining total pore volume, pore size distribution analyses achieve maximum pressure by a series of small pressure steps or by controlled-rate scanning. In step mode, pressure and volume area are measured after the establishment of intrusion (or extrusion) equilibrium. The cumulative intrusion volume of mercury at each measured pressure is determined by subtracting the volume of mercury remaining in

the stem from the original volume. Applying Washburn's equation (7) to each measured pressure provides the pore size associated with each pressure, that is, the pore size distribution.

### **3.2.3 Dilatation measurements**

Thermic, hydric and hygric dilatation of fine grained and medium grained sandstones were measured. Moreover, hydric dilatation measurements for surfactant treated samples as well as consolidant treated samples were also carried out.

Experiments on dilatation kinetics during hygric, hydric and thermal cycles have gained importance on the evaluation of deterioration state and efficiency of consolidation treatments. Under atmospheric conditions, cyclic temperature and moisture variations are very important parameters in stone degradation (Mertz and Jeanette, 2004). The dilatation is one of the most important physical characteristics of the material. It is the movement of the material itself that depends on the cyclic humidity, temperature variations and water uptake. The dilatation action results in the formation of microcracks and stone degradation dependant on the type of rock (Weiss et al., 2004).

Dilatation measurements are used both for the determination of the state of decay and for the evaluation of the conservation treatments (Felix, 1995; Mertz and Jeanette, 2004; Jimenez-Gonzalez et al., 2008). The measurements of dilatometric changes are done by recording the dilatation of the material during the cyclic changes of wetting, temperature and humidity as a function of time. It is also called "dilatation kinetics follow up" that give an overall idea about the material behaviour during those cycles of humidity and temperature variations and water uptake conditions (Mertz and Jeanette, 2004).

In this study, the linear expansion or free swelling strain ( $\xi_s$ ) is determined with inductive Linear-Variable Differential Transformer (LVDT) displacement captors. The range of measurement is  $\pm 10\text{m}^{-3}$  delivered by a 0,20mA electric signal. Captors are protected against water splash (IP65). The spring-load of the contact sensor is 2N. The captor accuracy is equal to 0.1 or 0.25% of the total measurement scale and the resolution values are 0.12 and 0.20  $\mu\text{m}$  according to captor type. Equipment is calibrated with a steel gauge block of nominal length 100 $\mu\text{m}$ .

Typical sample sizes were 50x10x10mm for the dilatation measurements. The expansion was measured in perpendicular direction to the bedding, first the sample was placed in a glass container then the captor LVDT (Linear Variable Differential Transformer) was placed on top of the sample, then the data was started to be collected, distilled water was poured into the glass container until it reached near the upper surface of the sample. As the sample got wet, it started swelling. The dilatation was measured by the LVDT until a plateau was reached. To calculate the linear free swelling strain, difference between the initial value and the plateau value was used.

### **3.2.4 Drying Rate Measurements at Site**

In order to understand the drying behaviour of the sandstones at the site; the sandstone cubes of 5cm size were weighed and soaked in distilled water for a day. They were then taken out and wiped with a tissue paper to take away the excess amount of water. The weight losses of the sandstone cubes by drying during six hours of exposure to atmospheric conditions were recorded. The graphs showing the decrease in weight versus time was obtained. During those measurements relative humidity, temperature and wind speed were also recorded.

### 3.2.5 Ultrasonic Velocity Measurements

Ultrasonic velocity of stone is dependent on bulk density and porosity of the substrate describing the general condition of the stone (Simon, 2001). The correlation between ultrasonic velocity/strength and degree of weathering has been found for marble and limestone (Caner-Saltik et al., 2001; Simon, 2001) and for other stone types as well. Ultrasonic velocity measurements are of use to follow the changes of the stone material in time non-destructively (Simon, 2001; Caner-Saltik et al., 2001, Bidner et al. 2001; Caner-Saltik et al., 2005; Calcaterra et al., 2004; Grinzato et al., 2004). Although ultrasonic velocity decreases by deterioration, it should be kept in mind that the interpretation of the ultrasonic velocity data is not always straightforward (Price, 1996). It is affected by water content, anisotropy etc. of the sample (Kandemir, 2010).

All ultrasonic velocity measurements both in the laboratory and at the site were done by using PUNDIT Plus test equipment with its transmitter and a receiver probes of 220 kHz.

The method basically depends on the calculations of velocity while passing through the specimen and uses the time required for the ultrasonic waves to traverse the minimum cross section of the test specimen. While generating the ultrasonic pulses PUNDIT plus measures the time elapsed between the generation and reception of the waves between the transmitter and receiver. The velocity of the waves is calculated by using the formula,

$$V = l / t \quad (8)$$

Where,

**V:** Velocity

**l:** the distance traversed by the wave (m)

**t:** travel time (s)

The speed of the sonic wave propagation,  $V$ , is expressed in meters per second, and the excitation frequency ( $f$ ) is in hertz. The wavelength ( $\lambda$ ) is the least distance in the propagation medium between identical particle displacements, and is given by  $\lambda = V / f$  (Bray and McBride, 1992, Kandemir, 2010). Thickness of the sample material, which the ultrasonic wave travels, should be greater than those  $\lambda$  values.

Ultrasonic measurements can be performed in direct, semidirect and indirect transmission modes. In direct mode, transmitter and receiver are placed at the opposite surfaces of the tested element. In the semidirect method, transducers are located at 90° angle, and in the indirect mode transmitter and receiver are arranged on the same surface of tested element.

There are laboratory studies investigating the relationship between direct and indirect P-wave velocity measurements (Kahraman, 2002; Kandemir, 2010). Although it is not always practical; the direct measurements seem to be the ideal way of measurements. Meola et al., (2005) indicated that indirect velocity measurement was the least sensitive arrangement for velocity calculations. In fact, the indirect velocity values were lower than the direct velocity values. Kahraman (2002) investigated that the indirect velocity values of rock samples were 0.57 times lower than that of direct velocity values.

In this study, UPV measurements were taken in the laboratory both in direct and indirect transmission modes in order to get a relationship between them. The changes in UPV values of saturated state and dry state were also noted, as well as, the changes of UPV values during drying of sandstones starting from saturated state. Furthermore, changes in UPV values with the progress of salt crystallization cycles were also followed.

At the site, UPV measurements could only be taken at indirect transmission mode. The relationships between the types and degree of deterioration at the site, the changes in UPV values due to moisture content of the sandstones were figured out by comparing the reference data collected in laboratory.

### **3.2.6 Infrared Thermography Analyses**

IR images of the materials are formed by the radiance emitted from its surface during the heating and cooling periods. They reflect thermal properties of the material affected by its physical and physicommechanical properties, its water content, etc.

In situ, Infra Red Thermography (IRT) imaging of the sandstones were done for the evaluation of their state of weathering as well as for the evaluation of the efficiency of the consolidation treatments. All the images were taken with the FLIR SC640 infrared thermography camera. The quantitative infrared thermography (QIRT) analyses of single and differential images were done by using the software provided by FLIR.

The human naked eye can only detect visible light waves or visible radiation of the electromagnetic spectrum (0.39-0.77  $\mu\text{m}$ ). The infrared radiation is not visible. It falls between the wavelengths of 2-15  $\mu\text{m}$  that is between the visible and microwave parts of the electromagnetic spectrum. Near IR waves (0.7-25  $\mu\text{m}$ ) are close to the visible light, far IR waves (25-1000 $\mu\text{m}$ ) are closer to microwave region (Kandemir, 2010). Infrared thermography (IRT) technique turns the emission pattern of an object into a visible image (Ocana, 2004). All objects radiate energy that is transported in the form of electromagnetic waves. Thermographic cameras measure the infrared radiation emitted by an object. Infact they do not measure the temperature but radiation of materials (Ocana, 2004). However it is possible to get the temperature. The quantity of energy leaving a heated surface given by

$$q = \sigma \varepsilon T^4 \quad (9)$$

where,

**q**: the radiated energy per unit area ( $\text{W/m}^2$ )

**$\sigma$** : the Stefan-Boltzman constant ( $5.67051 \times 10^{-8} \text{ W/m}^2 \text{ K}$ )

**$\varepsilon$** : emissivity of the surface ( $0 < \varepsilon < 1$ )

**T**: absolute temperature (K).

### 3.2.7 Color Measurements

Color measurements were done on relatively fresh and deteriorated samples at the site, artificially deteriorated sandstone samples by salt crystallization in order to see how the color changed with the state of deterioration, as well as before and after consolidation treatments to see their role in color change.

Color measurements were done by using a spectrophotometer KonicaMinolta 2600Cmd and according to the CIELAB coordinates. The spectral reflectance curves of each measurement allow the determination of three parameters in the LAB system (the three axis  $L^*$ ,  $a^*$  and  $b^*$ ), as proposed by CIE (ASTM E 308, 1993). It is also possible to compute color differences after the treatments ( $\Delta L^*$ ,  $\Delta a^*$ ,  $\Delta b^*$  and  $\Delta E$ ,  $\Delta C$ ), by using the initial color average of the untreated sample as reference and using color difference equations according to CIE (ASTM D2244, 1993) (Costa and Delgado Rodrigues, 1996).

In monitoring studies of the treatments, color changes due to treatment products or ageing processes can be computed as mean values. Total color differences or relevant color coordinates before and after treatments may evidence the changes promoted

by different products. Only a slight color change ( $\Delta E \leq 5$ ), and no darkening or gloss is required for a good consolidant (Sasse and Snethlage, 1997; Garcia-Talegon et al., 1997). The variations in color observed in treated/deteriorated stones can also be taken as a parameter showing the ageing or decay in time.

### **3.2.8 Artificial Salt Crystallization Tests**

To follow the changes in physical and physicochemical properties of sandstones the artificial weathering of sandstones were done by cyclic salt crystallization tests with  $\text{Na}_2\text{SO}_4 \cdot 10\text{H}_2\text{O}$  (14%) solution according to RILEM (1980). In this procedure the sandstones samples from the quarry nearby the Nemrut Mount Monument were cut into 5 cm cubes and those cubes were soaked into salt solution for 4 hours and dried at 60°C for at least 16 hours.

The changes in bulk density, effective porosity, UPV and color were followed during those cyclic salt crystallization tests.

### **3.3 Determination of Micro-Structural Properties**

The changes in microstructural properties of sandstones due to weathering were studied by following the changes in mineralogical and petrographical characteristics through examining thin sections under optic microscope, XRD analyses, SEM-EDS analyses and cation exchange capacity (CEC) measurements of sandstones and clay minerals.

### **3.3.1 Thin Section Analyses by Optical Microscopy**

The thin sections for the mineralogical and petrographical analyses of the samples were prepared in MTA (Maden Tetkik Arama Arama Genel Müdürlüğü – General Directorate of Mineral Research and Exploration) laboratories. Those thin sections were then examined using polarizing microscope Leica DMEP 4500 in MCL. Image Analyses of those sections were done by using the LAS (Leica Application Suit) software to determine the mean grain sizes and sorting characteristics and grain size distribution in sandstones.

### **3.3.2 X-Ray Diffraction (XRD) Analyses**

X-Ray diffraction (XRD) analyses were carried out on powdered samples to determine the mineralogical composition of the samples from deteriorated areas and relatively interiors of the sandstone. Clay minerals and iron oxides extracted from the sandstone were also studied by XRD. A Bruker D8 Advanced X-Ray diffractometer emitting  $\text{CuK}\alpha$  radiation in MCL was used for the analyses. The instrument was adjusted to 40 kV and 40 mA and traces were taken for  $2\theta$  values. Goebel mirror accessory of the system made possible to take XRD traces of the small samples non-destructively when their examination were then followed by SEM analyses.

*Sample Preparation for XRD Analyses:* The powdered stone samples were prepared by crushing and grinding them to powder size in an agate mortar. They were dried at 60°C for a night to get rid of the non-compositional water. Then the powdered samples were placed onto the sample holder of the Bruker D8 Advanced X Ray diffractometer to get their XRD traces.

*Extraction of Clay Mineral:* Due to the low percentage of clay minerals in sandstones, it was necessary to extract them from the sandstone body with a suitable extraction method to be identified by XRD. The stages of extraction of clay minerals are explained below.

*Crushing and grinding of sandstone samples:* Samples should be dry crushed and grinded until obtaining a coarse powder of the stone. The crushing and grinding should be done by hand using an agate mortar in order not to break up the existing fragments of any mineral including clays.

*Decarbonation treatment:* It was necessary to clear off the carbonates from the sandstone samples. 20g of powdered sample was mixed in 50 cm<sup>3</sup> distilled water with the help of a magnetic stirrer, concentrated HCl was added drop by drop while stirring continuously for not to increase the local concentration too much. It was continued until the natural pH was obtained, then the suspension was poured in a container for mixing.

*Placing the solution:* The powdered and decarbonised solution was *stirred* at 2000rpm of a magnetic stirrer for 2 to 5 minutes, the top part of the solution with clayey particles was collected and put into centrifuge containers together with distilled water.

*Washing:* If they are free from salts and other chemicals the clay minerals flocculate in water. Therefore, it was necessary to wash the solution with clay particles till obtaining a stable suspension. The solution was accepted as stable if the sedimentation of the clayey particles was not completed after 12 hours or they stayed suspended at 3000 rpm of centrifuge for 10 minutes. In order to obtain the solution containing clay particles the washing had to be done in the following two consequent steps:

Decanting by centrifugation: Centrifugation of the clayey particles were started by 2000 rpm for during 5 minutes. To achieve that, the centrifugation speed could be up to 2500rpm for 8 minutes.

Agitation in distilled water: The water was carefully poured in the containers to get only the residue. Then water was added up to 2/3 of containers and the solutions were mixed in the containers with the help of a magnetic stirrer for 2 minutes. The steps from decanting by centrifugation and agitation in distilled water were repeated till obtaining a stable suspension. Stable suspensions were collected and finally clay minerals were precipitated at 3500 rpm of centrifuge for the duration of 40 minutes.

*Final Extraction of Clay Fraction:* Sedimentation time of the particles in the solution could be calculated according to the Stocke's Law:

$$v = [(2a^2(dp-dl)g) / 9n] \quad (10)$$

where,

v: velocity of the sedimentation (cm/s)

a: radius of the particles

dp: density of the particle (which is 2.6 for clays)

dl: density of the liquid (which is 1 for water)

g: mass acceleration

n: viscosity of the liquid (0.01 for water at 20°C)

Thus the time 't' to descend 1cm for a particle having a diameter d was calculated as

$$t(mn) = 190/d^2 \text{ with } d(\mu m) \quad (11)$$

Consequently, the clay minerals in suspension in water are put in a beaker, the solution was left for 100 minutes and the top 2.5cm part of the solution which contained the clay particles was taken with the help of a pipette.

*Preparation of Oriented Samples of Clay Minerals for XRD Examination:* Oriented samples were used for the identification of clay minerals to enhance their basal or *00l* reflections (Moore and Reynolds, 1997).

Traditionally the solution containing clay minerals is placed on the glass slide and left to dry calmly. In this study, the solution with clay particles was put into the ultrasonic bath for 1h15mn, it was filtered with the help of a Millipore paper, transferred onto a glass slide and left to dry to obtain an oriented sample.

*XRD Patterns obtained after further treatments:* Oriented samples permit the qualitative identification of most of the clay minerals. However, further treatments as heating at 490°C for 4 hours and exposure to ethylene glycol atmosphere are necessary to make precise identification of clay minerals by XRD.

Heating at 490°C for 4 hours: Heating treatment leads to the dehydrolyxation of kaolinite and as a result the major peak of kaolinite disappears. Heating also has an effect on chlorites, vermiculites and smectites that can be followed by XRD (Table 3.1).

Ethylene Glycol Treatment: Leaving the glass slide in an ethylene-glycol atmosphere for a night cause swelling of smectites and in some types of vermiculites. It also affects the some types of chlorites (Table 3.1).

**Table 3.1** The changes in basal reflections of clays by treatments.

<b>Clay / Treatment</b>	<b>Air Drying (A°)</b>	<b>Heating (A°)</b>	<b>Ethylene Glycol Treatment (A°)</b>
<b>Kaolinite</b>	7	Peak disappears	7
<b>Halloysite</b>	9.5-10	Peak disappears	9.5-10
<b>Chlorite (Mg)</b>	14	14	14
<b>Chlorite (Fe)</b>	7(14)	14 (7)	7(14)
<b>Illite</b>	10	10	10
<b>Vermiculite (Ca, Mg)</b>	14	10	14
<b>Smectite</b>	12-15	10	16-17

### **3.3.3 Cation Exchange Capacity (CEC) Measurements**

In this study, powdered samples of deteriorated and non-deteriorated sandstone samples were analyzed for their CEC to make a quantitative estimation of the clay mineral content in those samples. Determination of CEC of clay minerals was also investigated in the accumulated soil between two scales of sandstone that started to be detached (Shooneydt and Heughebaert, 1992; Potgieter and Strydom, 1999; Ramasamy et al., 2008).

The method investigates the adsorption of the MB by the sample being put into the MB solution of known concentration (Shooneydt and Heughebaert, 1992; Topal, 1996; Potgieter and Strydom, 1999; Ramasamy and Anandalakshmi, 2008).

At 630 nm, the maximum absorbance of methylene blue was obtained (Potgiere and Strydom, 1999). A calibration curve of absorbance against concentration of methylene blue was obtained in studies of Ramasamy and Anandalakshmi (2008), Potgieter and Strydom (1999); which indicate that the Beer-Lambert law was obeyed up to a concentration of 20 mg/L. The Beer-Lambert law explains a linear relationship between the absorbance measured at a constant wavelength and the concentration of a solution (Potgieter and Strydom, 1999). Beyond the concentration of 20mg/L, a deviation from the linear relationship between concentration and absorbance of methylene blue solution was observed (Potgieter and Strydom, 1999; Ramasamy and Anandalakshmi, 2008).

In this study, maximum absorption of MB was at 632nm. A standard curve was drawn to show the relationship between the concentration of MB solution and its absorption at 632nm. To determine the clay mineral content of deteriorated and non-deteriorated sandstone samples, the powdered samples were magnetically stirred for 2h with 150mL of a methylene blue solution of 20 mg/L. Then the solutions were centrifuged for 5 min and the absorbance at 632 nm was measured on an OPTIMA SP-3000 Plus UV–vis spectrometer in MCL. The CEC of soil accumulated between the two scales was also determined with the same procedure, expressing the CEC as meq/100g of sample.

### **3.3.4 Scanning Electron Microscopy (SEM) Coupled with Energy Dispersive X-Ray (EDX) Analyzer**

In this study SEM images were taken by JEOL/EO JSM 5610 model Scanning Electron Microscope and the elemental analyses were done by using an OXFORD Energy dispersive X-Ray analyzer in LRMH. The deteriorated sandstone samples of about half centimetres size coated with gold, no further sample preparation was done.

### **3.4 Application of Surfactants**

The surfactants that are used in study are *diaminoethanedihydrochloride* or *ethylenediaminedihydrochloride*, *hexadecylmethylamonium (HDTMA)* and *tetraethylenediammoniumdichloride* (Antihygro). Very dilute solutions of those surfactants were prepared for the treatments in accordance with the amount of clay minerals present in the sandstones' composition. The dilution was done according to an average value of the cation exchange capacity for halloysite and chlorite. It was approximated as 40meq for 100g clay. Thus the surfactant was diluted to  $0.8 \times 10^{-3}$  mol/L for the treatment of 100 g sandstone. In the laboratory the sandstone samples were soaked in that surfactant solution. That treatment was repeated at least five times for *ethylenediaminedihydrochloride* and *tetraethylenediammoniumdichloride* to reach the necessary surfactant amount in the stone. The sandstone treated with *HDTMA* was soaked in the surfactant solution only once, since the HDTMA was reported having water blocking capacity when it was used in increasing amounts (Xi et al., 2010, Bildiren et al., 2009). After the treatments with the surfactants samples were dried. The hydric dilatation measurements were done during wetting of the treated sandstones.

### **3.5 Application of Consolidants**

In this study, Syton X30, Funcosil KSE500STE, KSE100 and KSE300 were used as the consolidation agents. SytonX30 was a suspension of nano-silica having average particle size of 30nm in water. Funcosil KSE500STE was elastified silicic acid ester with an average particle size of 350nm and the amount of gelation was about 70%. KSE100 was also a silicic acid with an ethylester base and described as tetraethyl silicate hydrolyzate in organic solvent being ethylalcohol. It had low gel deposit rate of about 10%, and active ingredient component was approximately 20% by mass. KSE300 was another silicic acid ethylester described as silicic acid ethylic ester; it had 30% gel deposit rate and approximately 99% of active ingredient by mass.

Diluted solution of Funcosil KSE500STE (10% by weight) in alcohol; diluted solution of SytonX30 (5% by weight) in water were used for the consolidation treatments of Nemrut sandstones. In the field, the consolidants were applied drop by drop on their surfaces. In the laboratory the consolidants were applied on trial samples by soaking the stones in the solution. KSE100 and KSE300 were used without any dilution by soaking the sandstones in their solutions in the laboratory.

## CHAPTER 4

### EXPERIMENTAL RESULTS

Diagnostic studies of sandstone deterioration, selection of treatments targeted to the control of deterioration mechanisms and the studies on the effectiveness of those conservation treatments were carried out by using some non-destructive analyses performed at the site and several analytical techniques as well as non-destructive analyses performed in the laboratory. Those experimental results are presented below under the general titles of “Mapping of Visual Weathering Forms”, “Determination of Physical and Physicomechanical Properties”, “Determination of Microstructural Properties”. Experimental results cover the analyses of deteriorated samples, relatively non-deteriorated samples as well as treated samples with surfactants and consolidants.

#### 4.1 Mapping of Visual Weathering Forms

The site of Nemrut Mount Monument possesses the weathering forms mainly as separation by layering especially along the bedding planes, back weathering due to loss of scales, cracking, granular disintegration, rounding/notching and discoloration/biological deposition (Figure 4.1, 4.2). The most important weathering forms of Nemrut Sandstones are material loss due to i) loss of scales and ii) granular disintegration (Figure 4.1, 4.2).

Two mapping examples representing weathering forms of the site, being a stele (DTKM058) and the Lion statue (DTKM066) at the East Terrace are given here.

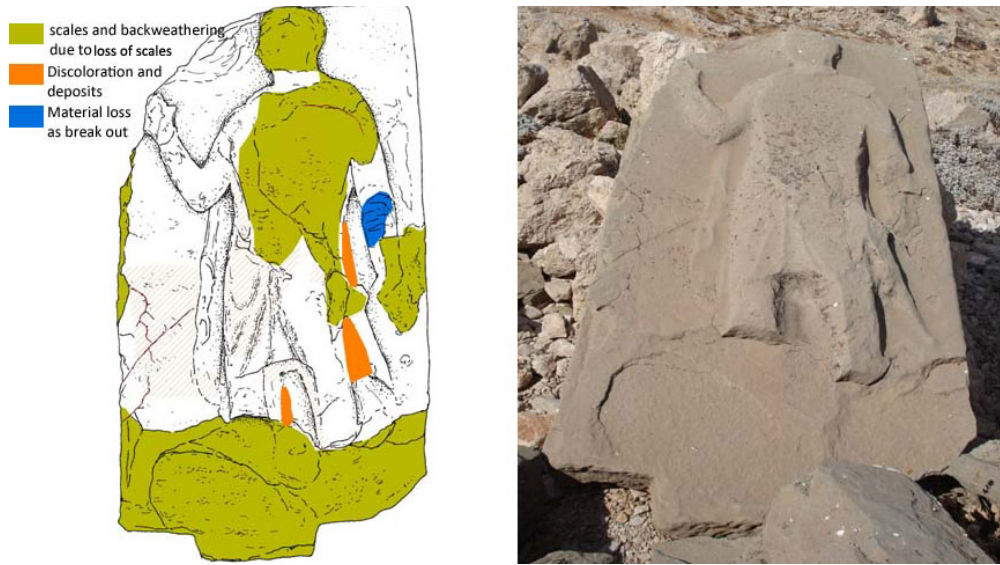


**Figure 4.1** Mapping of visual weathering forms of a relief (DTKM058) in the East Terrace (CNCDP, Final Report, 2011) (left) and its photo (right).

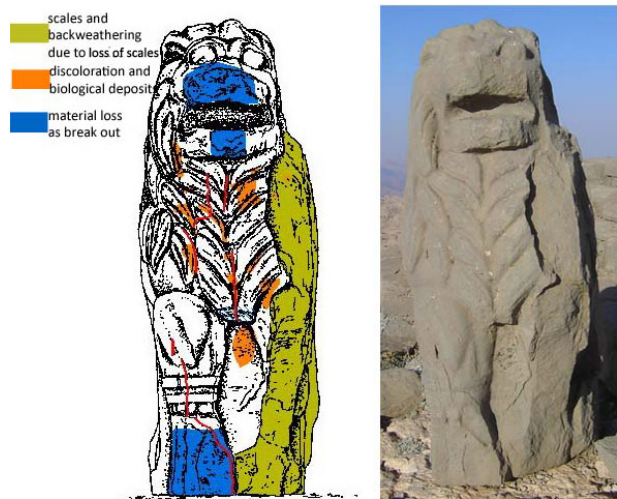


**Figure 4.2** Mapping of visual weathering forms of West face of Lion Statue (DTKM066) at East Terrace (CNCDP Final Report, 2011) (left) and its photo (right)

*Previous Treatments:* At Nemrut Mount Monument some wrong interventions were done by the previous teams. Among those harmful interventions repairs with cement mortars and epoxy resins could be observed at the site, moreover, some consolidation interventions with polyvinyl acetate were also reported by Sanders (1996). Sanders (1996) reported that polyvinyl acetate (PVA) solutions in acetone were used on the animal statues around the altar and on some fragile sandstone pieces either by spraying or using brushes. Such a previous application was detected in this study in some breakout surfaces of lion horoscope in the temporary laboratory at the site. By using a UV lamp in the dark, the old PVA applications got florescent and became visible to the naked eye (Simon, 2011); and could be photographed (Figure 4.3)



**Figure 4.3** The old PVA applications got florescent and became visible under UV light

## **4.2 Physical and Physicomechanical Characteristics**

Analyses of physical and physicomechanical properties of sandstones were evaluated after the mapping studies. Sampling of deteriorated sandstones from the Nemrut Mount Monument site next to the sandstone steles and relatively non-deteriorated samples from the sandstone quarry were done. The sandstones from quarry were cut into 5cm cubes and subjected to salt crystallization tests to produce reference data on gradual change of UPV, bulk density, effective porosity. Comparison of those results with the deteriorated samples was done. Those results are given below.

### **4.2.1 Results of UPV Measurements**

Direct UPV measurements were done on the sandstone cubes of 5cm size before they were subjected to salt crystallization cycles and after each 5th cycle during the progress

of salt crystallization tests. 5 successive direct UPV measurements were taken from 5 points on each three surfaces facing each other, resulting in 25 UPV measurements for each direction being a, b, c and they did not refer to any particular direction since it was difficult to detect the bedding directions of the sandstone cubes. Thus different directions were not named as x, y, z in order to avoid any miscomprehension (Figure 4.4; Table ).

The direct UPV measurements showed that there were directional differences in the sandstone cubes. Generally one of the UPV values of three directions was smaller than the two others which indicated the bedding direction of the sandstones. The very

different value for Sample 19 in c - direction ( $707\pm 50$  m/s) was due to a very large crack from one side to the other side of the sample (Figure 4.3).

The change in the UPV values were followed for the sandstone cubes at different salt crystallization cycles being after 5<sup>th</sup>, 10<sup>th</sup> and 15<sup>th</sup> cycles (Figures 4.5 - 4.7). Although UPV values decreased, there was no consistent decrease in average UPV values during the progress of salt crystallization, most probably due to heterogenous nature of the sandstones (mixed grain sizes, poor sorting of grains etc.). On the other hand, a systematic decrease in UPV was observed at each cube during the progress of salt crystallization e.g. for the cube having high UPV, a:3689m/s, b:3578 m/s, c:3478 m/s; UPV values drop to a':3048, b':2769, c':2757 at 15th cycle, for another cube having UPV values a:2255, b:2323, c:1966; at 15th cycle UPV values drop to a': 1442, b':1429, c':1312 (Figure 4.4, Figure 4.7; Table 4.1)

The assessment of differences between the indirect and direct UPV measurements was also done. It was seen that indirect measurements were lower than the direct measurements on the sandstone cubes. When the samples were saturated with water both direct and indirect measurements were further decreased e.g, in fresh sandstone cube, while  $UPV_{DIRECT} = 3581$ m/s;  $UPV_{INDIRECT} = 2347$ m/s were measured in dry state (33% RH); while  $UPV_{DIRECT} = 3675$ m/s; and  $UPV_{INDIRECT} = 2220$ m/s were measured in saturated state. For the deteriorated sandstone cubes at 20th cycle of salt crystallization,  $UPV_{DIRECT} = 2800$ m/s;  $UPV_{INDIRECT} = 1530$  were measured in dry state (at 33% RH),  $UPV_{DIRECT} = 1500$ m/s and  $UPV_{INDIRECT} = 463$ m/s were measured in saturated state. For fresh sandstones there was no considerable decrease neither in direct nor in indirect UPV values by saturation with water. On the other hand, for deteriorated sandstones there was a decrease both in direct and indirect UPV values by saturation with water (Figures 4.8 – 4.11; Tables 4.2 – 4.4 ).

The in-situ UPV measurements were done for sandstones at different degrees of deterioration and these were compared to the ones taken in the laboratory (Figure 4.12-4.15). The sandstones with granular disintegration had UPV values generally below 1000 m/s indicating lower physicommechanical properties (Figure 4.11, 4.12). The detaching scales themselves had  $UPV_{INDIRECT}$  values between 1000-2500 m/s indicating sufficient physicommechanical properties (Figure 4.15, 4.18).

The UPV values of the sandstone cubes before and after treatments with Syton X30, Funcosil KSE500STE, KSE300 and KSE100 in laboratory and the sandstone blocks at the site before and after treatment were measured and evaluated together for the assessment of the treatments success (Figures 4.16, 4.17; Tables 4.5, 4.6). After the treatment with Syton X30 and Funcosil KSE500STE a slight increase in UPV values of sandstones was noticed (Figure 4.16, Table 4.5). After the treatment with KSE300 and KSE100 a slight increase in UPV was more noticeable parallel to the bedding plane (Figure 4.17; Table 4.6).

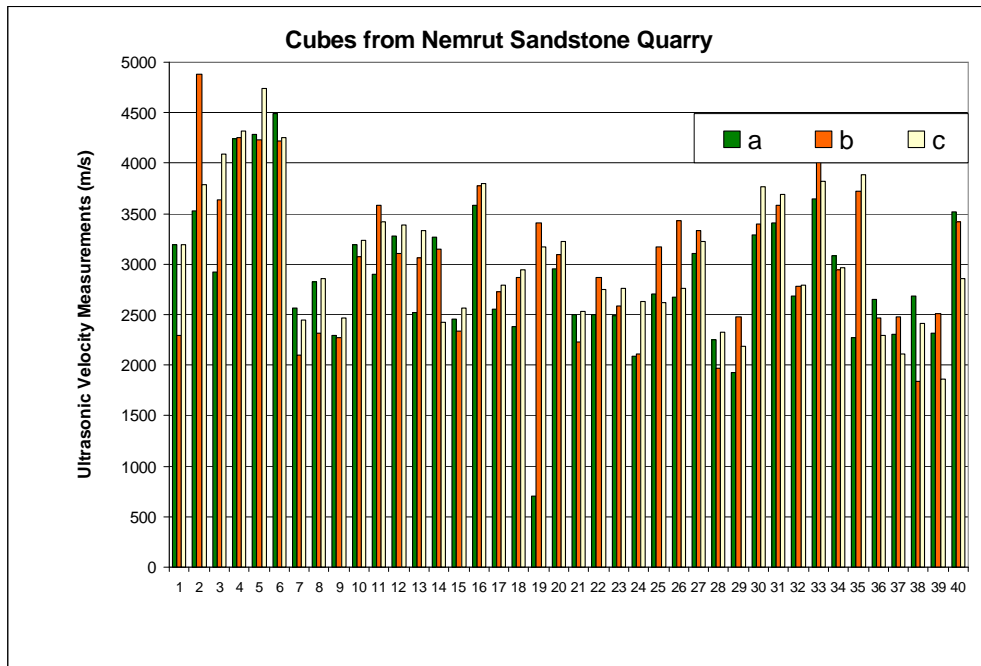


**Figure 4.4** UPV<sub>(a,b,c)</sub> values for each sandstone cube before salt crystallization tests.

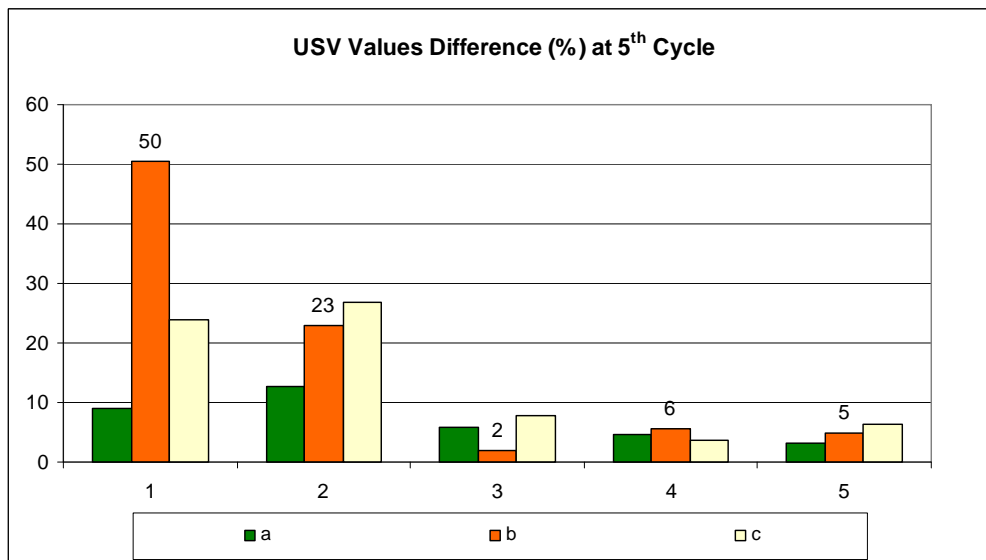


**Figure 4.5** Percentage change in the UPV<sub>(a,b,c)</sub> values for each sandstone cube after 5<sup>th</sup> cycle of salt crystallization in comparison to their fresh state.

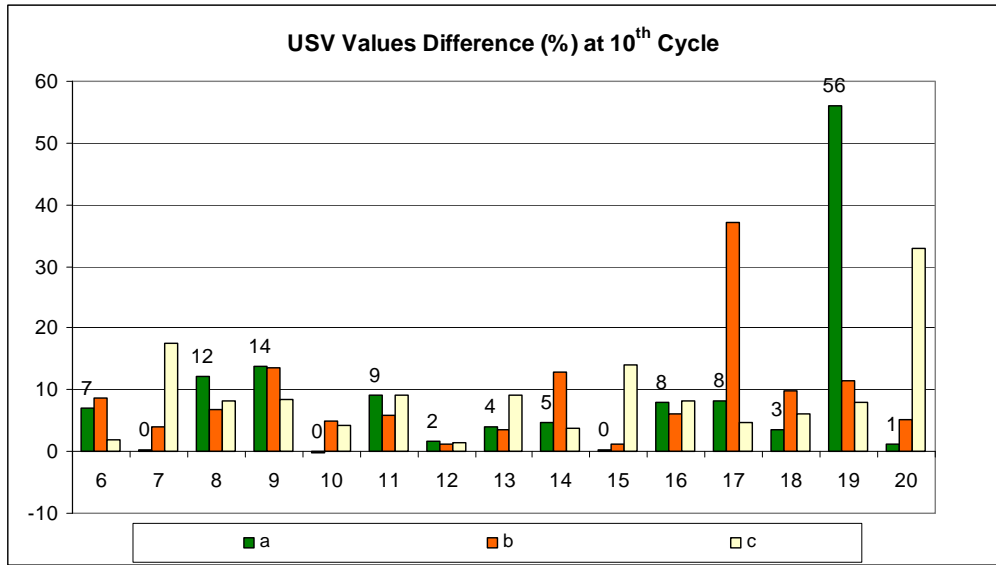


**Figure 4.6** Percentage change in the  $UPV_{(a,b,c)}$  values for each sandstone cube after 10th cycle of salt crystallization in comparison to their fresh state.

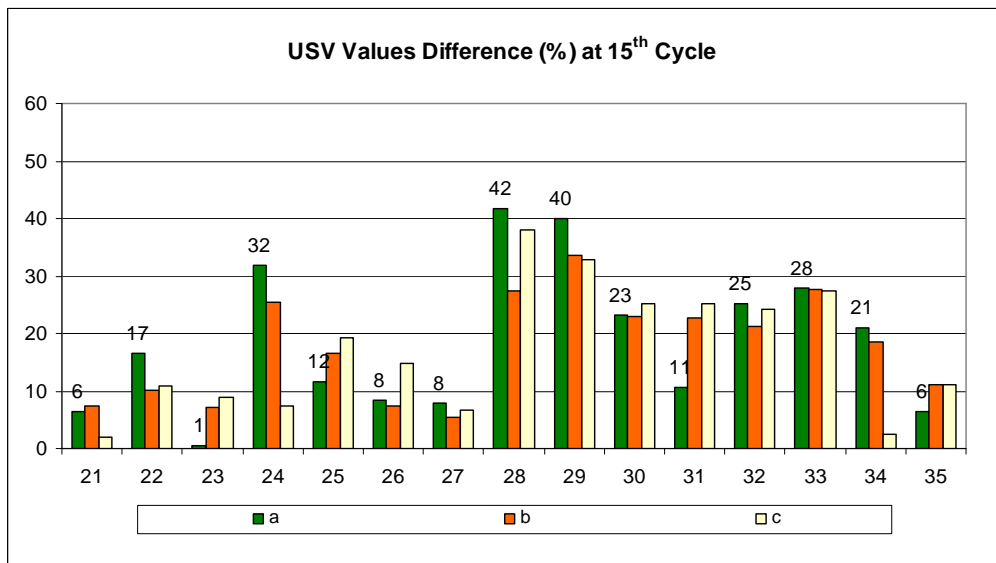


**Figure 4.7** Percentage change in the  $UPV_{(a,b,c)}$  values for each sandstone cube after 15th cycle of salt crystallization in comparison to their fresh state.

**Table 4.1** Average UPV values of sandstone cubes at different salt crystallization cycles.

Average UPV (m/s) values of sandstone cubes at different salt crystallization cycles.				
Sample No.	0 <sup>th</sup> cycle	5 <sup>th</sup> cycle	10 <sup>th</sup> cycle	15 <sup>th</sup> cycle
1-5	3839±222	3648±254		-----
6-20	2965±150	-----	2877±36	-----
21-35	2889±58	-----	-----	2543±19
1-40	2990±22	-----	-----	-----

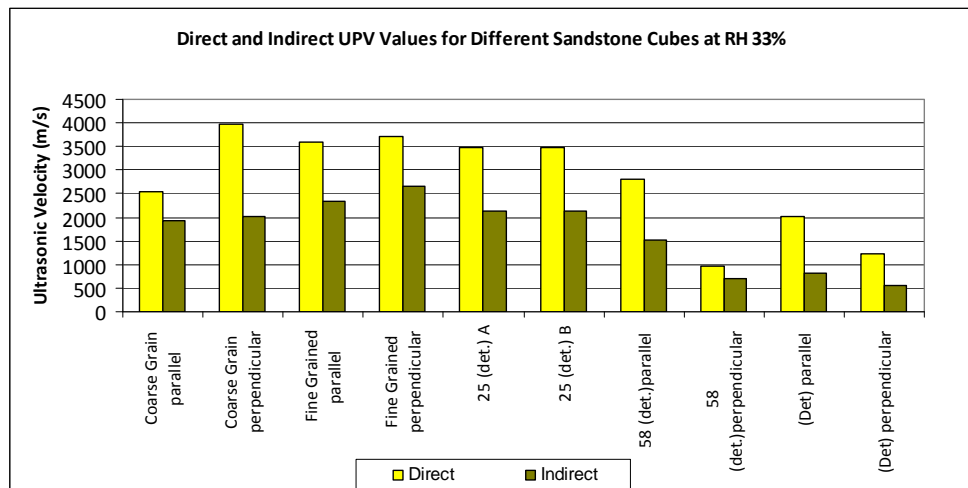


**Figure 4.8** Indirect and direct UPV values of undeteriorated and deteriorated sandstone cubes taken parallel and perpendicular to bedding planes at dry state (33% RH).

**Table 4.2** Indirect and direct UPV values of undeteriorated and deteriorated sandstone cubes taken parallel and perpendicular to bedding planes at dry state (33% RH).

33 % RH		
UPV Measurement	Direct	Indirect
Coarse Grain parallel	2534	1929
Coarse Grain perpendicular	3971	2019
Fine Grained parallel	3581	2347
Fine Grained perpendicular	3716	2647
25 (det.) A	3484	2121
25 (det.) B	3474	2130
58 (det.)parallel	2802	1530
58 (det.)perpendicular	979	697
(Det) parallel	2005	825
(Det) perpendicular	1221	545

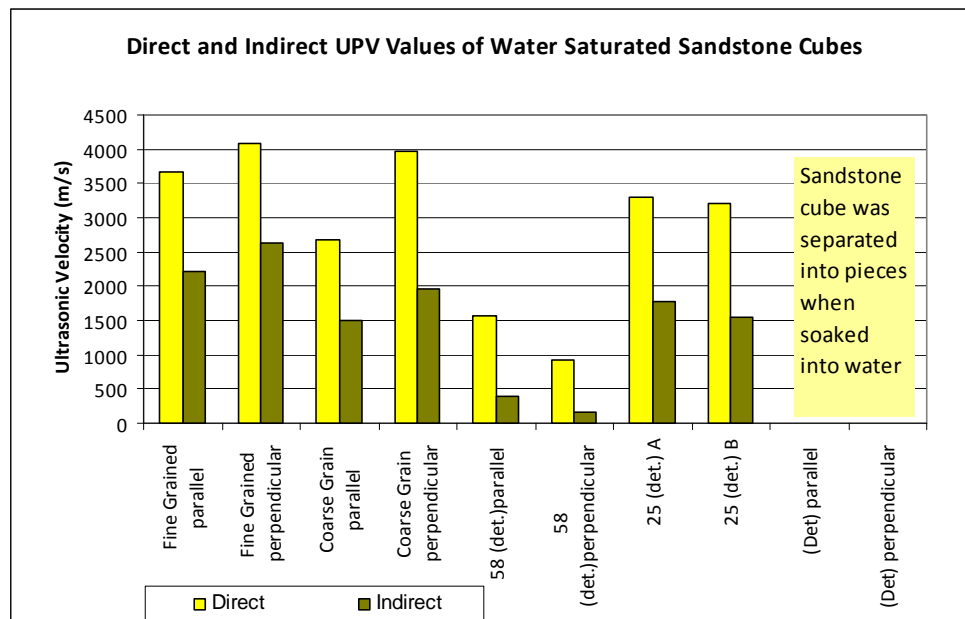


**Figure 4.9** Indirect and direct UPV values of water saturated undeteriorated and deteriorated sandstone cubes taken parallel and perpendicular to bedding planes.

**Table 4.3** Indirect and direct UPV values of water saturated undeteriorated and deteriorated sandstone cubes taken parallel and perpendicular to bedding planes.

Water Saturated		
UPV Measurement	Direct	Indirect
Fine Grained parallel	3675	2220
Fine Grained perpendicular	4085	2626
Coarse Grain parallel	2668	1509
Coarse Grain perpendicular	3968	1956
58 (det.)parallel	1572	403
58 (det.)perpendicular	922	171
25 (det.) A	3306	1780
25 (det.) B	3200	1552
Deteriorated sample	Sample separated into pieces when soaked into water	

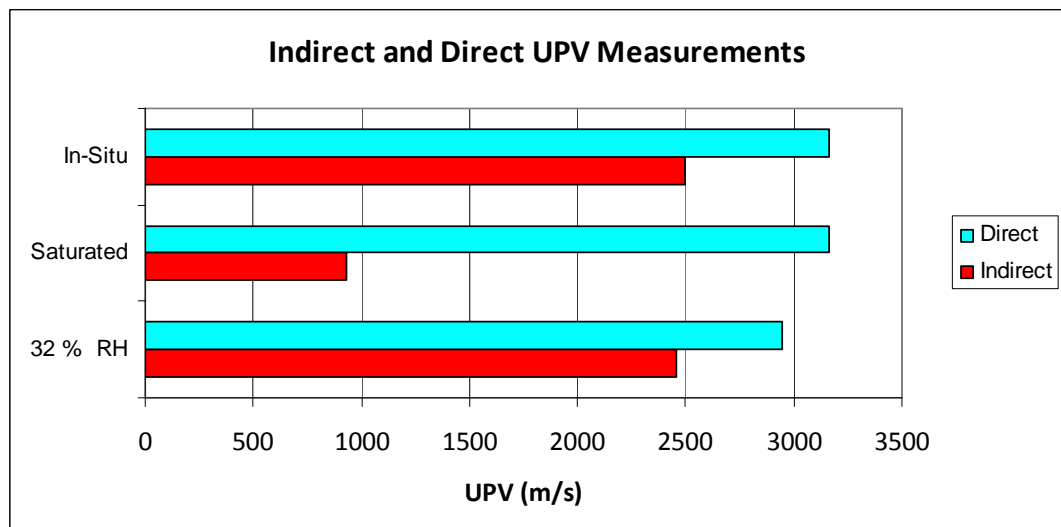


**Figure 4.10** Indirect and direct UPV values of a sandstone sample taken from the site (Figure 4.11) in situ, dry and water saturated states.

**Table 4.4** Indirect and direct UPV values of a sandstone sample taken from the site (Figure 4.11) in situ, dry and water saturated states.

Measurement	32 % RH	Saturated	In-Situ
Indirect	2458	933	2499
Direct	2950	3161	3160

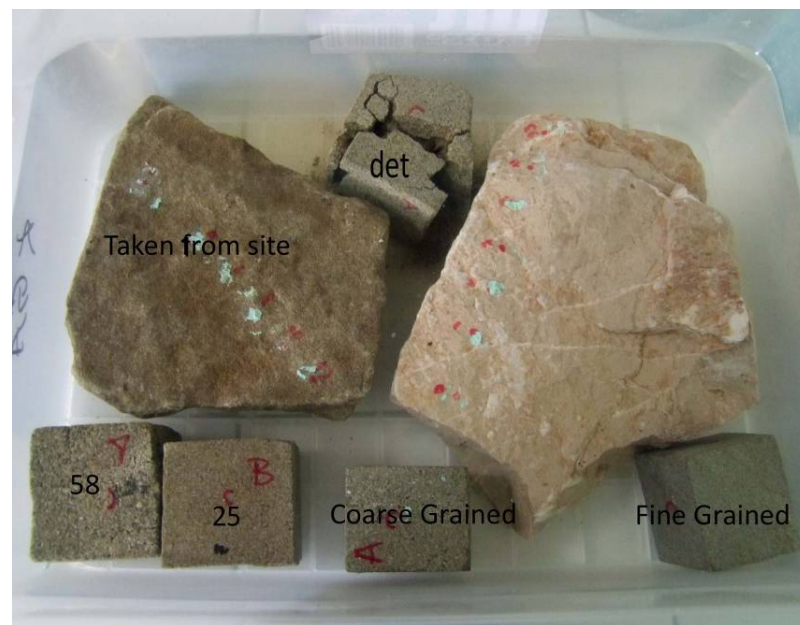


**Figure 4.11** Sandstone cubes that were soaked into water.

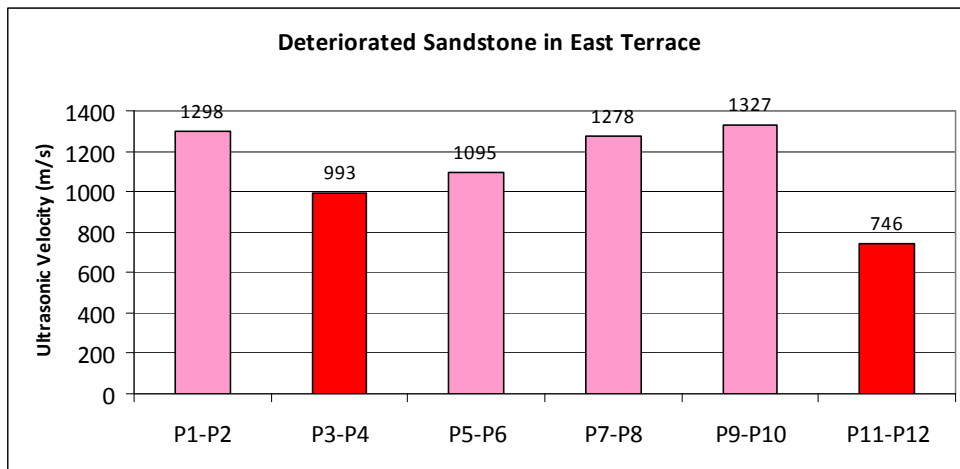


**Figure 4.12** Indirect UPV measurement taken from different points of a deteriorated sandstone block (above) in East Terrace, and graphic representation of the UPV values for each point pairs, red: very deteriorated parts, pink: deteriorated parts.

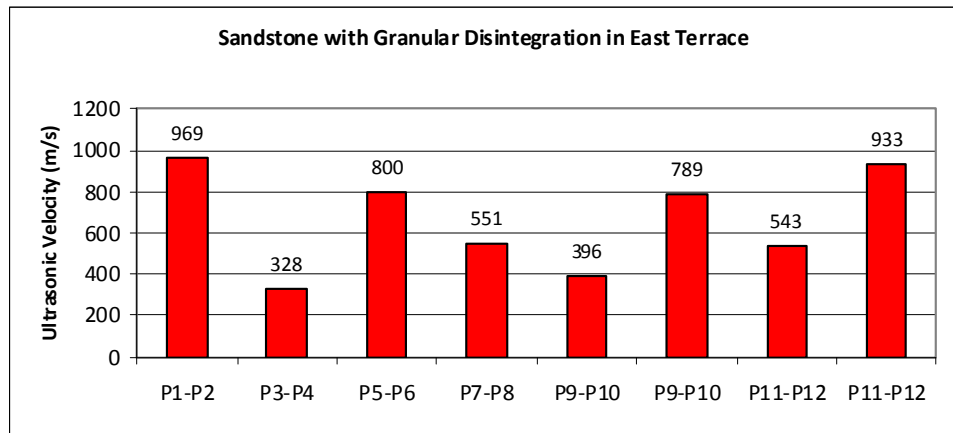
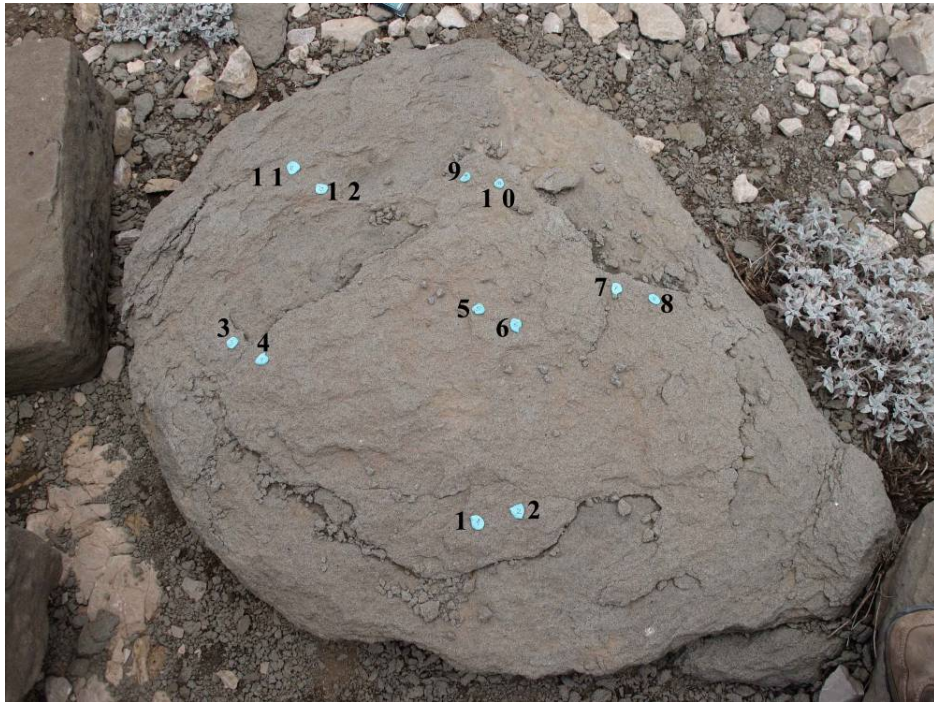


**Figure 4.13** Indirect UPV measurement taken from a sandstone showing granular disintegration (above) at East Terrace, and graphic representation of the UPV values for each point pairs, red: very deteriorated parts.

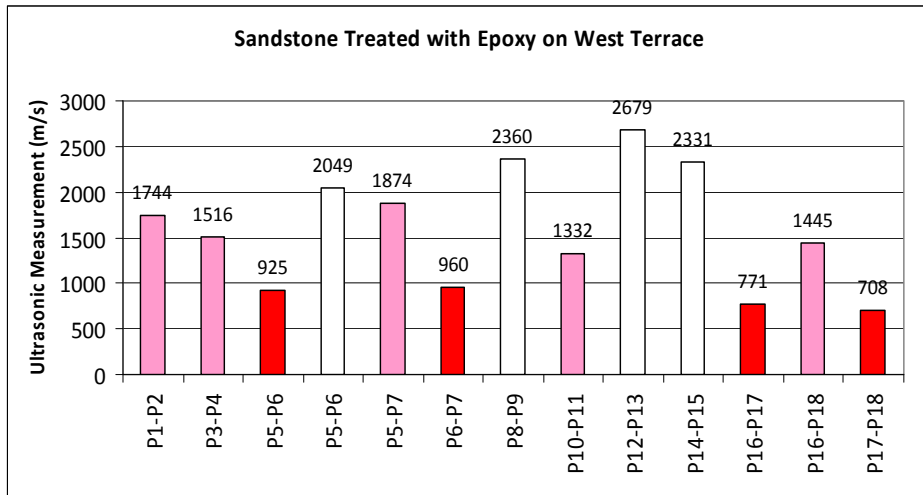


**Figure 4.14** Indirect UPV measurements from sandstone treated with epoxy by the old conservation team (East Terrace), and graphic representation of the UPV values for each point pairs, red: very deteriorated parts, pink: deteriorated parts, white: sound

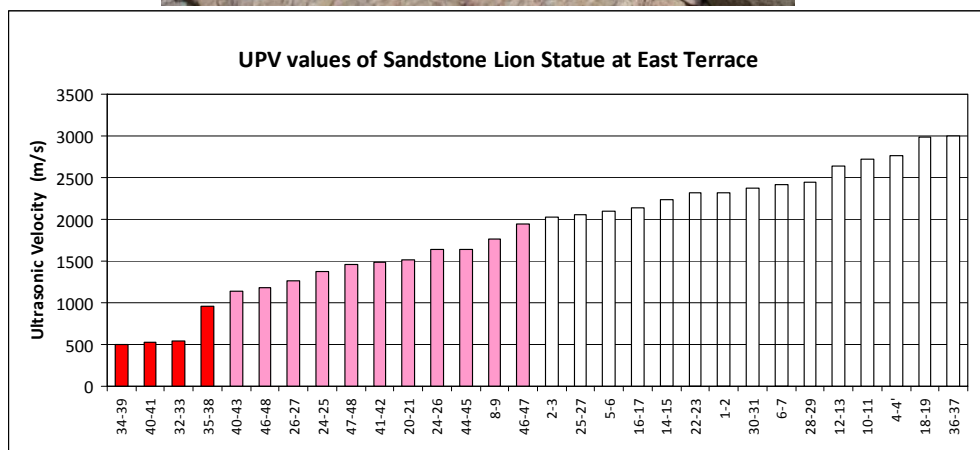


**Figure 4.15** UPV measurements from different points on Sandstone Lion Statue at East Terrace; the measurement points (above); and UPV values of those points pairs; red: very deteriorated parts, pink: deteriorated parts, white: sound.

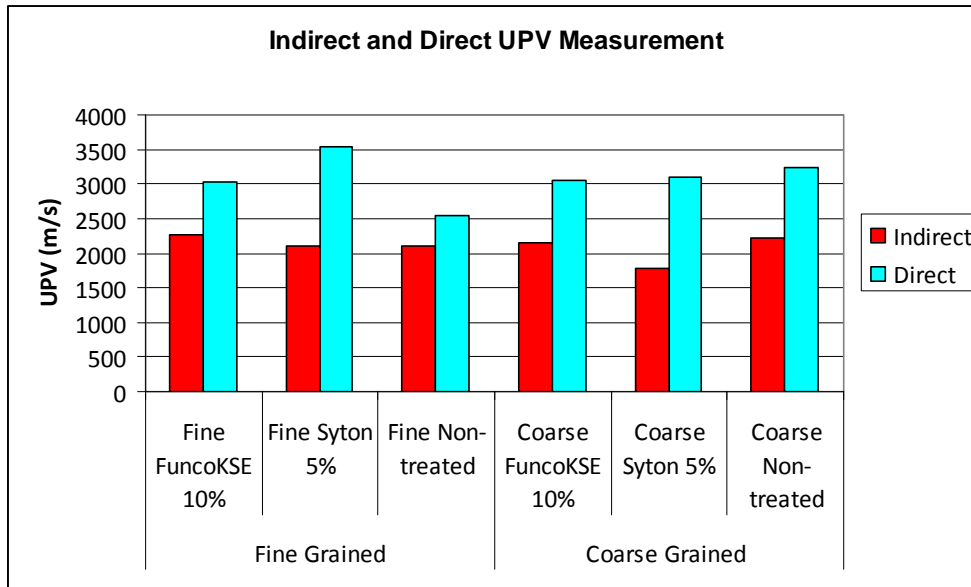


**Figure 4.16** Indirect and direct UPV values of sandstone cubes before and after consolidation treatments.

**Table 4.5** Indirect and direct UPV values of sandstone cubes before and after consolidation treatments.

Treated Sandstones		Velocity (m/s)	
		Indirect	Direct
Fine Grained	<b>Fine FuncoKSE 10%</b>	2264	3038
	<b>Fine Syton 5%</b>	2114	3541
	<b>Fine Non-treated</b>	2104	2545
Coarse Grained	<b>Coarse FuncoKSE 10%</b>	2139	3056
	<b>Coarse Syton 5%</b>	1787	3108
	<b>Coarse Non-treated</b>	2231	3247

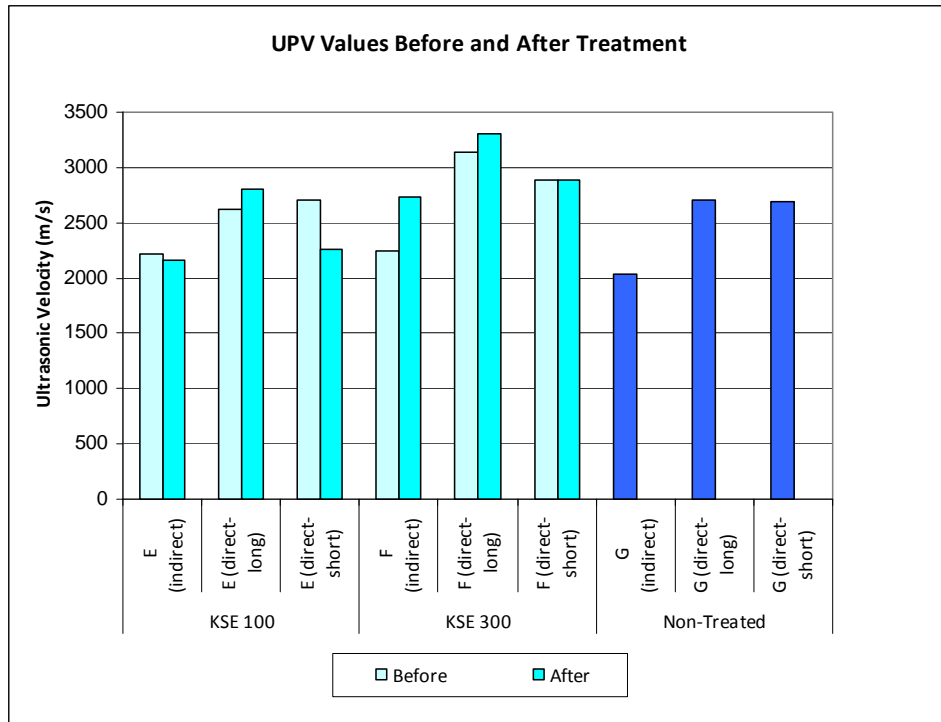


**Figure 4.17** Indirect and direct UPV values of sandstones blocks before and after consolidation treatments; direct (long) measurements are parallel to the bedding and the direct (short) being perpendicular to bedding.

**Table 4.6** Indirect and direct UPV values of sandstones blocks before and after consolidation treatments; direct (long) measurements are parallel to the bedding and the direct (short) being perpendicular to bedding.

Treatment	Sample	UPV Values (m/s)	
		Before	After
<b>KSE 100</b>	<b>E (indirect)</b>	2217	2156
	E (direct-long)	2626	2798
	E (direct-short)	2707	2260
<b>KSE 300</b>	<b>F (indirect)</b>	2247	2730
	F (direct-long)	3132	3301
	F (direct-short)	2890	2890
<b>Non-Treated</b>	<b>G (indirect)</b>	2036	
	G (direct-long)	2705	
	G (direct-short)	2696	

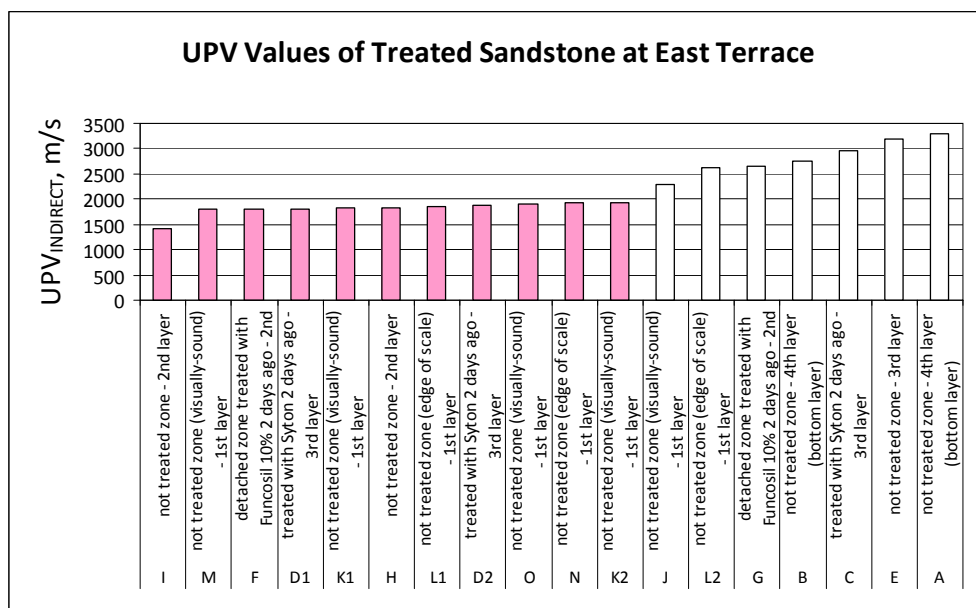
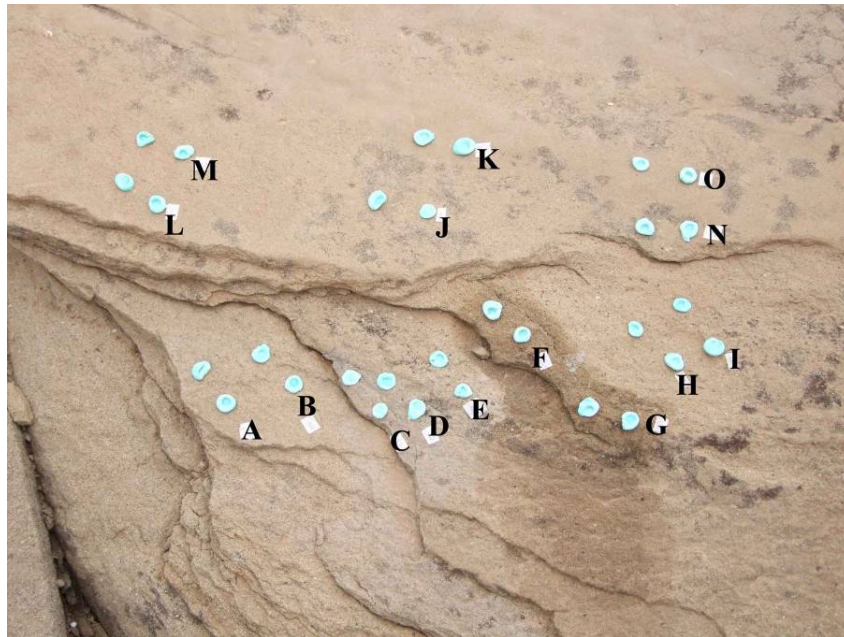


**Figure 4.18** Indirect UPV values of the points of UPV measurements of untreated and treated Layers of sandstone on North Terrace, the areas C and D are treated with Syton X30, areas F and G are treated with Funcosil KSE 500 (above).

#### 4.2.2 Quantitative IR Thermography (QIRT) Results

In-situ IR images were taken for the evaluation of the degree and depth of deterioration and the success of the treatments that were done during the field studies. QIRT analyses revealed the areas with deterioration problems (Figure 4.18). QIRT analyses and UPV measurements together had given the complementary information on the degree and depth of deterioration and in situ evaluation of the treatments' success. Detaching layers were observed as hot areas in the single IR image, however they were seen as colder areas in the differential IR images in cooling period indicating their lowered thermal inertia by weathering. (Figure 4.18). Detaching layers had lower UPV values depending on their degree of deterioration (Figure 4.19).

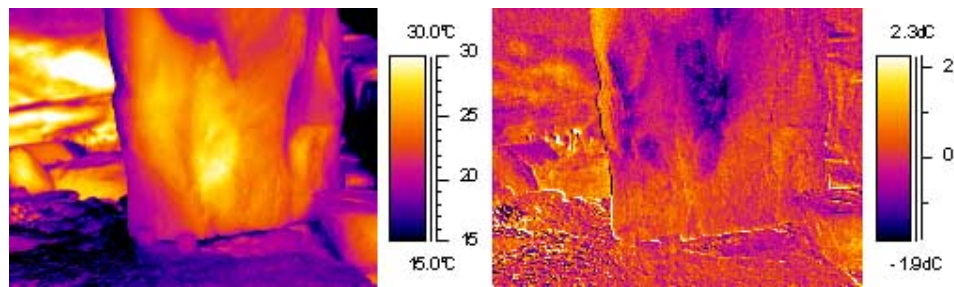


**Figure 4.19** Photograph of Lion Statue at East Terrace (left), single IR image of the statue showing the relatively hot surfaces and the cold surfaces of the statue (above left), differential IR image in cooling period (above right).

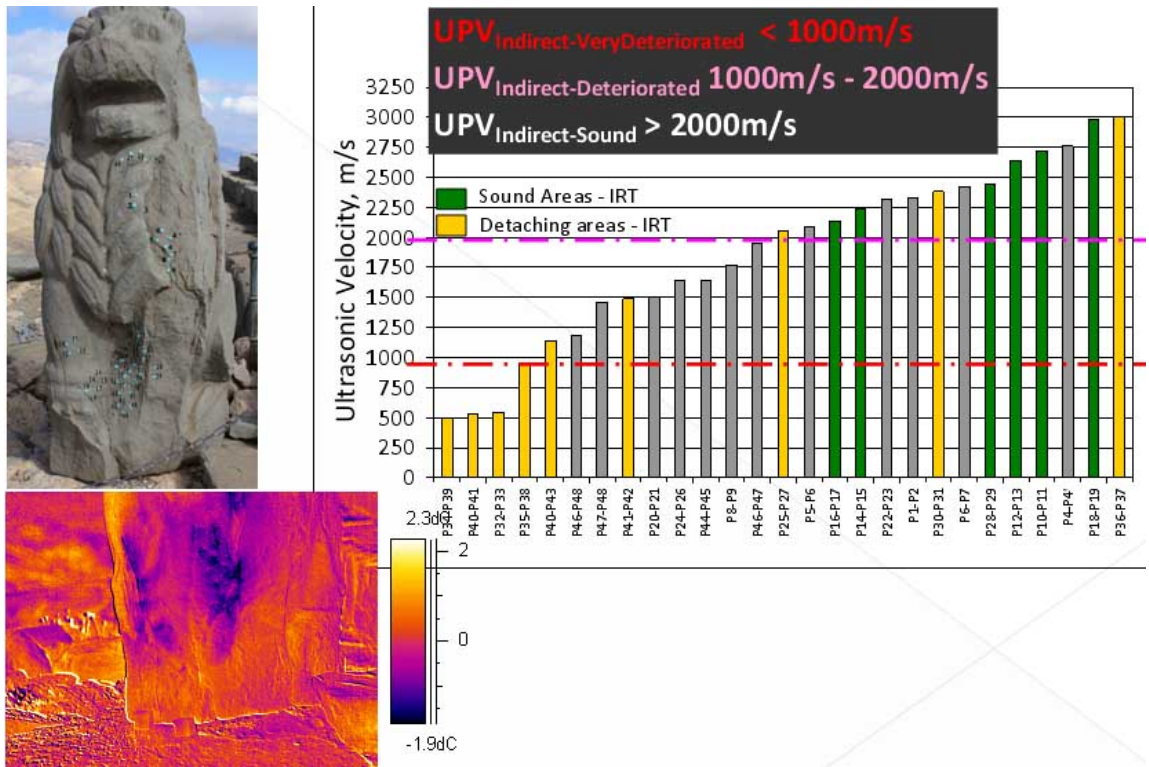


**Figure 4.20** Differential IR image and UPV measurements of the detaching scales. The degree of deterioration of detaching parts can be determined by the changes in UPV measurements that are taken parallel to the surface.

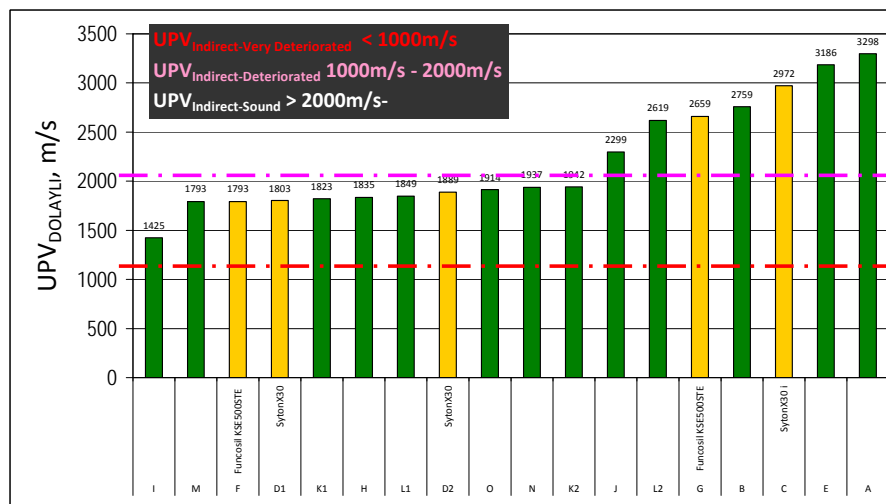
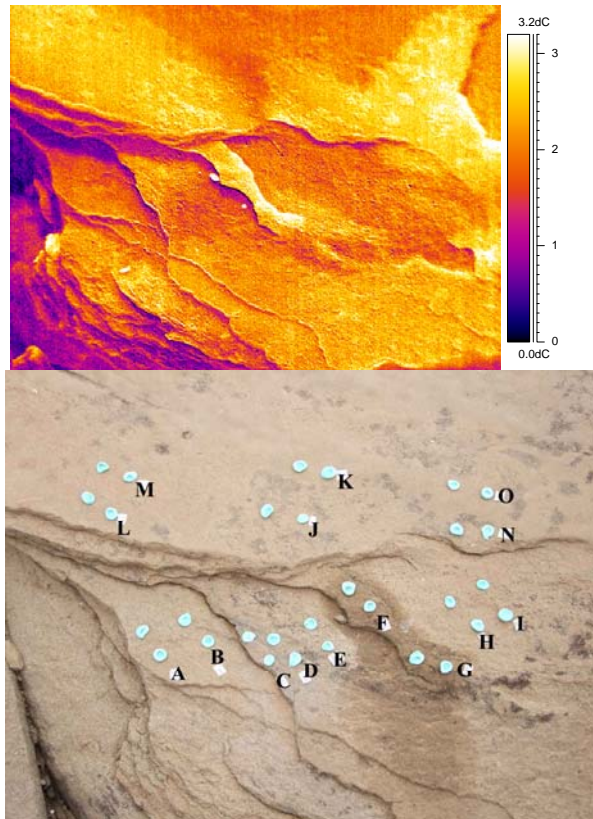


**Figure 4.21** Treated and non-treated layers of sandstone in North Terrace. The UPV and Differential IR images showing that the consolidation treatments done with Funcosil KSE500STE and SytonX30 improve the sandstones' UPV and thermal inertia characteristics.

The treatments with Funcosil KSE500STE and SytonX30 have increased the thermal inertia of the detached layers followed during heating. Increase in UPV values indicated improvement in physicomechanical properties of sandstone by those treatments (Figure 4.21).

#### **4.2.3 Color Measurements**

L\*ab values of sandstone cubes from quarry at 0<sup>th</sup>, 10<sup>th</sup> and 15<sup>th</sup> cycles of salts crystallization were measured to evaluate the color change by weathering. Color values were also determined before and after treatments with consolidants, i.e., Funcosil KSE 500STE, Syton X30, Funcosil 300 KSE and Funcosil 100 KSE to evaluate the effect of treatments on the color (Figure 4.21-4.29).

The color changes of sandstones were visible to eye even after the 5<sup>th</sup> cycle of salt crystallization (Figure 4.22). Main difference was in “b” –yellow-blue– component of the color which indicated yellowing; a slight change also existed in “a” –red-blue component– the browning of the sandstones was observed through weathering (Figure 4.22, 4.24, 4.26). The color changes caused by the application of the consolidants were evaluated by colorimetric measurements of the surface. Color values were measured before and after consolidation treatments. Only a slight color change ( $\Delta E \leq 5$ ), and no darkening or gloss was required for a good consolidant (Sasse and Snethlage, 1997). Syton X30 (Figure 4.27, 4.28) and KSE 100 (Figure 29) were found to be the most successful treatments resulting in minimum color change having values  $\Delta E=4.98$  and  $\Delta E=3.51$  respectively (Figure 4.28, 4.29).

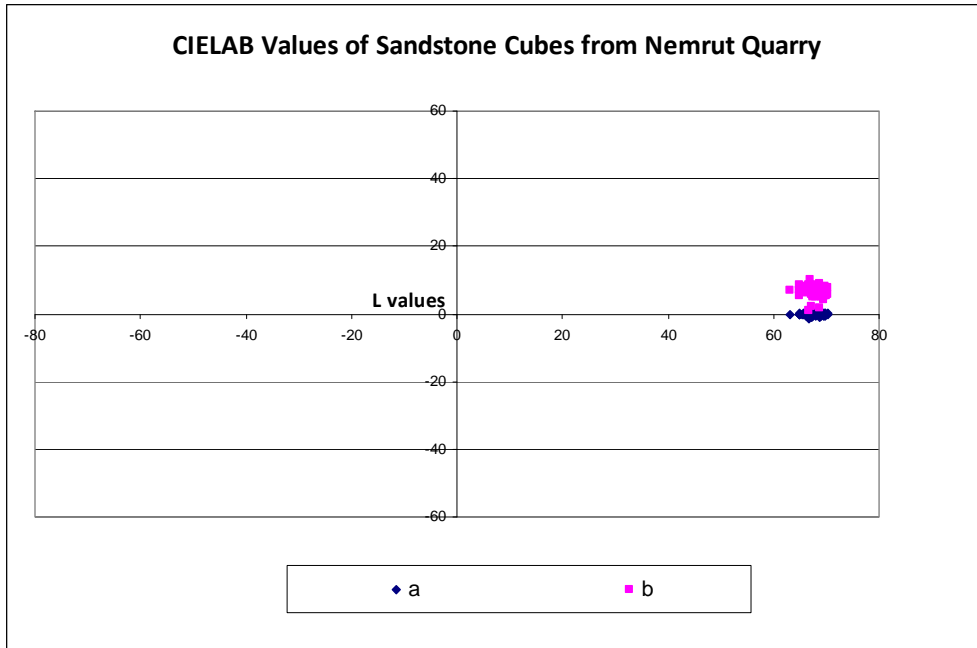


**Figure 4.22** CIELAB color values of sandstone cubes from Nemrut Quarry

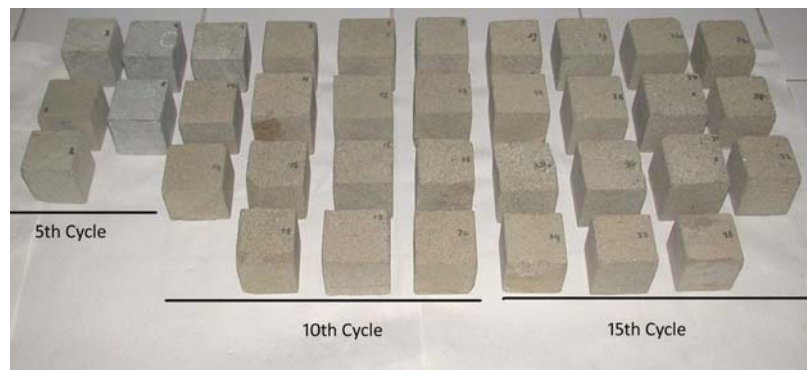


**Figure 4.23** Sandstone cubes from 5<sup>th</sup>, 10<sup>th</sup> and 15<sup>th</sup> cycle of salt crystallization.

**Table 4.7** CIE La\*b\* values of sandstone cubes before subjected to salt crystallization cycles

SAMPLE	L	a	b
1	63.204	-0.064	7.13
2	69.408	0.018	6.888
3	69.61	-0.478	4.032
4	66.696	-1.384	1.008
5	68.658	-1.152	1.696
6	67.328	-1.132	2.124
7	67.572	-0.334	5.426
8	65.734	-0.156	7.85
9	69.408	-0.36	5.034
10	67.59	-0.406	4.882
11	69.892	-0.446	5.454
12	65.362	-0.238	6.788
13	65.882	0.086	8.102
14	66.086	-0.008	7.444
15	65.616	0.088	7.934
16	66.302	-0.406	6.434
17	70.328	0.362	7.642
18	64.82	0.054	8.538
19	69.812	0.028	6.322
20	67.528	0.456	8.642
21	69.422	-0.066	7.452
22	67.864	-0.496	5.004
23	65.016	-0.076	7.166
24	68.752	0.168	8.874
25	66.9	0.316	8.588
26	66.632	-0.21	8.64
27	66.984	-0.264	7.332
28	69.744	0.256	8.27
29	68.48	0.18	7.45
30	67.408	-0.112	5.968
31	70.228	-0.27	5.702
32	67.55533	0.185333	8.150667
33	67.19267	-0.31133	5.868667
34	68.31867	0.066667	7.853333
35	69.04467	-0.33067	5.168
36	66.97867	1.082	10.07933
37	68.05067	0.332667	8.024667
38	69.11067	-0.41133	5.500667
39	67.316	0.421333	8.055333
40	67.442	-0.08933	5.898667
Average	67.63188	-0.12752	6.610383
SD	1.662662	0.449434	1.977514

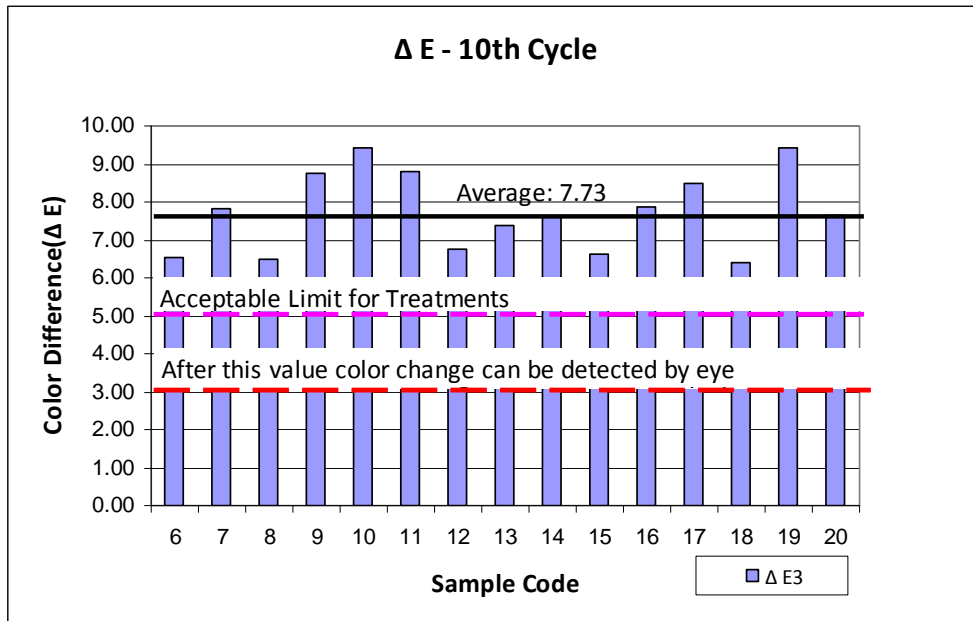


Figure 4.24  $\Delta E$  values of artificially weathered sandstone samples after 10<sup>th</sup> cycle of salt crystallization.

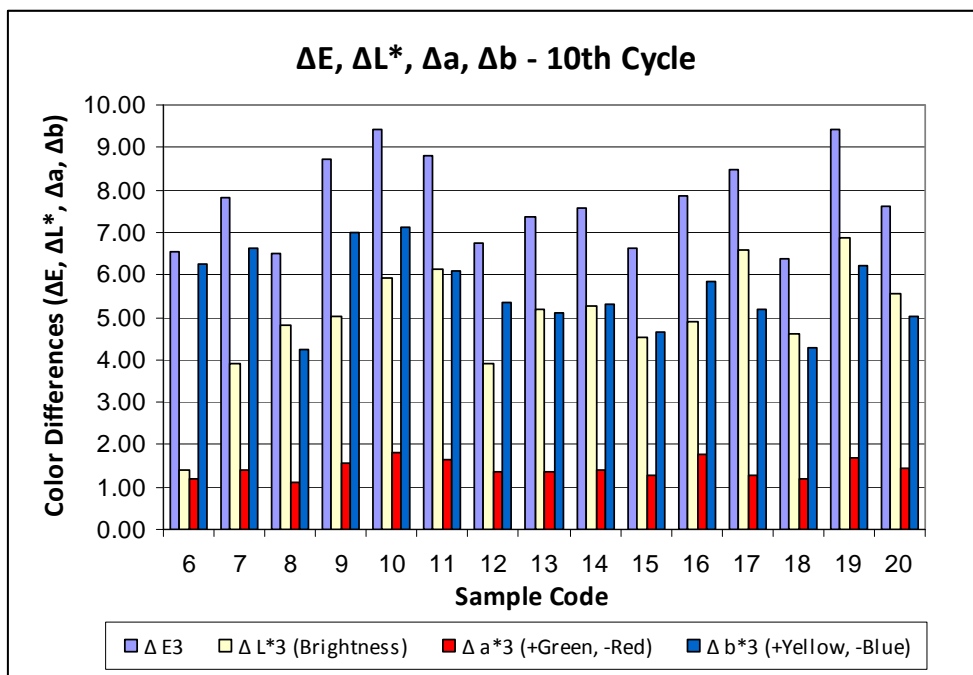
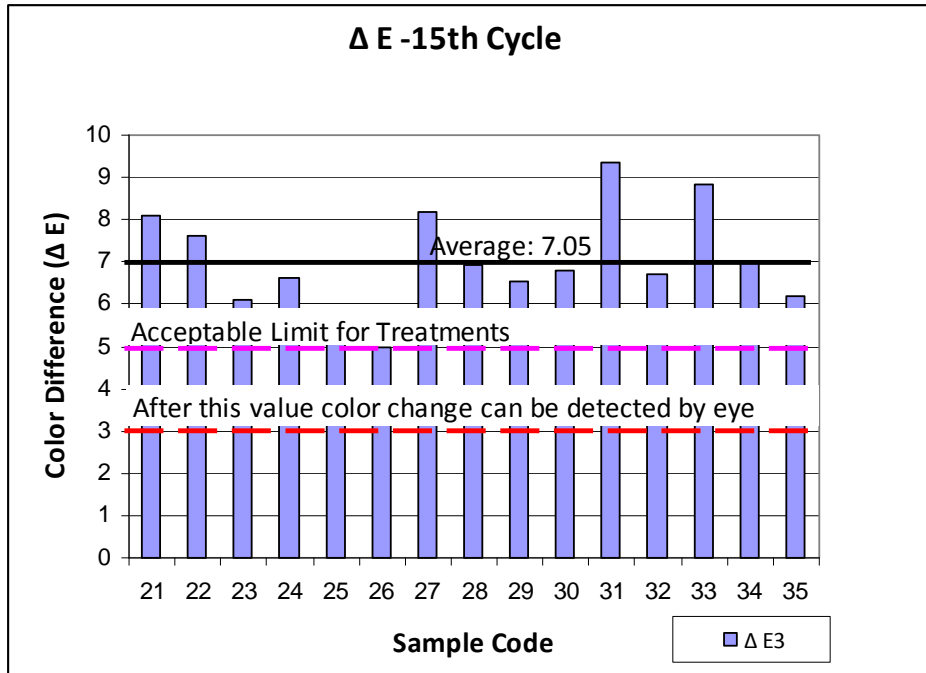
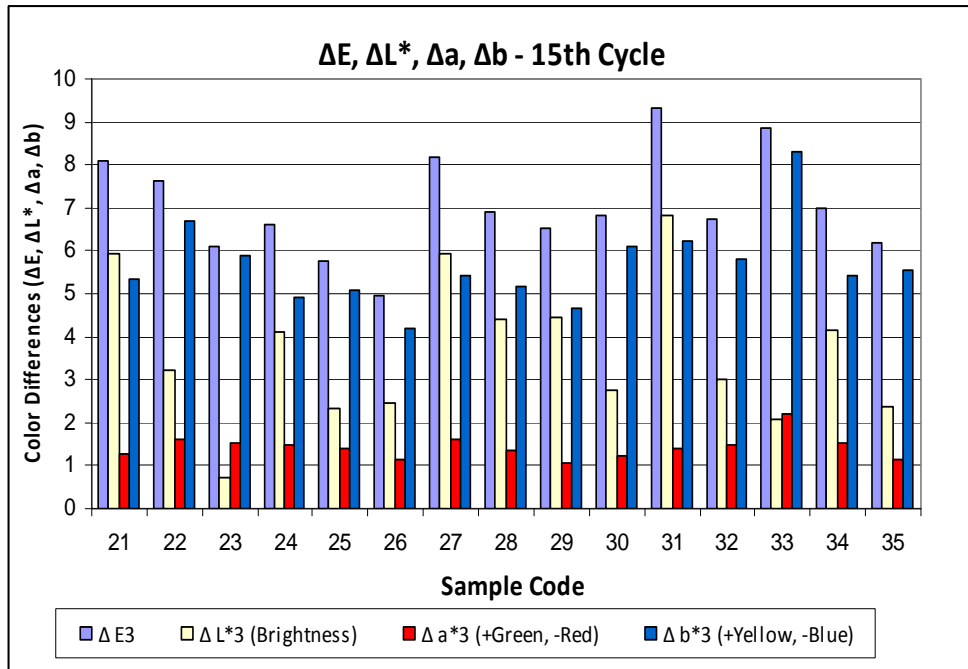


Figure 4.25  $\Delta E$ ,  $\Delta L^*$ ,  $\Delta a$ ,  $\Delta b$  values of artificially weathered sandstone samples after 10<sup>th</sup> cycle of salt crystallization.



**Figure 4.26** ΔE values of artificially weathered sandstone samples after 15<sup>th</sup> cycle of salt crystallization.



**Figure 4.27** ΔE, ΔL\*, Δa, Δb values of artificially weathered sandstone samples after 15<sup>th</sup> cycle of salt crystallization.

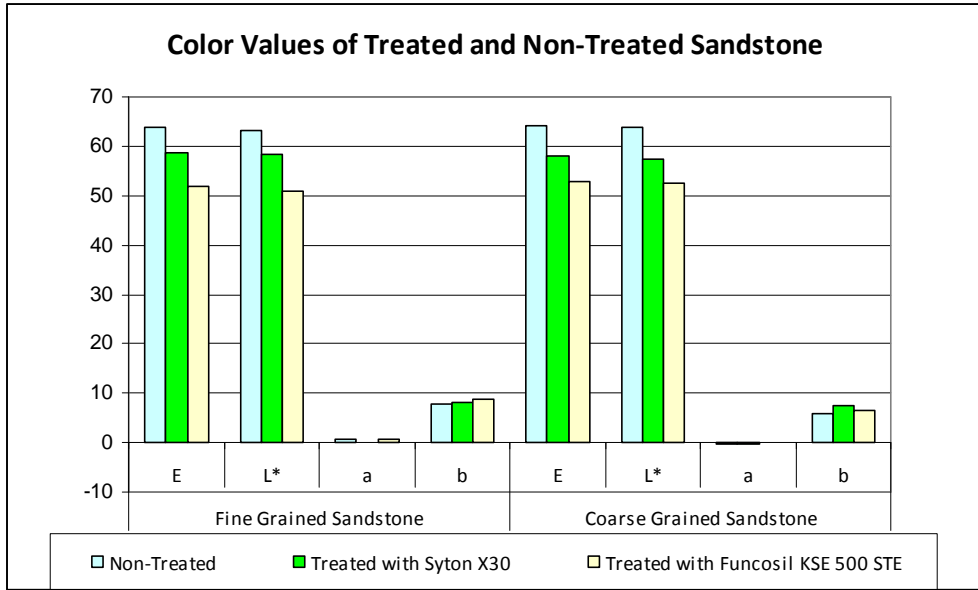


**Figure 4.28** Color values of non-treated and treated sandstone cubes with Syton X30 and Funcosil KSE500STE.

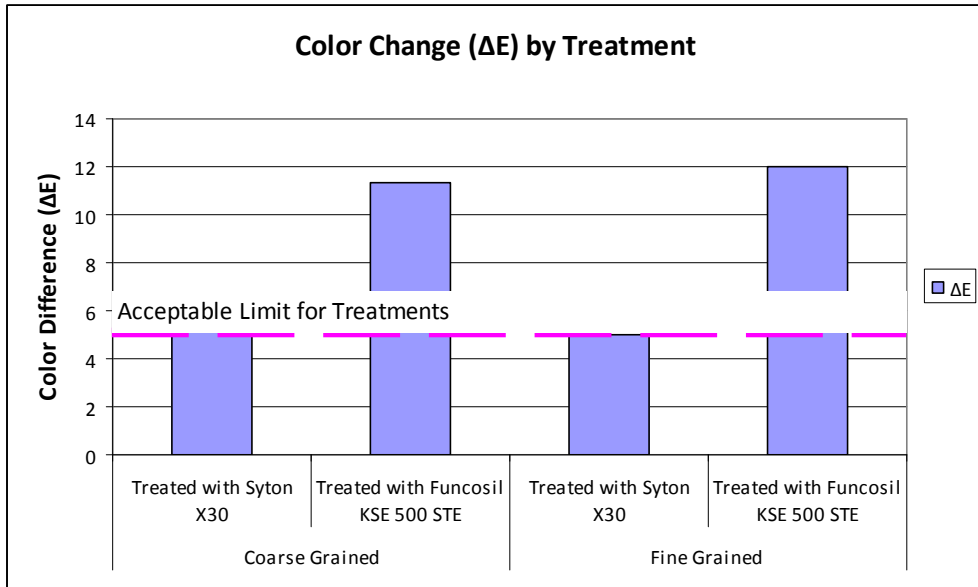


**Figure 4.29**  $\Delta E$  values of fine and medium grained sandstones treated with Syton X30 and Funcosil KSE500STE.

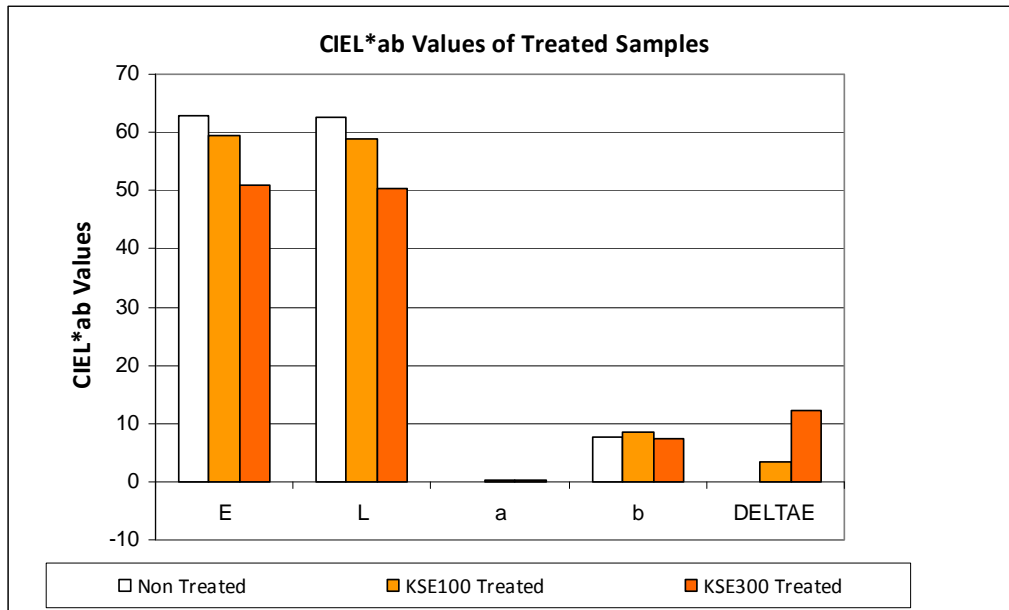


**Figure 4.30** Color values of non-treated and treated sandstone cubes with KSE100 and KSE300.

#### 4.3.4 Results of Effective Porosity and Bulk Density Experiments

Bulk density of the sandstone cubes from the quarry were found to be between 2.48 g/cm<sup>3</sup> - 2.66 g/cm<sup>3</sup> and with an average value 2.58± 0.04 g/cm<sup>3</sup>. The porosity of sandstone cubes were found to be between 0.43 - 4.05 % with an average value 3.57 ± 1.33 % (Figure 4.31, Table 4.8).

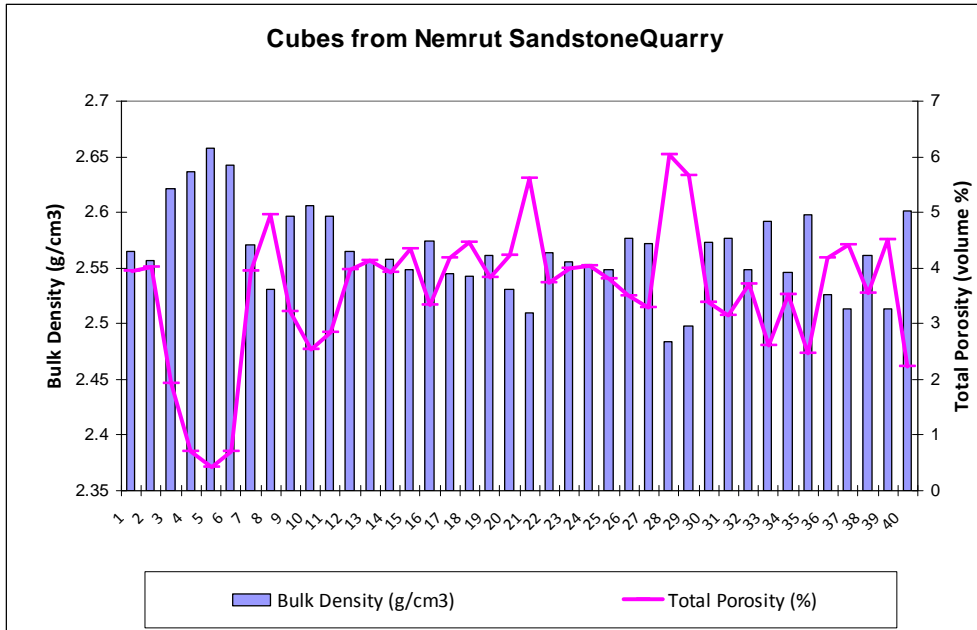


**Figure 4.31** Bulk density and total porosity of sandstone cubes from Nemrut Sandstone Quarry.

**Table 4.8** Bulk Density and Porosity values of sandstone cubes before salt crystallization test.

<b>SAMPLE</b>	<b>Bulk Density (g/cm<sup>3</sup>)</b>	<b>Total Porosity (%)</b>	<b>WAC</b>
1	2.57	3.94	1.54
2	2.56	4.03	1.57
3	2.62	1.92	0.73
4	2.64	0.71	0.27
5	2.66	0.43	0.16
6	2.64	0.70	0.26
7	2.57	3.95	1.54
8	2.53	4.95	1.96
9	2.60	3.22	1.24
10	2.61	2.53	0.97
11	2.60	2.85	1.10
12	2.57	3.97	1.55
13	2.56	4.14	1.62
14	2.56	3.91	1.53
15	2.55	4.34	1.70
16	2.57	3.33	1.29
17	2.54	4.18	1.64
18	2.54	4.45	1.75
19	2.56	3.84	1.50
20	2.53	4.23	1.67
21	2.51	5.60	2.23
22	2.56	3.75	1.46
23	2.56	3.99	1.56
24	2.55	4.05	1.59
25	2.55	3.80	1.49
26	2.58	3.49	1.36
27	2.57	3.30	1.28
28	2.48	6.05	2.43
29	2.50	5.65	2.26
30	2.57	3.38	1.31
31	2.58	3.14	1.22
32	2.55	3.70	1.45
33	2.59	2.60	1.00
34	2.55	3.52	1.38
35	2.60	2.48	0.95
36	2.53	4.18	1.65
37	2.51	4.40	1.75
38	2.56	3.55	1.38
39	2.51	4.52	1.80
40	2.60	2.23	0.86

The effective porosity had increased gradually while the bulk density decreased during the artificial weathering by salt crystallization (Figures 4.31, 4.32; Tables 4.8 – 4.10 ).

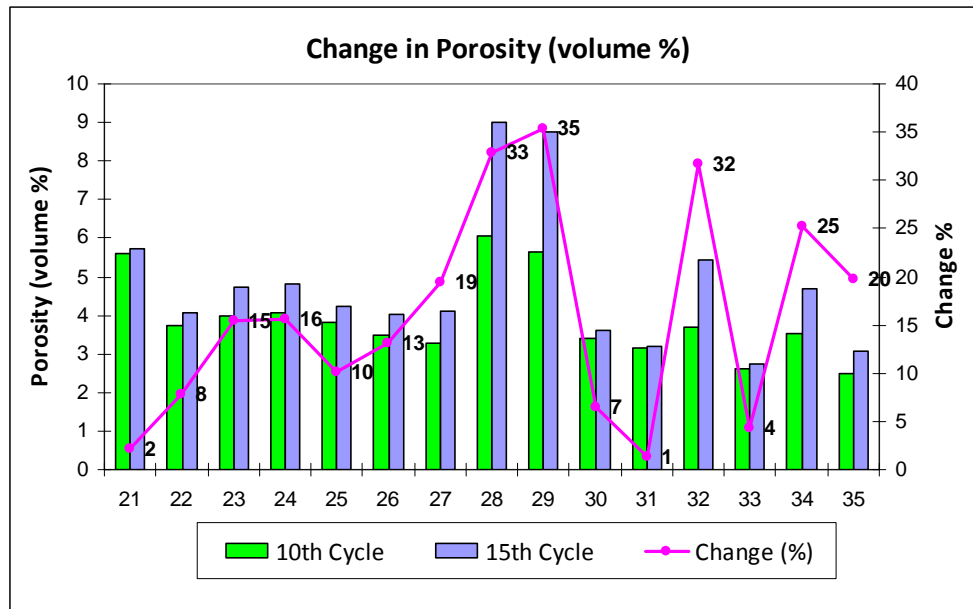


**Figure 4.32** Percentage change in the bulk density and porosity values with salt crystallization cycles

**Table 4.9** Porosity change (%) of each sandstone cube after the 5<sup>th</sup> cycle of salt crystallization test.

SAMPLE	Porosity (%)		Change (%)
	0 <sup>th</sup> cycle	5 <sup>th</sup> cycle	
1	3.88	3.94	1.5
2	1.42	4.03	66
3	0.67	1.92	32
4	0.44	0.71	7
5	0.18	0.43	6

**Table 4.10** Porosity change (%) of each sandstone cube after the 10<sup>th</sup> cycle of salt crystallization test.

SAMPLE	Porosity (%)		Change (%)
	0thcycle	10th cycle	
6	0.66	0.70	5
7	3.46	3.95	14
8	4.23	4.95	17
9	2.59	3.22	24
10	1.92	2.53	31
11	1.76	2.85	62
12	2.69	3.97	47
13	3.35	4.14	24
14	3.19	3.91	23
15	3.73	4.34	16
16	2.00	3.33	67
17	3.40	4.18	23
18	3.99	4.45	12
19	2.95	3.84	30
20	3.15	4.23	35

**Table 4.11** Porosity change (%) of each sandstone cube after the 15<sup>th</sup> cycle of salt crystallization test.

SAMPLE	Porosity (%)		Change (%)
	0 <sup>th</sup> Cycle	15 <sup>th</sup> Cycle	
21	5.60	5.73	2
22	3.75	4.06	8
23	3.99	4.71	15
24	4.05	4.80	16
25	3.80	4.23	10
26	3.49	4.02	13
27	3.30	4.09	19
28	6.05	9.01	33
29	5.65	8.75	35
30	3.38	3.62	7
31	3.14	3.18	1
32	3.70	5.43	32
33	2.60	2.72	4
34	3.52	4.70	25
35	2.48	3.09	20

#### 4.2.5 Mercury Intrusion Porosimetry

The pore size distribution of several sandstone samples, including the ones from the sandstone formations nearby the monument as well as the samples representing the main weathering forms on the monuments and artificially weathered sandstones were studied e.g., non-weathered fine grained and non-weathered coarse grained sandstones from the formation near the site, naturally weathered sandstones showing layering and showing granular disintegration and artificially weathered sandstones subjected to different cycles of salt crystallization.

Pore size distribution of sandstones were in the range of 100-0.01  $\mu\text{m}$ . The medium grained sandstones were found to have lower effective porosity ( $\sim 0.8\%$ - $1.5\%$ ) than the fine grained ones ( $\sim 5.2\%$ ) (Figures 4.32 and 4.33). In the medium grained sandstones the effective porosity was formed mainly by the pores having diameters of  $100\mu\text{m}$ . In the fine grained sandstones majority of the pores had diameters in the range of  $0.5 \mu\text{m}$  (Figure 4.32 and 4.33).

It was seen that the total porosity of the weathered surface of the sandstones that exhibited granular disintegration was about  $6\%$  whereas its relatively unweathered deeper part had  $4.5\%$  of effective porosity. Pore size distribution of the weathered part has shown that while the fine pore percentage stayed almost the same, medium size pores increased when compared with deeper part of the stone, and the average pore diameter have slightly shifted to a higher value (Figure 4.33, 4.34). In the detaching scales, total porosity of the weathered exterior surface was about  $4.5\%$ , whereas the detaching surface having clayey accumulation was  $3.3\%$  (Figure 4.35, 4.36). On the other hand, pore size distribution of the detaching scale at the weathered exterior surface show increase in both fine and medium pore sizes (Figure 4.37).

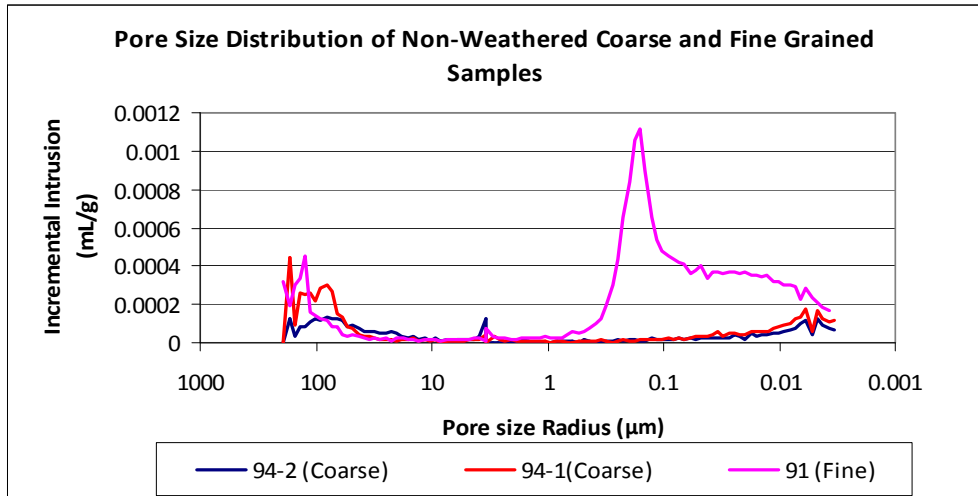


Figure 4.33 Pore size distribution of medium and fine grained sandstones from quarry.

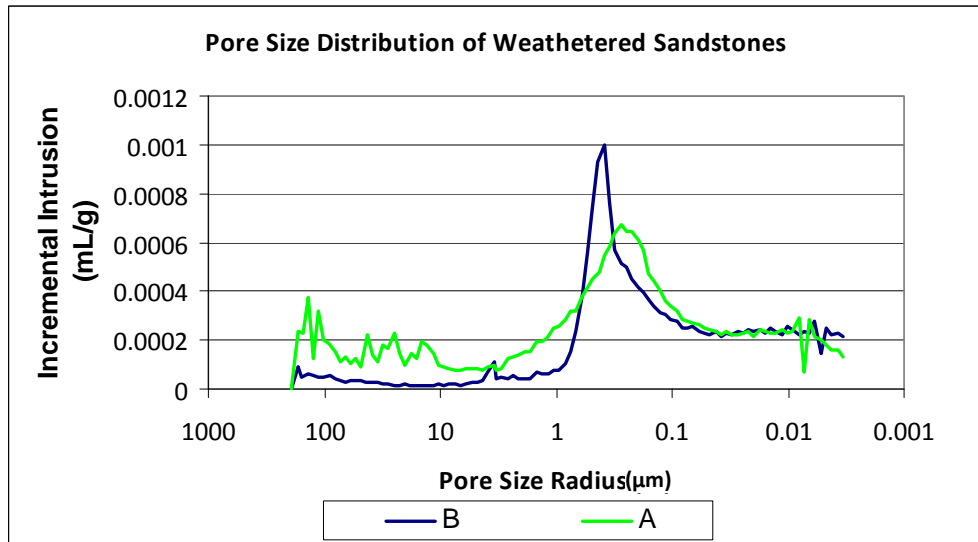
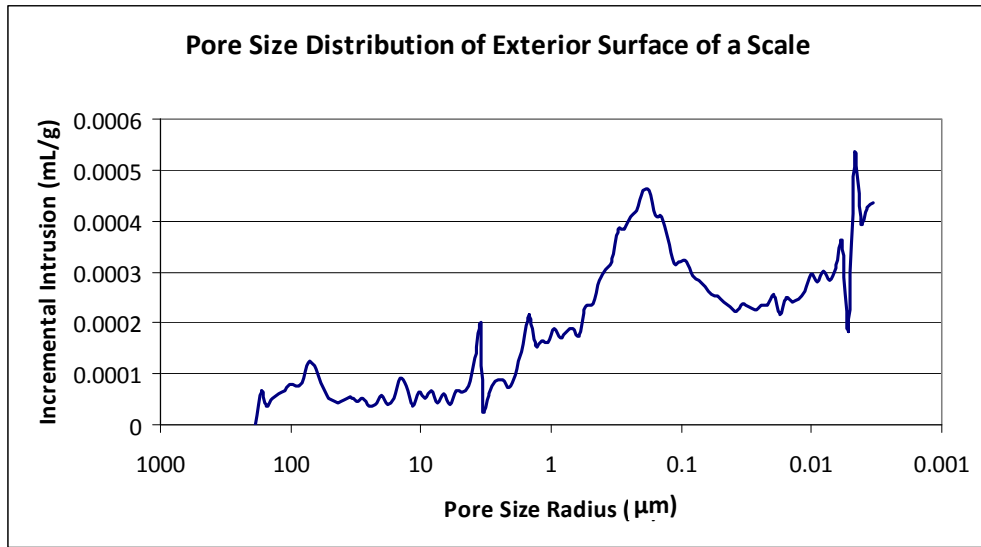
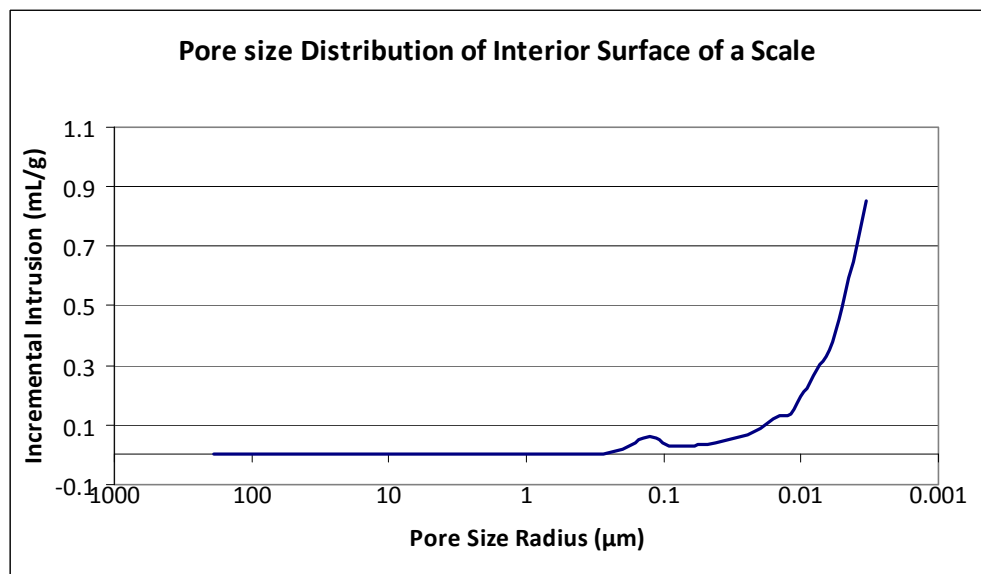


Figure 4.34 Pore size distribution of weathered sandstone samples from site.



**Figure 4.35** Pore size distribution of exterior surface of a scale from site.



**Figure 4.36** Pore size distribution of interior surface of a scale from site.

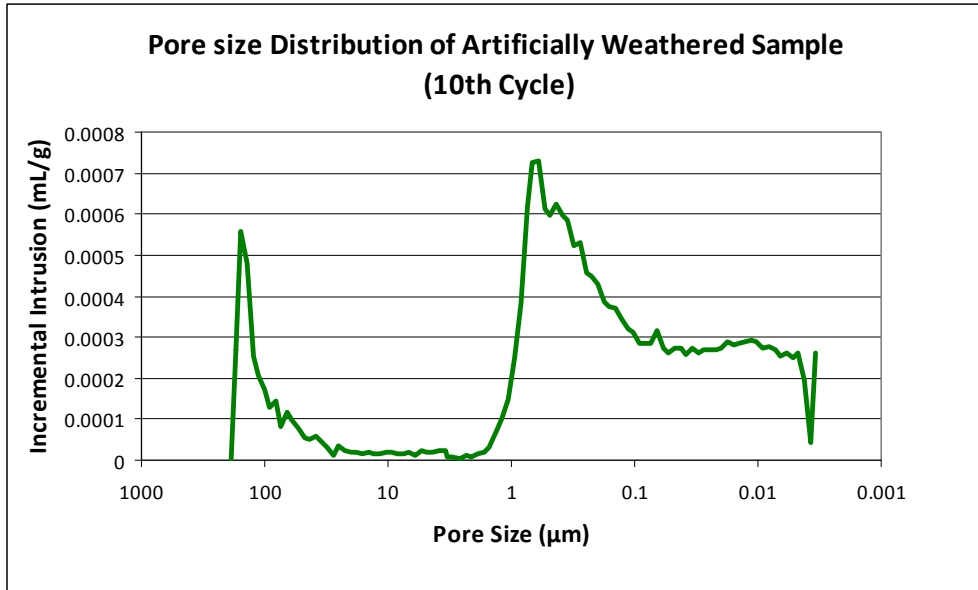


**Figure 4.37** Pore size distribution of artificially weathered sample from 10th cycle of salt crystallization.

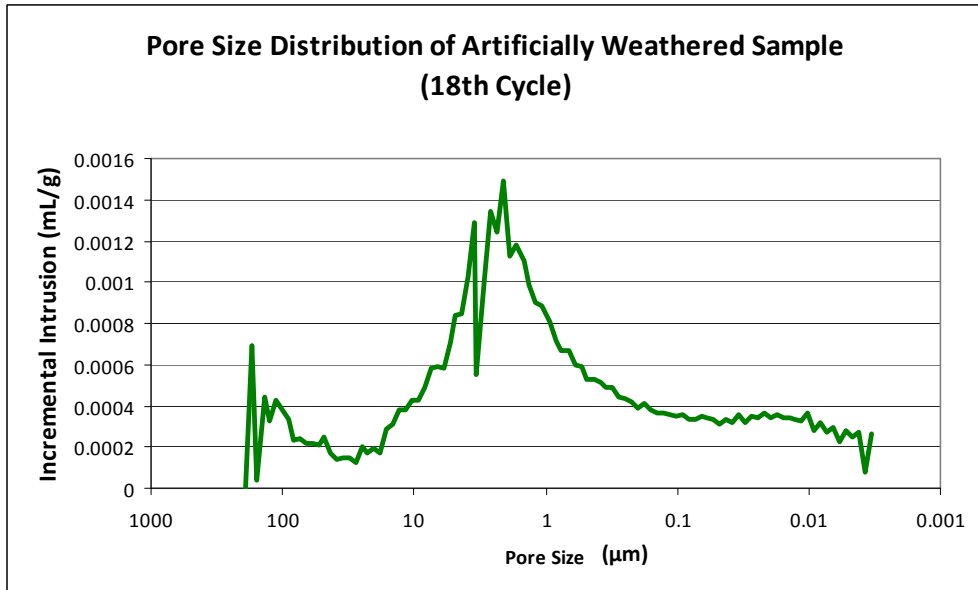


**Figure 4.38** Pore size distribution of artificially weathered sample from 18th cycle of salt crystallization.

#### 4.2.6 Dilatation Measurement Tests

Thermal, hydric and hygric dilatation measurements for sandstones from Nemrut were carried out in MCL (hydric dilatation measurements) and LRMH (thermal and hygric dilatation measurements) laboratories. The dilatation perpendicular to bedding at 95 % RH was  $0.01\mu\text{m}$  per millimeter for fine grained sandstones and  $0.06\pm 0.02\mu\text{m}$  per millimeter for medium grained sandstones (Figure 4.39). The thermal dilatation of medium and fine grained sandstones perpendicular to bedding plane was around  $0.35\pm 0.02\mu\text{m}$  per millimeter between 0 - 45°C (Figure 4.40). Hydric dilatation of medium and fine grained sandstones perpendicular to the bedding plane was about  $0.3\pm 0.02\mu\text{m}$  per millimeter (Figure 4.41).

Hydric dilatation measurements of surfactant treated sandstones showed some decrease in swelling. For HDTMA treated sample that decrease was from 0.324 to  $0.246\mu\text{m}/\text{mm}$  (Figure 4.42); for Antihydro from 0.32 to  $0.257\mu\text{m}/\text{mm}$  (Figure 4.43) and for DAA from 0.32 to  $0.197\mu\text{m}/\text{mm}$  (Figure 4.44).

The hydric dilatation of the sandstones treated with SytonX30 decreased from  $0.33\pm 0.02\mu\text{m}/\text{mm}$  to  $0.28\pm 0.02\mu\text{m}/\text{mm}$  for fine grained sandstones and  $0.41\pm 0.02\mu\text{m}/\text{mm}$  to  $0.37\pm 0.02\mu\text{m}/\text{mm}$  for medium grained sandstones (Figure 4.44). The hydric dilatation of sandstones treated with FuncosilKSE500STE decreased from  $0.32\pm 0.02\mu\text{m}/\text{mm}$  to  $0.27\mu\text{m}/\text{mm}$  for medium grained sandstones and  $0.32\pm 0.02\mu\text{m}/\text{mm}$  to  $0.25\pm 0.02\mu\text{m}/\text{mm}$  for fine grained sandstones (Figure 4.45).

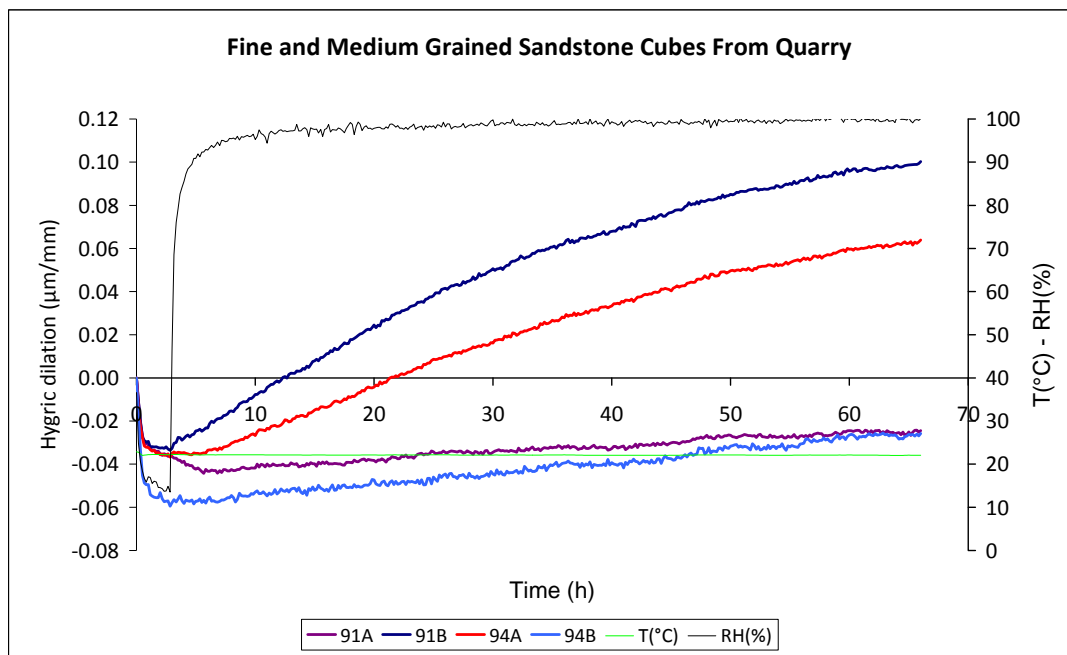


**Figure 4.39** Hygric Dilatation measurement of medium and fine grained sandstones; 94A: hygric dilatation of medium grained sandstone perpendicular to bedding; 94B: hygric dilatation of medium grained sandstone parallel to bedding; 91A: Hygric dilatation of fine grained sandstone perpendicular to bedding, 91B: Hygric dilatation of fine grained sandstone parallel to bedding.

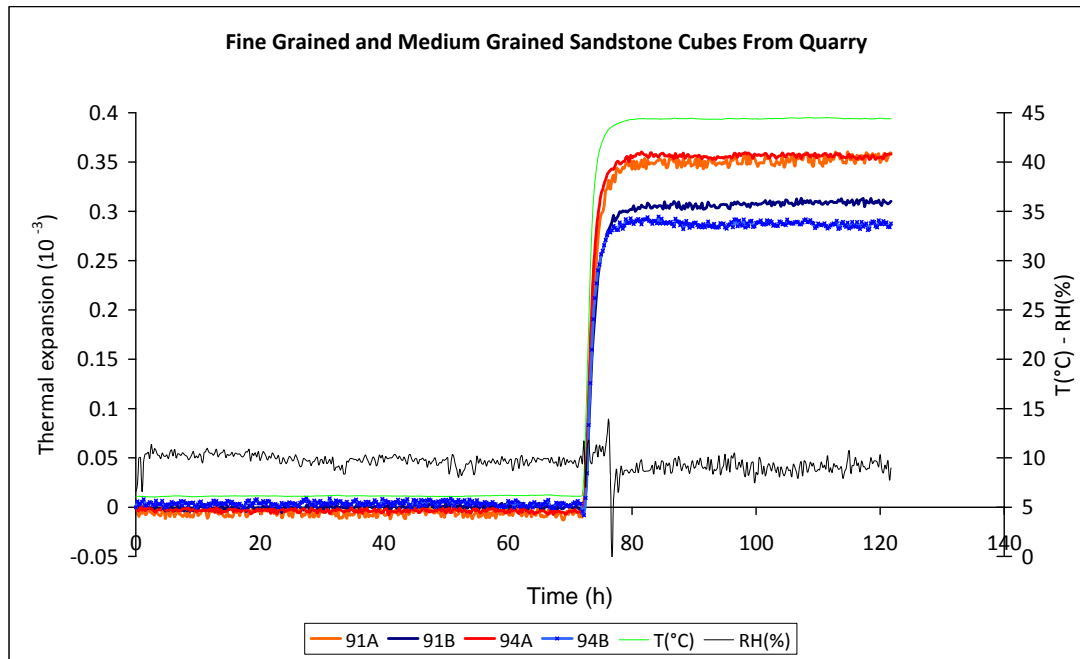


**Figure 4.40** Thermal Dilatation measurement of medium and fine grained sandstones; 94A: thermal dilatation of coarse grained sandstone perpendicular to bedding; 94B: thermal dilatation of medium grained sandstone parallel to bedding; 91A: thermal dilatation of fine grained sandstone perpendicular to bedding, 91B: thermal dilatation of fine grained sandstone parallel to bedding.

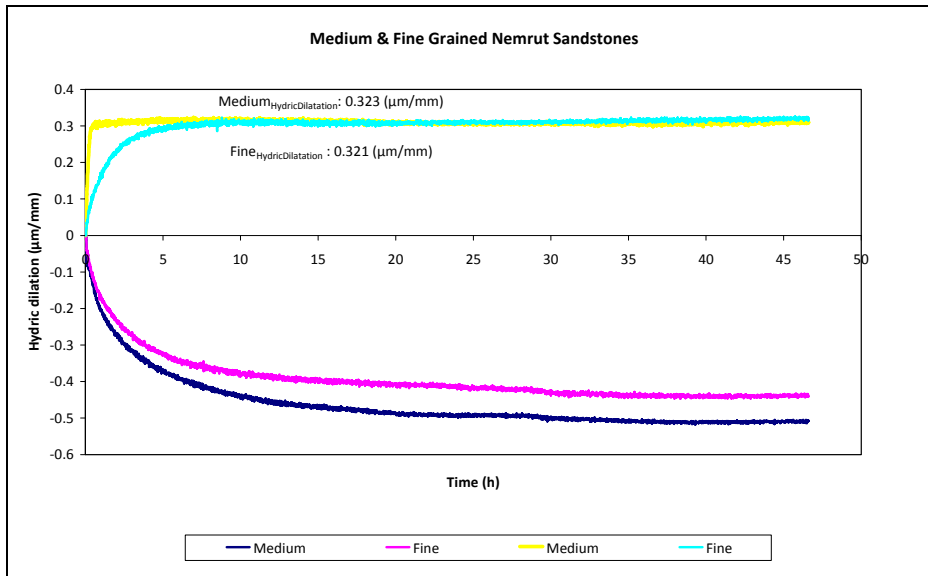


**Figure 4.41** Hydric Dilatation measurement of medium and fine grained sandstones perpendicular to bedding.

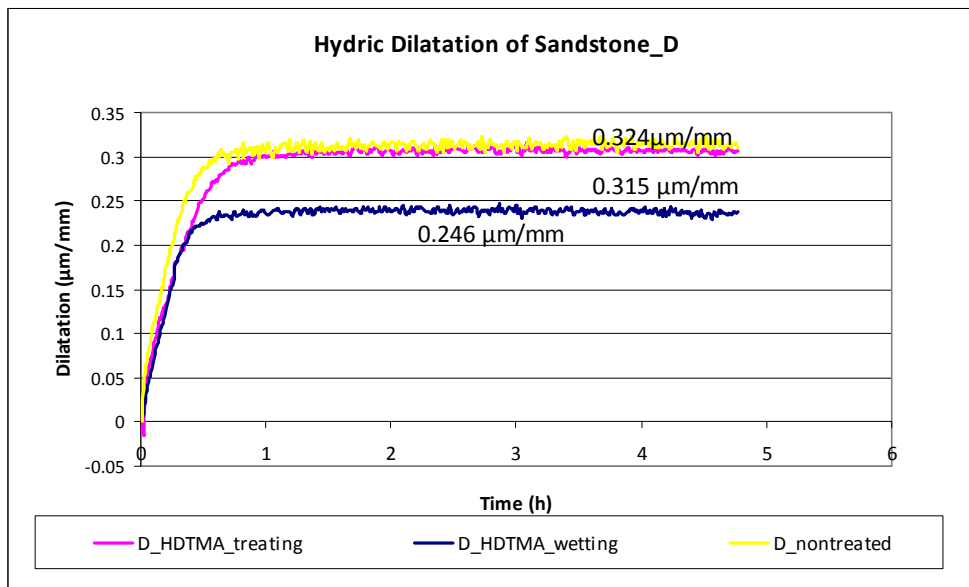


**Figure 4.42** Hydric Dilatation measurement of sample Sandstone\_D before treatment with HDTMA, as well as treatment with HDTMA and wetting after the treatment.

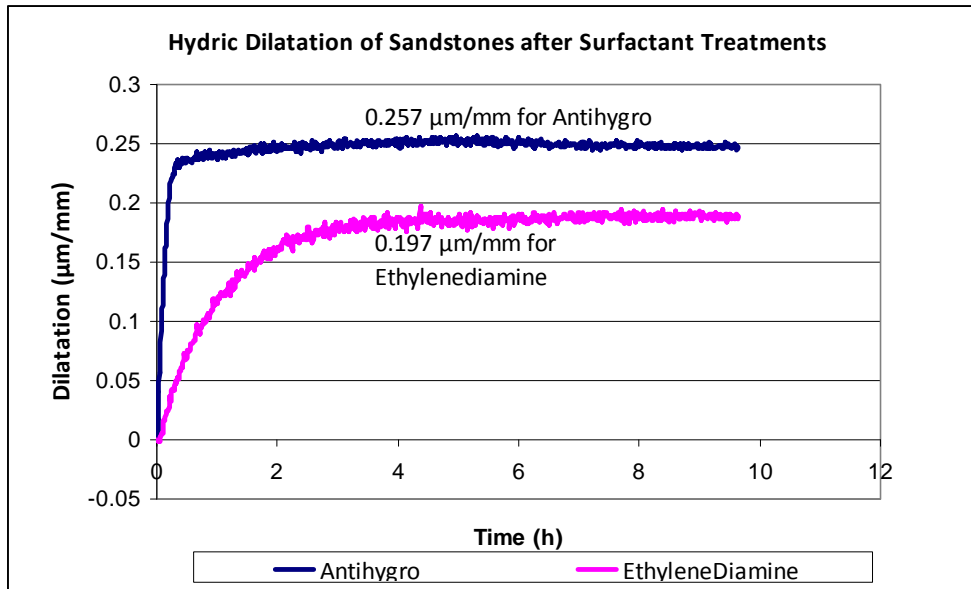


**Figure 4.43** Hydric dilatation measurement of sandstone after treatment with antihydro and ethylenediamine.

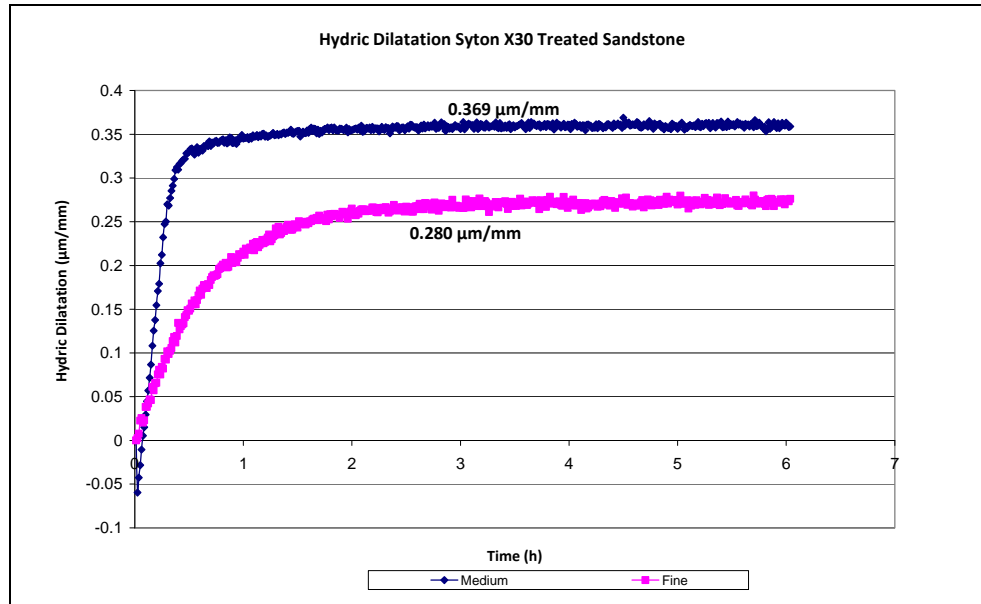


**Figure 4.44** Hydric dilatation measurement of medium and fine grained sandstones after treatment with SytonX30.

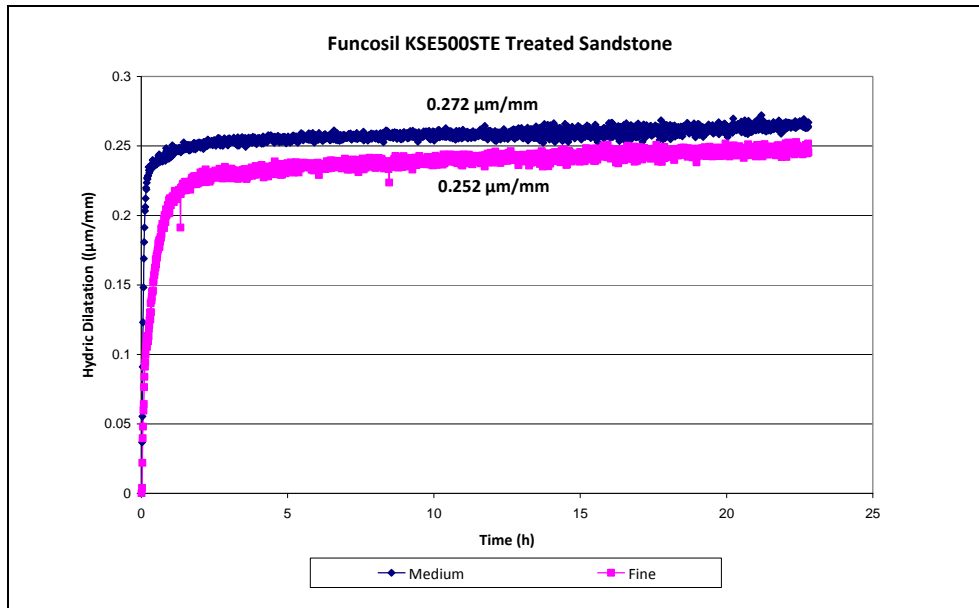


**Figure 4.45** Hydric dilatation measurement of medium and fine grained sandstones after treated with FuncosilKSE500STE.

#### 4.2.7 Drying Rate Measurements at Site

Drying rates of four saturated sandstone cubes were evaluated during the field study done in September 2009. While the measurements were taken, the climatic conditions, i.e., relative humidity, temperature and wind speed were also measured and an average for each parameter was calculated. The average temperature was 20°C, average relative humidity was 34% and the average wind speed was 3.6 km/h. Complete drying was achieved at the end of 6 hours for all sandstone cubes by reaching their initial dry weights (Figure 4.46).

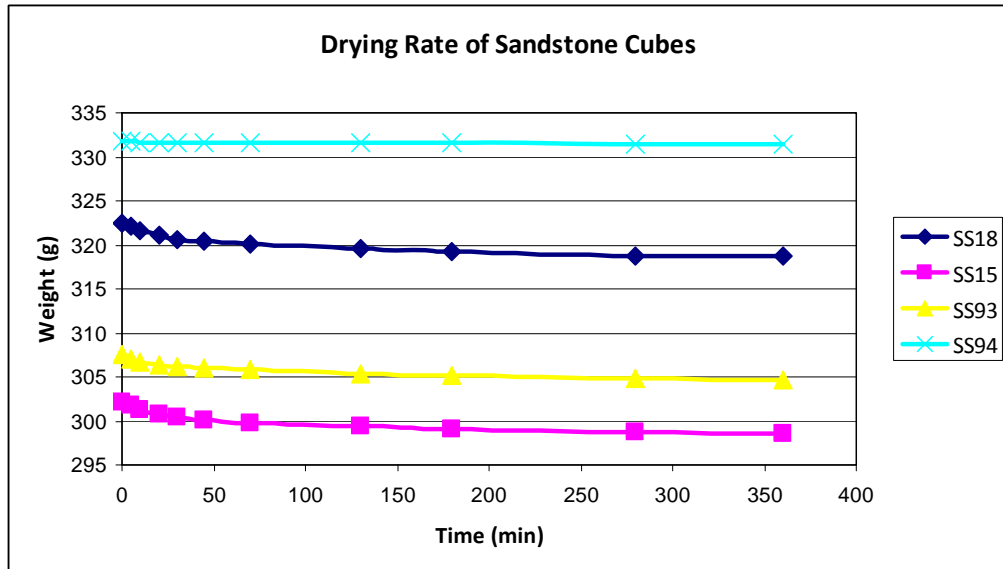


**Figure 4.46** Drying rate of saturated sandstone cubes at site.

### 4.3 Determination of Micro-Structural Properties

#### 4.3.1 Thin Section Analyses by Optical Microscopy and Image Analyses

Thin section analyses of nonweathered quarry sandstones (Figures 4.47-4.49), weathered sandstones in the site from different locations i.e., east and north terraces (Figures 4.50-4.59) and artificially weathered sandstones by salt crystallization were done (Figure 4.60). Moreover image analyses of fine grained and coarse grained sandstones were done in order to figure out the sorting and the average grain sizes of the medium and fine grained sandstones.

The sandstones of Nemrut consisted of considerable range of rock fragments and minerals such as limestones, granite, quartzite and minerals like feldspars, quartz, biotite and clay minerals (Figures 4.47, 4.48). Chlorite (Figures 4.47, 4.60) and opaque minerals were also observed in the thin sections (Figures 4.47-4.60). Those fragments of rocks and minerals were in a fine grained carbonatic-clayey matrix. The fabrics of

sandstones were generally matrix supported, in addition, grain supported matrix and point contacts were also observed. According to the grain sizes observed in thin sections, Nemrut sandstones could be classified as fine and medium grained sandstones. Medium grained sandstones had average grain size as  $333\mu\text{m}$  with a range of  $1300$  to  $60\mu\text{m}$  (Figures 4.61, 4.62). Fine grained sandstones had average grain size as  $176\mu\text{m}$  in the range of  $40$ - $450\mu\text{m}$  (Figures 4.63, 4.64). Both fine and medium grained sandstones were poorly sorted sandstones (Figures 4.62, 4.64).

In the thin section analyses of the deteriorated sandstones, the micro crack formations parallel to each other were observed which indicated the increase in the porosity (Figures 4.50 - 4.52, 4.56 - 4.59). Those micro cracks were the regions for the accumulation of clay minerals together with the iron oxides (Figures 4.50, 4.52, 4.56).



**Figure 4.47** Thin section photomicrograph of a fresh sandstone sample (crossed nicols). Showing the presence of quartz, plagioclase feldspar, granite, igneous rock fragments, alkali feldspar, biotite, orthoclase, calcedony, quartzite, calcite, Limestone particles

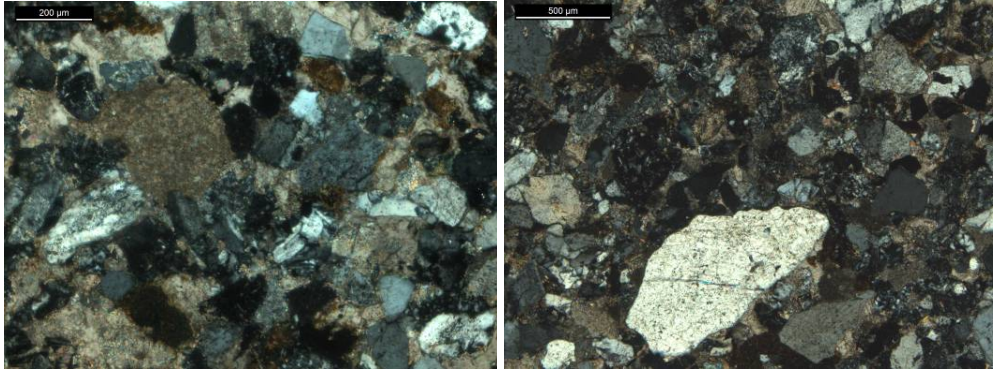


**Figure 4.48.** Thin section photomicrographs of fresh sandstone, fine grained (left), cross nicols; medium grained (right) crossed nicols.

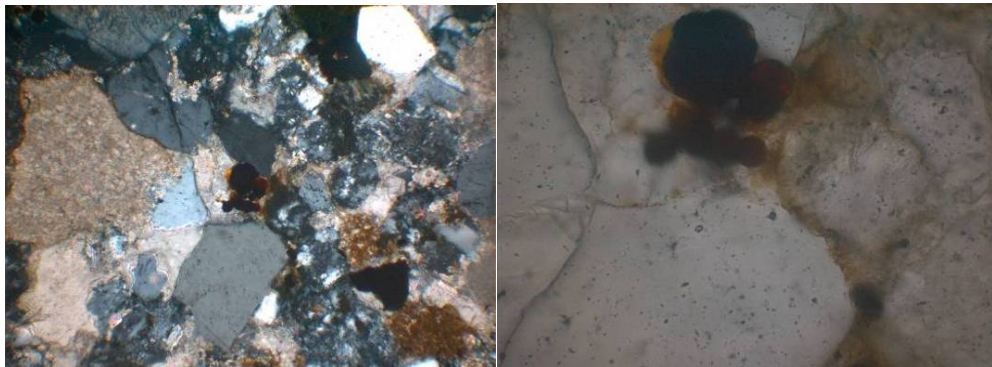


**Figure 4.49.** Thin section photomicrograph of a fresh sandstone sample, crossed nicols X10 (left) and single nicol X63 (right), showing opaque minerals as iron oxides and some amorphous phases around them observed as small spheres.

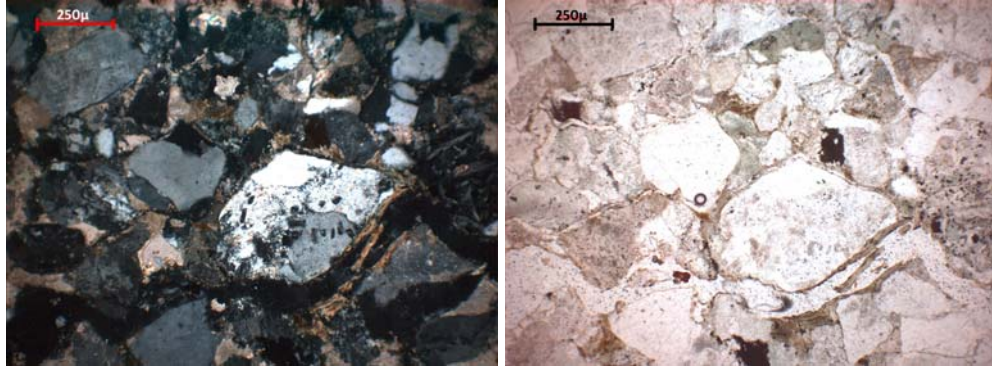


**Figure 4.50.** Thin section photomicrograph of naturally weathered sample crossed nicols (left) and single nicol (right). Cracks in the microstructure and clay accumulations on the surfaces of cracks are observed.

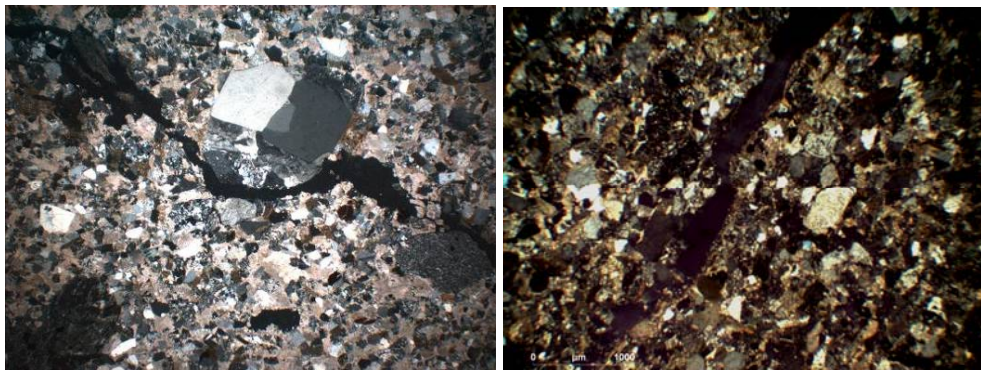


**Figure 4.51.** Thin section views from naturally weathered samples. Micro-cracks are observed in the microstructure.

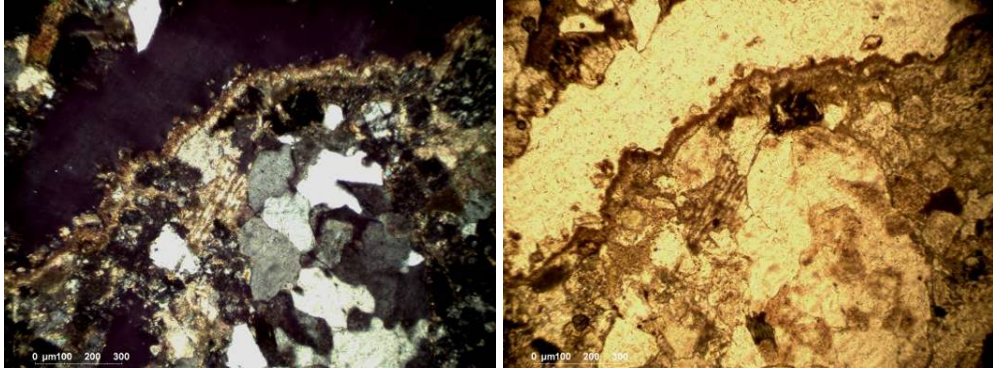


**Figure 4.52.** Thin section photomicrograph of naturally weathered sample crossed nicols (left) and single nicol (right). A crack of  $\sim 300\mu\text{m}$  size, accumulation of micritic calcite and clay minerals on one of its surfaces.

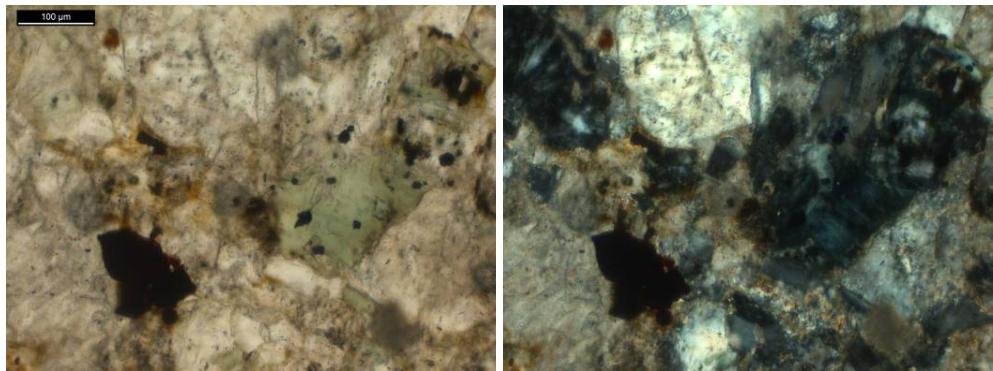


**Figure 4.53.** Chlorite and iron oxide minerals in deteriorated fine grained sandstone can be seen in the single nicol (left), cross nicols (right).



**Figure 4.54.** Aggregates of colloidal iron oxide in the matrix of deteriorated sandstone around the iron oxide minerals, single nicol.

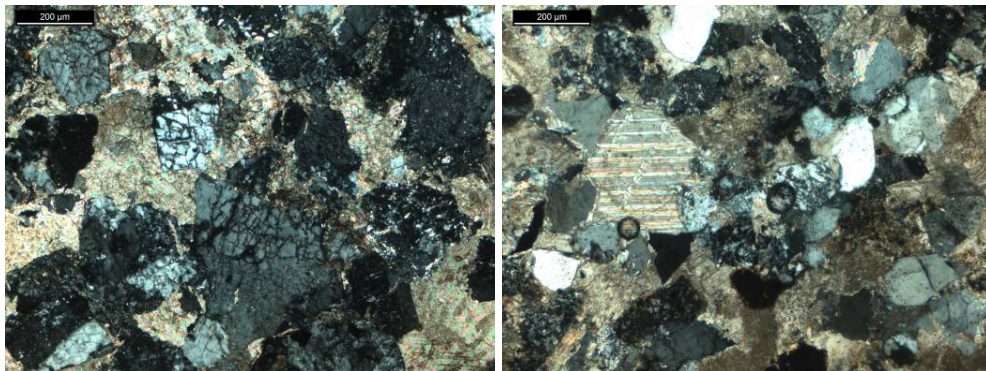


**Figure 4.55.** Thin section photomicrograph of fine grained deteriorated sandstone, crossed nicols, deterioration of feldspar minerals (left) and calcite in the matrix (right).

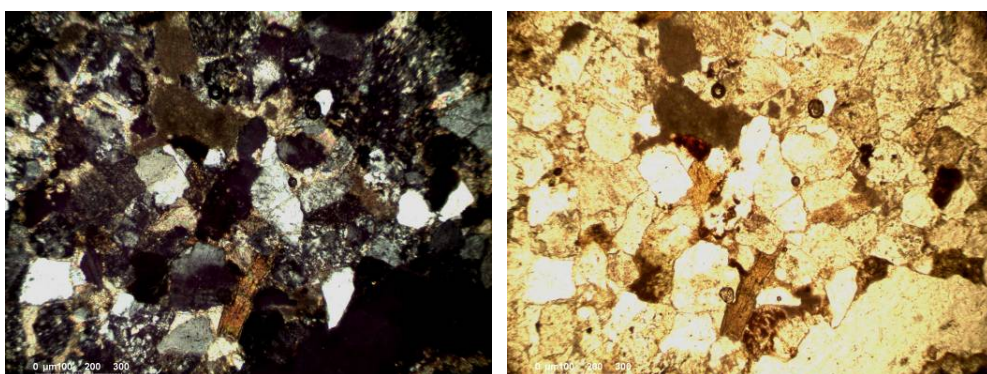


**Figure 4.56.** Thinsection photomicrograph of deteriorated sandstone from north terrace crossed nicols (right), single nicol (left)

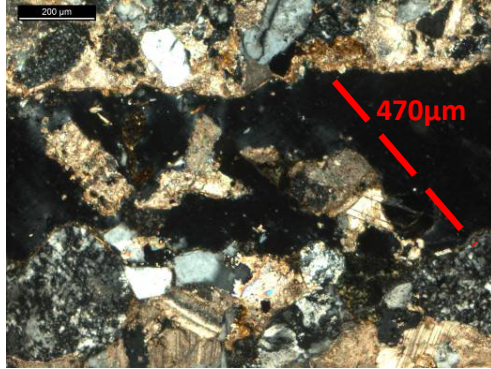


**Figure 4.57** Thin section photomicrograph of deteriorated sandstone from north terrace (crossed nicols), a closer look into the microcrack of about 470 $\mu$ m, detached minerals can be seen in the crack.

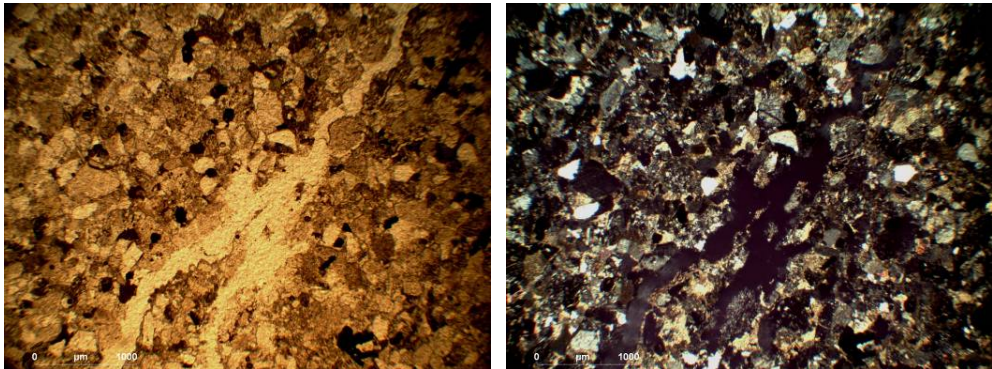


**Figure 4.58.** Thin section photomicrograph of naturally weathered sample (NS1) crossed nicols (left) and single nicol (right). A crack network can be seen.

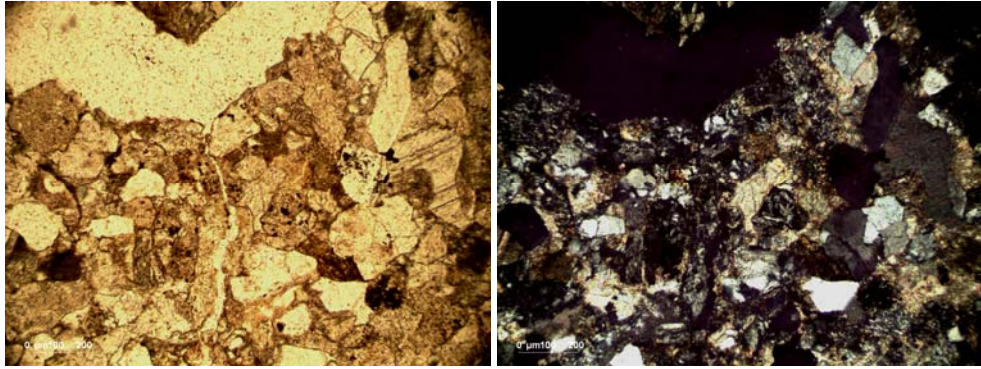


**Figure 4.59.** Thin section photomicrograph of deteriorated sandstone from east terrace, presence of opaque minerals, single nicol (left), crossed nicols (right).

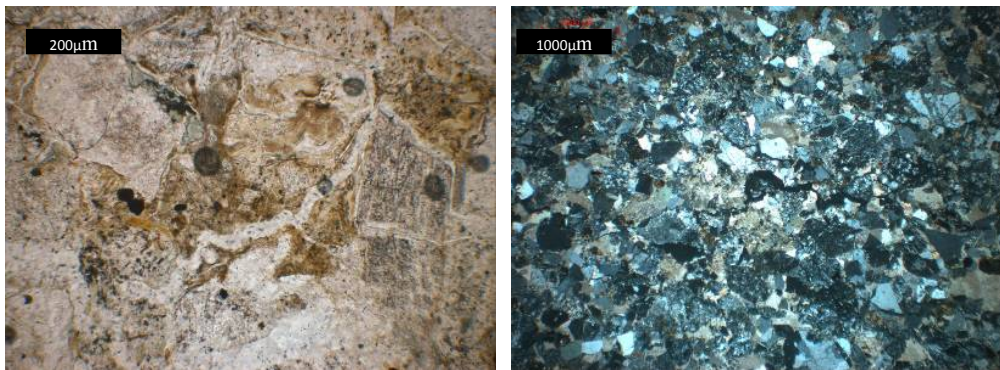


**Figure 4.60.** Thin section photomicrographs of artificially deteriorated sandstone presence opaque minerals single nicols (left) cross nicols (right).

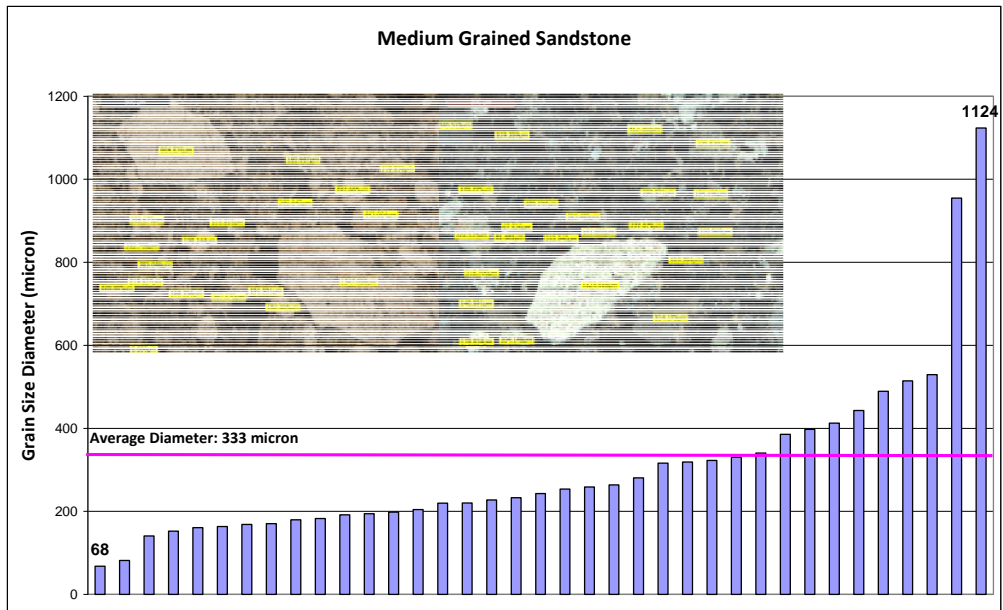


**Figure 4.61** Image analysis of medium grained sandstone. The average diameter was found to be 333 $\mu$ m.

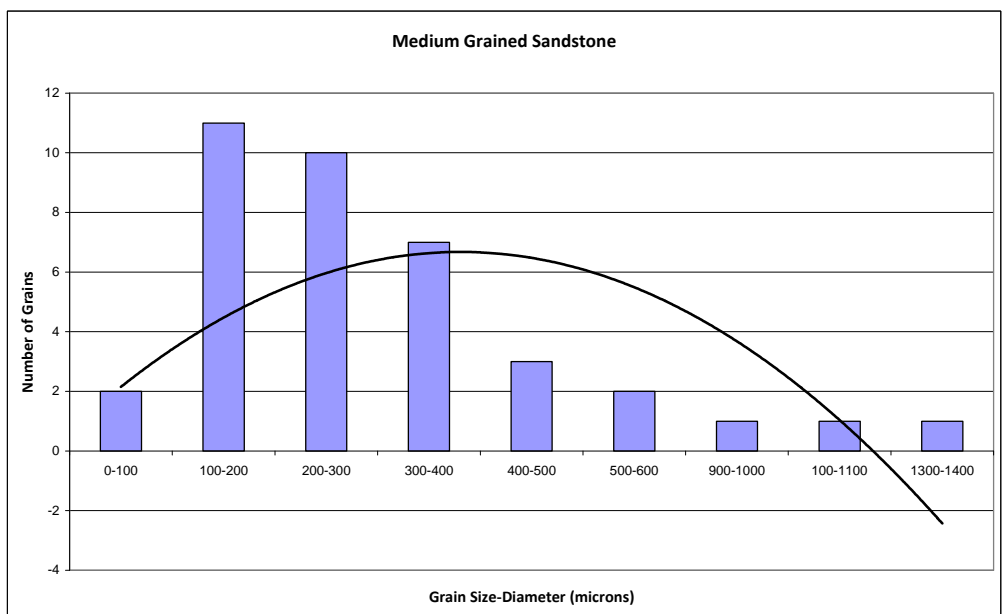


**Figure 4.62.** Frequency distribution of medium grained sandstone, it was found to be poorly sorted.

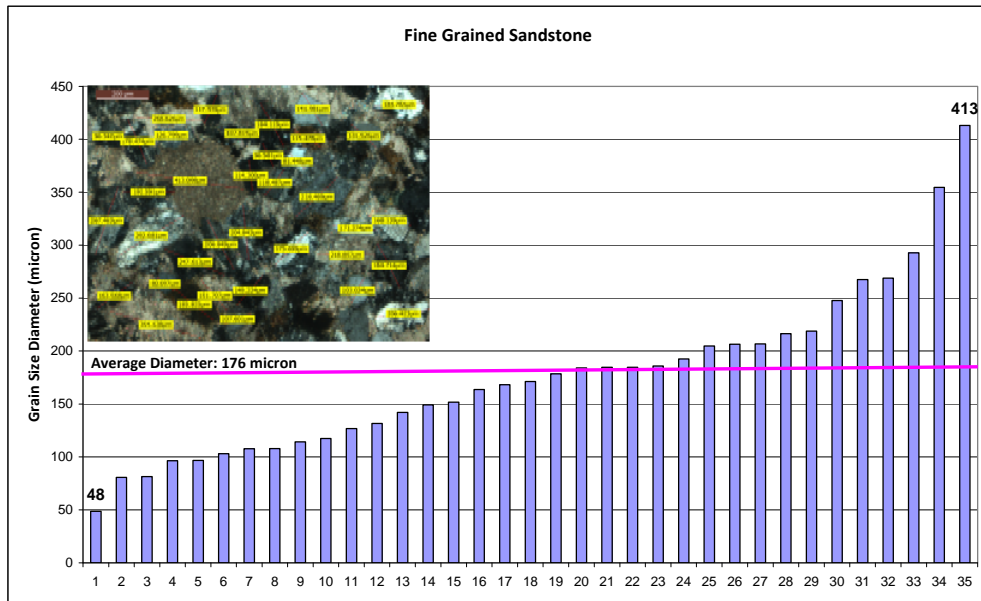


**Figure 4.63.** Image analysis of fine grained sandstone. The average diameter was found to be 176 $\mu$ m

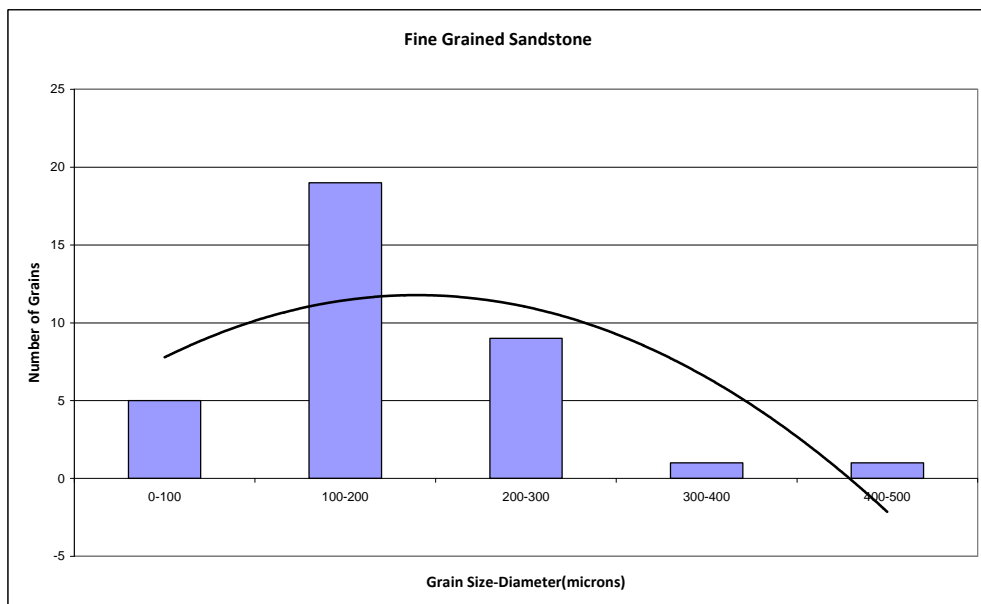


**Figure 4.64.** Frequency distribution of fine grained sandstone, it was found to be poorly sorted.

### 4.3.2 X Ray Diffraction (XRD) Analyses

XRD traces of powdered samples from the sandstone quarry of Nemrut, surface accumulations of a non treated sample, HCl treated powdered sandstone samples were obtained. XRD patterns of air dried, ethylene glycolated and heated clay extractions from non-deteriorated and deteriorated sandstones were studied for the identification of clay minerals. The extracted clay ratio was found to be 4% by weight in sandstones and that fraction was the same for deteriorated and nondeteriorated sandstones. The clayey accumulations between two scales of weathered sandstones were also studied by XRD analyses.

Fine grained and medium grained sandstones had the similar XRD traces, having the same main components such as quartz, calcite, and feldspars being anorthite and albites (Figure 4.65, 4.66). HCl treated sandstone powder showed the same peaks except the absence of calcite and the existence of chlorite (Figure 4.67).

The XRD analyses of the clays extracted showed the presence of chlorite and halloysite in the sandstones (Figure 4.70, 4.71). The clay fraction of the weathered sandstone also showed presence of chlorite and halloysite. Main chlorite peak at  $14^{\circ}\text{A}$  showed a minor shift to  $13.87^{\circ}\text{A}$  (Figure 4.71) in deteriorated layer upon ethylene glycolation. Accumulations between two detaching scales in the weathered sandstone also showed chlorite, illite, kaolinite and mixed layers having swelling characteristics (Figure 4.72).

During the extraction of clay minerals the iron oxides were collected magnetically and the XRD of that fraction was also studied. Maghemite/magnetite, hematite and goethite were the iron oxides detected by XRD (Figure 4.69).

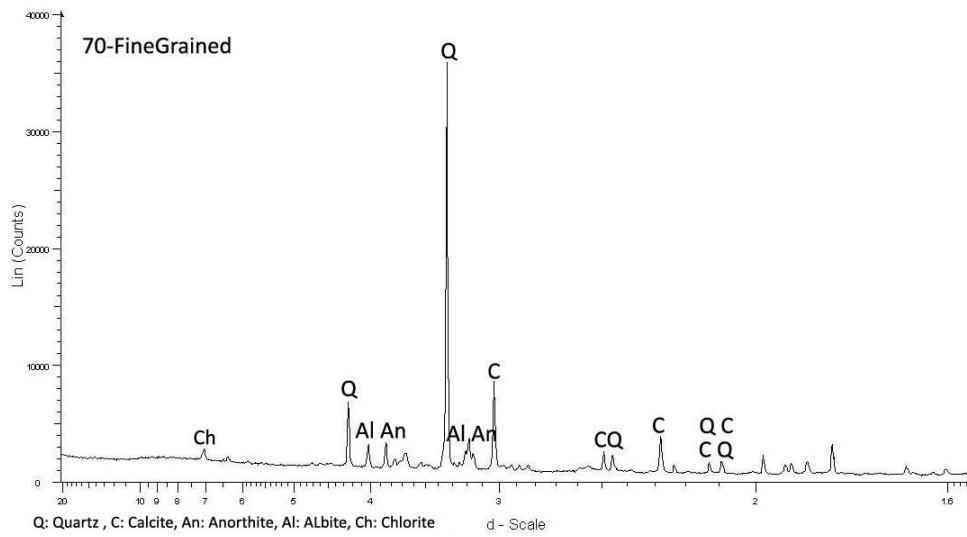


**Figure 4.65** XRD trace of fine grained powdered sandstone from Nemrut Quarry, C: Calcite, Q: Quartz, Al: Albite, An: Anorthite, Ch: Chlorite

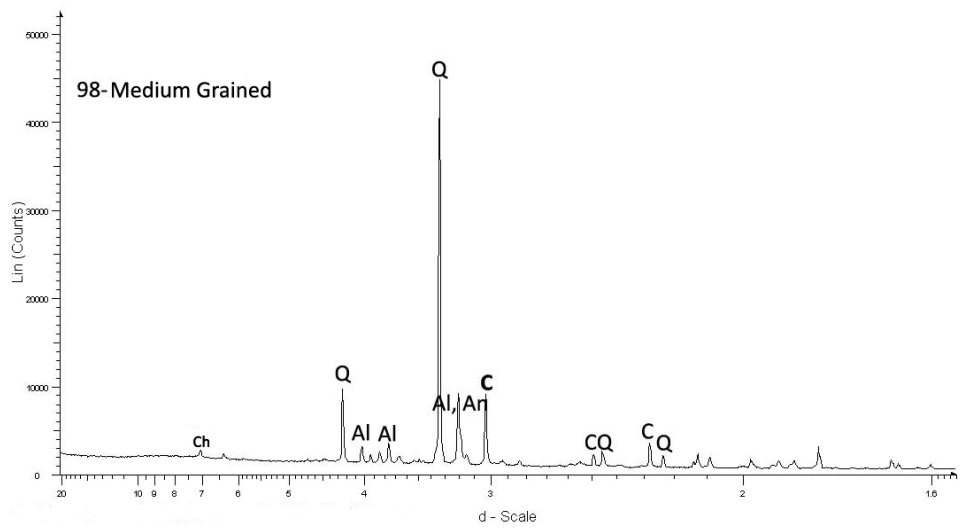


**Figure 4.66** XRD trace of medium grained powdered sandstone from Nemrut Quarry, C: Calcite, Q: Quartz, Al: Albite, An: Anorthite, Ch: Chlorite

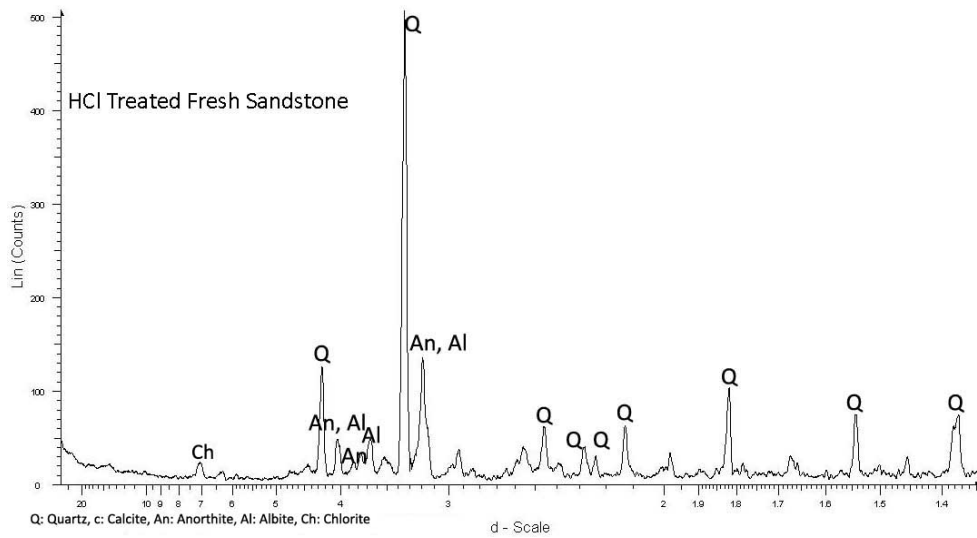


**Figure 4.67** XRD trace of HCl Treated powdered sandstone from Nemrut Quarry, C: Calcite Q: Quartz, Al: Albite, An: Anorthite, Ch: Chlorite.

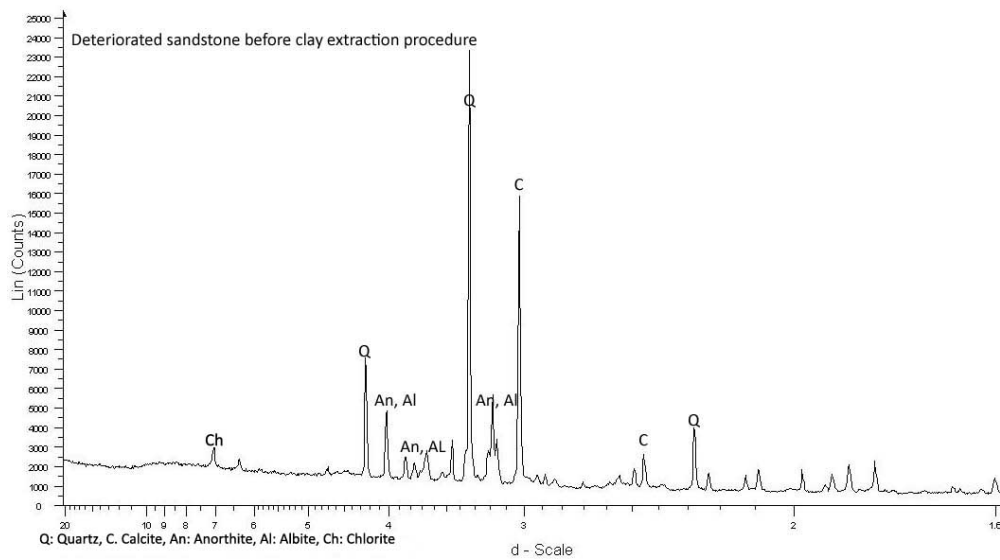


**Figure 4.68** XRD trace of powdered deteriorated sandstone before clay extraction , C: Calcite Q: Quartz, Al: Albite, An: Anorthite, Ch: Chlorite

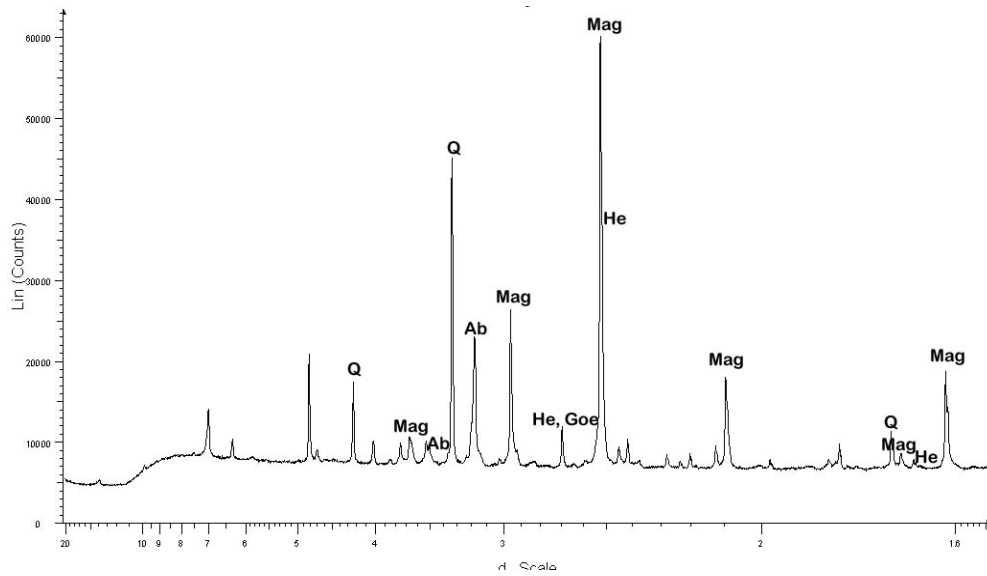


**Figure 4.69.** XRD trace of magnetically collected iron oxides during clay extraction procedure. He: Hematite, Goe: Goethite, Mag: Magnetite/Maghemite, Q: Quartz, Al: Albite

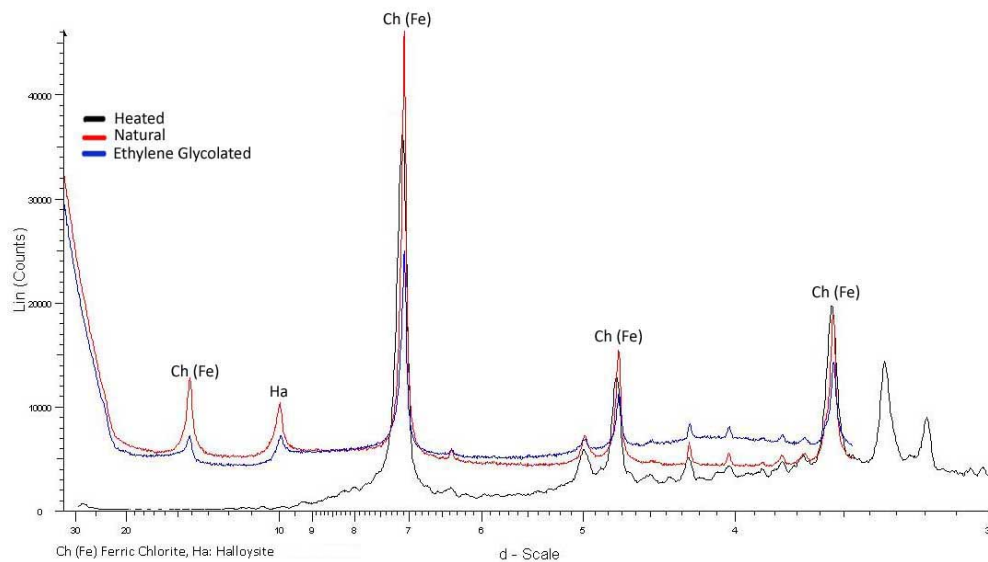


**Figure 4.70.** XRD trace of air dried, ethylene glycolated and heated clay extraction from nondeteriorated sandstone, Ch(Fe): Chlorite Ferric, Ha: Halloysite.

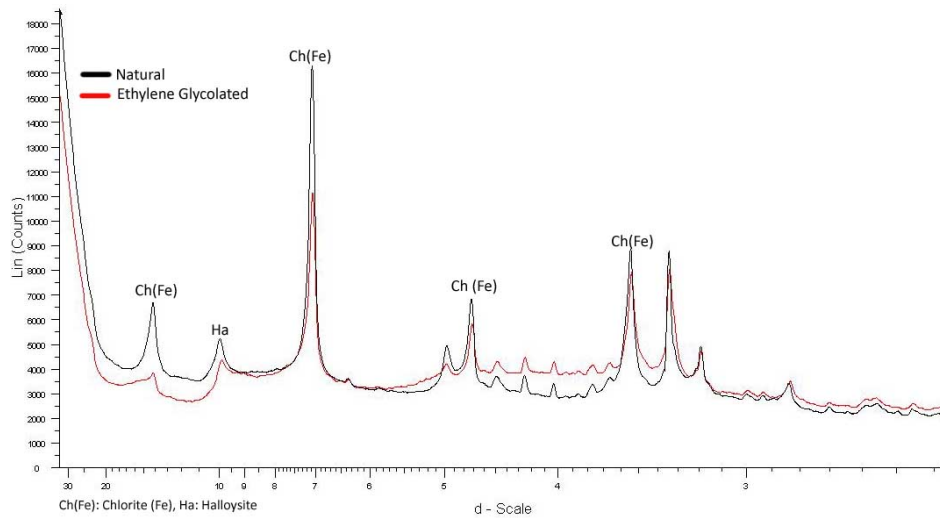


**Figure 4.71.** XRD trace of air dried and ethylene glycolated clay extraction from deteriorated sandstone Ch(Fe): Chlorite Ferric, Ha: Halloysite.

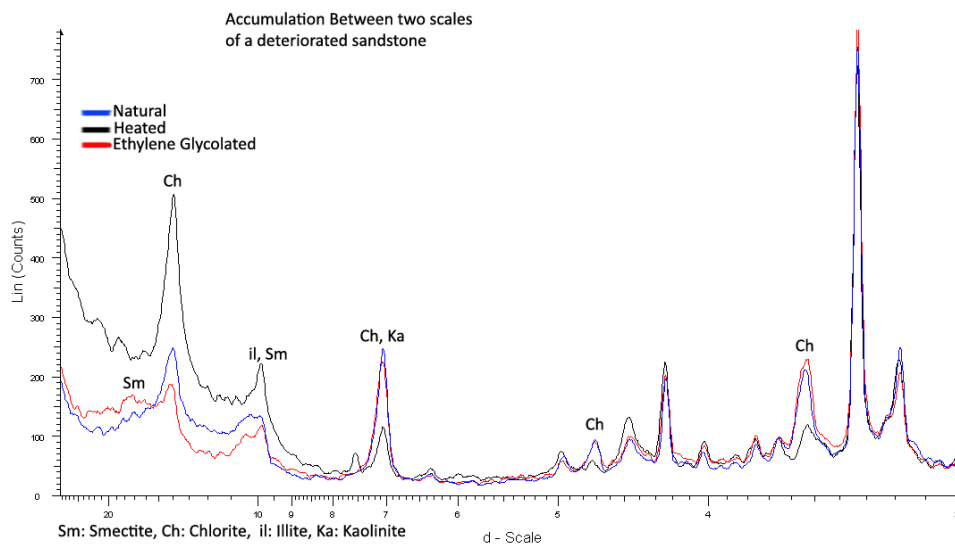


**Figure 4.72.** XRD trace of air dried, ethylene glycolated and heated accumulation between two scales of a naturally deteriorated sandstone sample, Sm: Smectite, Ch: Chlorite, Il: Illite; Ka: Kaolinite.

**Table 4.12** Observed “d values” of minerals in XRD traces

First three d values (Å) of unoriented samples			
Quartz	3.34	4.25	1.817
Albite	3.19 (4.03)	3.78 (3.22)	3.68 (6.39)
Anorthite	3.19 (3.20)	3.75 (3.18)	3.21 (4.04)
Calcite	3.03	2.28	2.09
Hematite	2.7	2.51	1.69
Magnetite	2.53	1.48	2.97
Maghemite	2.51	2.95	1.614
Gothite	4.18	2.45	2.69

### 4.3.3 CEC Determination by UV-Vis Spectrometry

The Cation Exchange capacity of the clay fraction extracted from both deteriorated and nonweathered sandstones were also studied as well as clayey accumulations between two detaching scales of a deteriorated sandstone (Figure 4.73, Table 4.13).

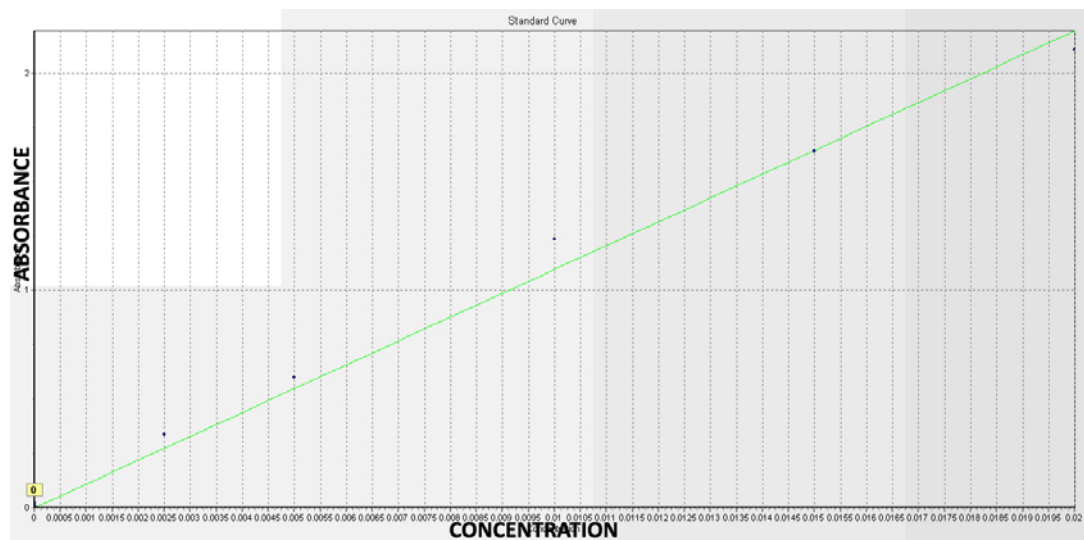


**Figure 4.73** Standard curve of methylene blue concentration versus absorption at 632 nm.

**Table 4.13** Determination of Cation Exchange Capacity by UV-Vis Spectrometry

Sample	mg	ml	Concentration (mg/ml)	spend mg/250ml	g/100g	CEC mEq/100g
Sandstone Powder	100	150	0.018	0.15	0.15	0.47
Deteriorated Sandstone Powder	100	150	0.018	0.15	0.15	0.47
Clayey Accumulation between two Scales of Weathered Sandstone	7.3	11	0.002	0.187	0.187	0.58
Kaolinite/Halloysite	From the literature (Caroll, 1974; Grim,1968)					3-15
Chlorite	From the literature (Caroll, 1974; Grim,1968)					10-40

The average value of CEC of the clay minerals in Nemrut sandstones were taken as 10 considering the literature values and the types of the clay minerals in the stone (Table 4.3). Using the measured CEC  $\sim 0.47$  meq/100g and the average CEC of the clay minerals in the Nemrut Mount sandstone taken as 10 meq/100g, the clay amount for non-deteriorated sandstone powders was calculated to be  $\sim 4.7\%$  by weight.

#### **4.3.4 Scanning Electron Microscopy (SEM) Coupled with Energy Dispersive X-Rays (EDX) Analyses**

The SEM images and the elemental mapping of pieces representing deteriorated sandstone scales revealed the existence of iron oxides and clay minerals, in the distribution maps of Si, Al, K, Mg and Na (Figure 4.74, 4.75). The SEM analyses have further verified the existence of clay minerals and iron oxides in the composition of Nemrut Sandstones (Figures 4.74 – 4.82).

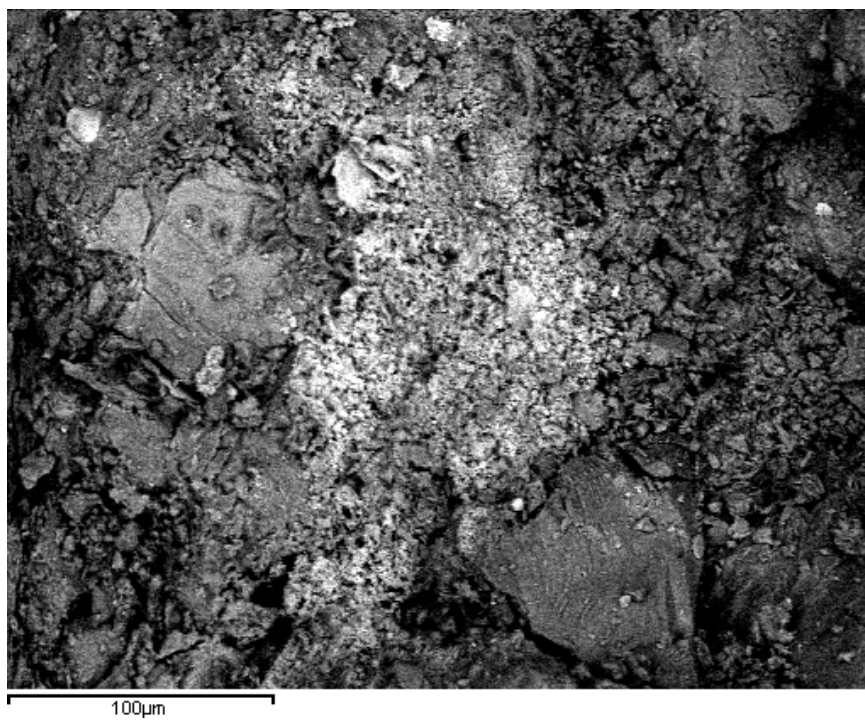
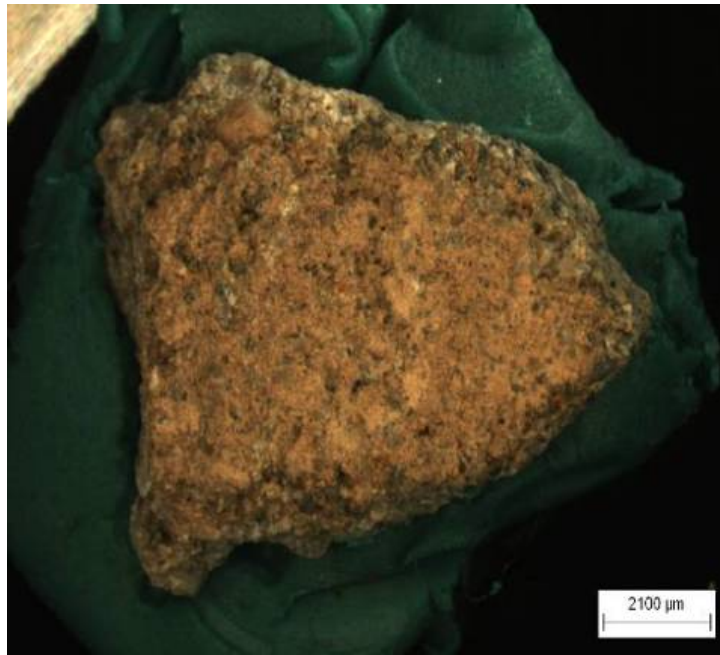


**Figure 4.74** Macro view of deteriorated sandstone sample (left), SEM image of interior face of deteriorated sandstone sample (right)

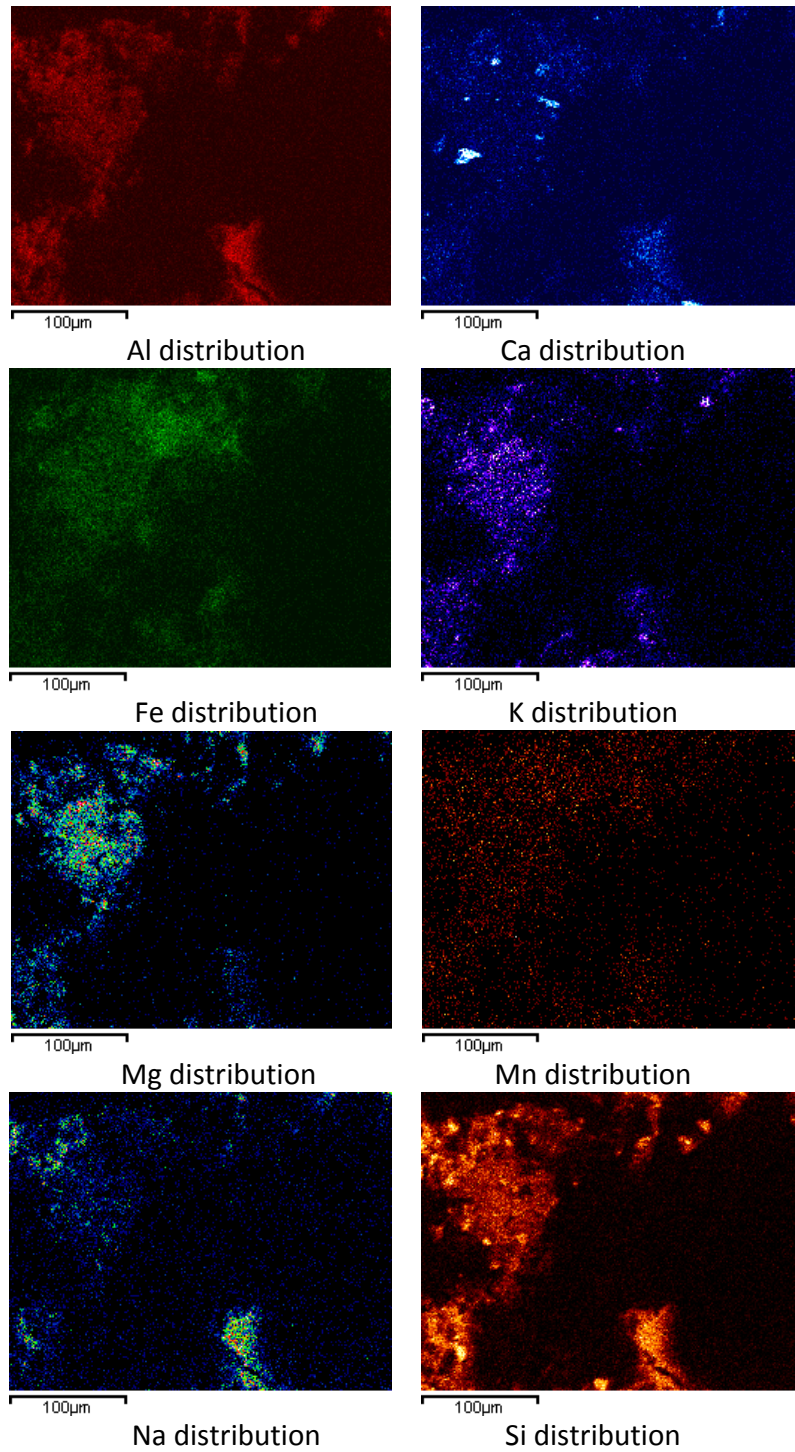


**Figure 4.75** Elemental (Ca, Al, K, Fe, Mn, Mg, Si, Na) mapping of surface of deteriorated sandstone sample.

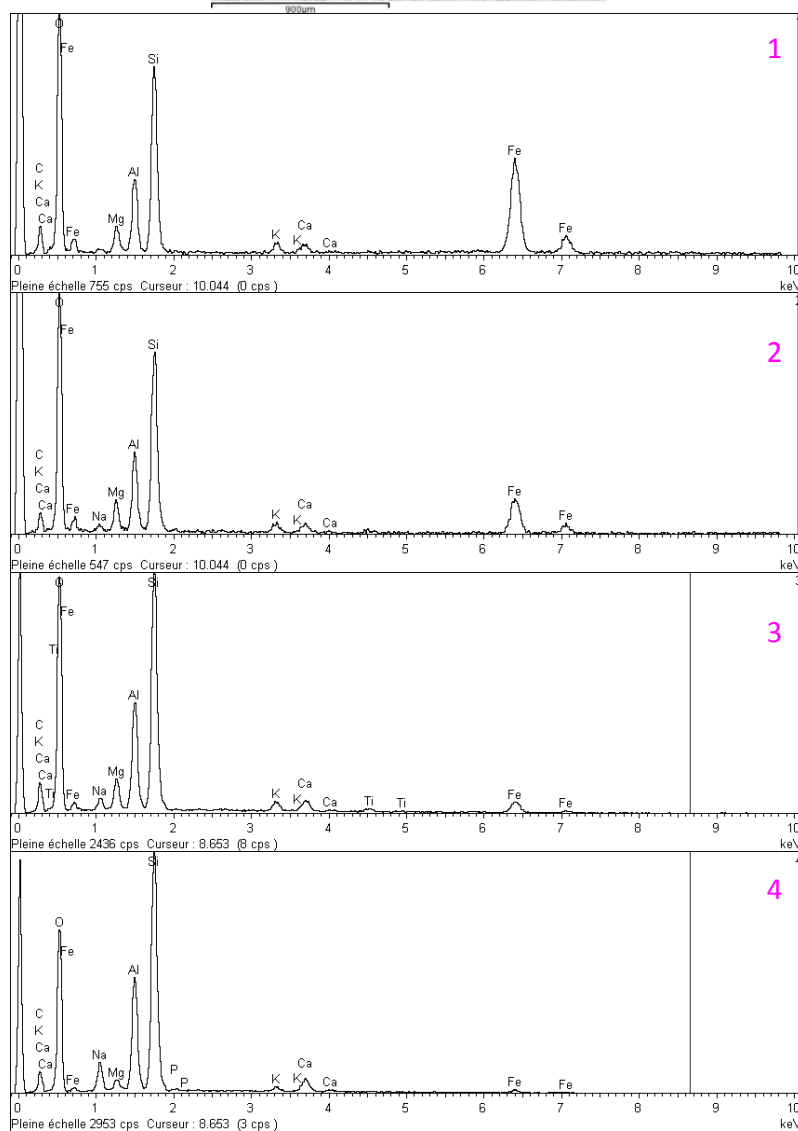
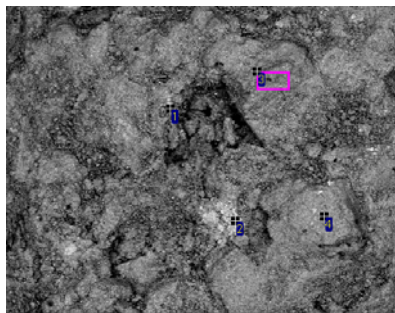


**Figure 4.76** SEM view from surface of deteriorated sandstone sample (on top) and EDX analyses from points (1, 2, 3,4) shown on the image.

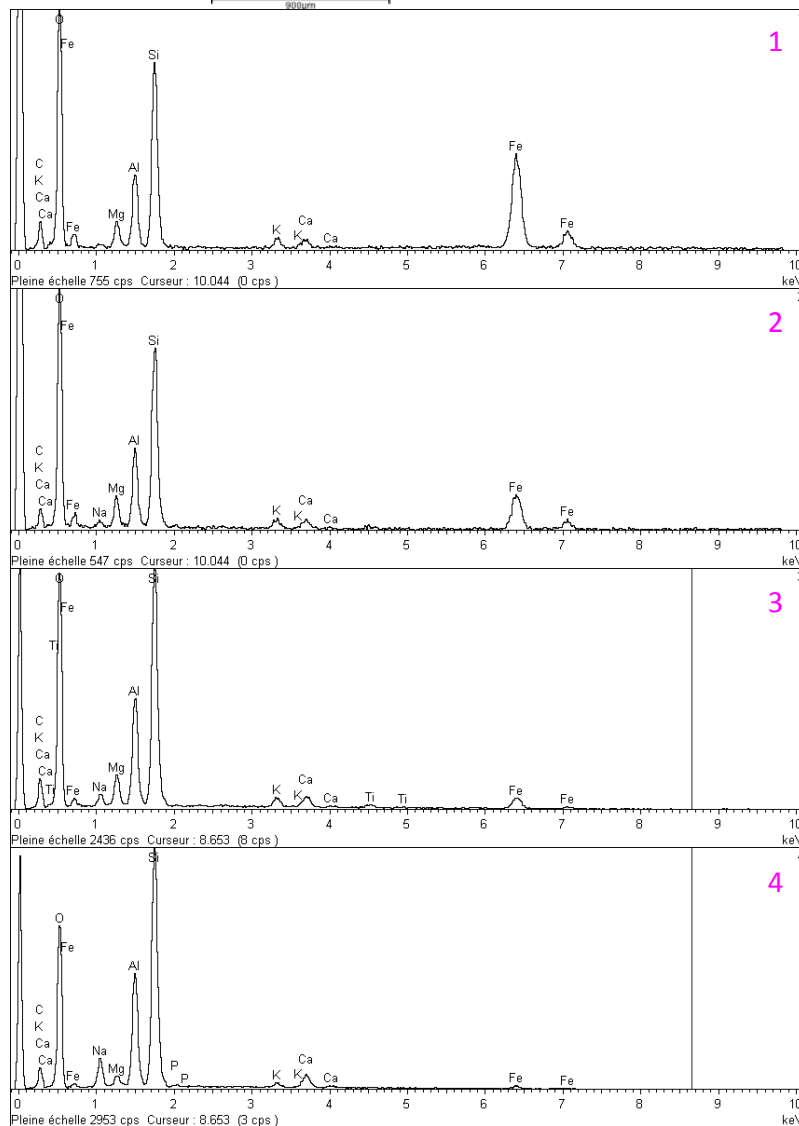
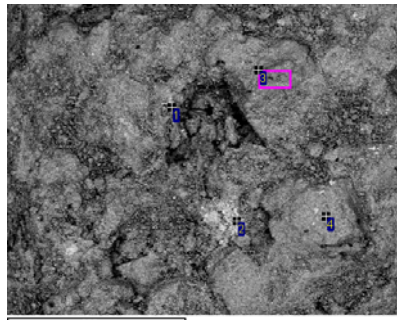


**Figure 4.77** SEM view from surface of deteriorated sandstone sample (on top) and EDX analyses from points (1, 2, 3,4) shown on the image.

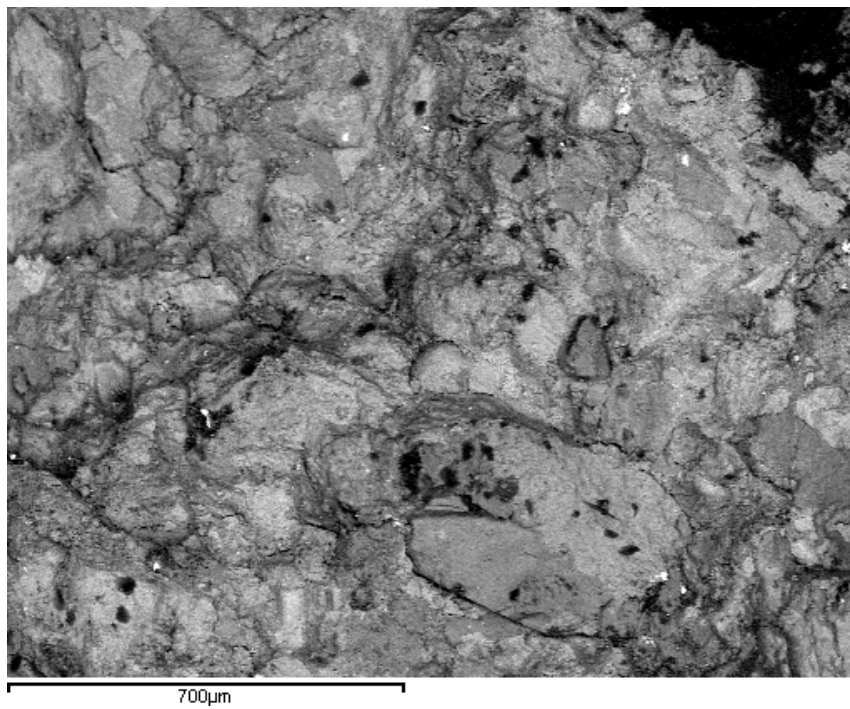


**Figure 4.78** Macro view of interior face of relatively nondeteriorated deteriorated sandstone sample (top), SEM image of interior face of deteriorated sandstone sample (bottom)

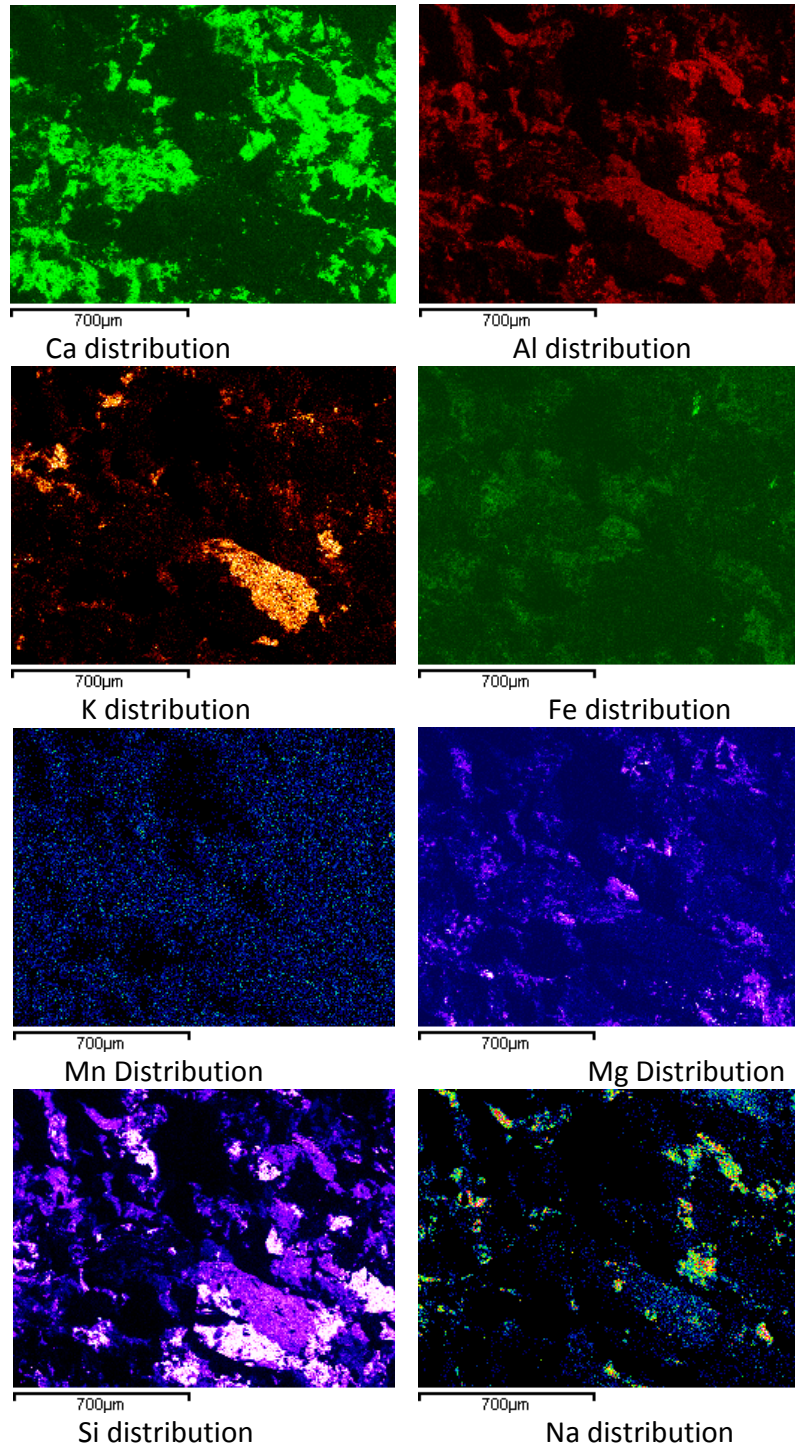


**Figure 4.79** Elemental (Ca, Al, K, Fe, Mn, Mg, Si, Na) mapping of interior face of deteriorated sandstone sample shown in Figure 4.77.

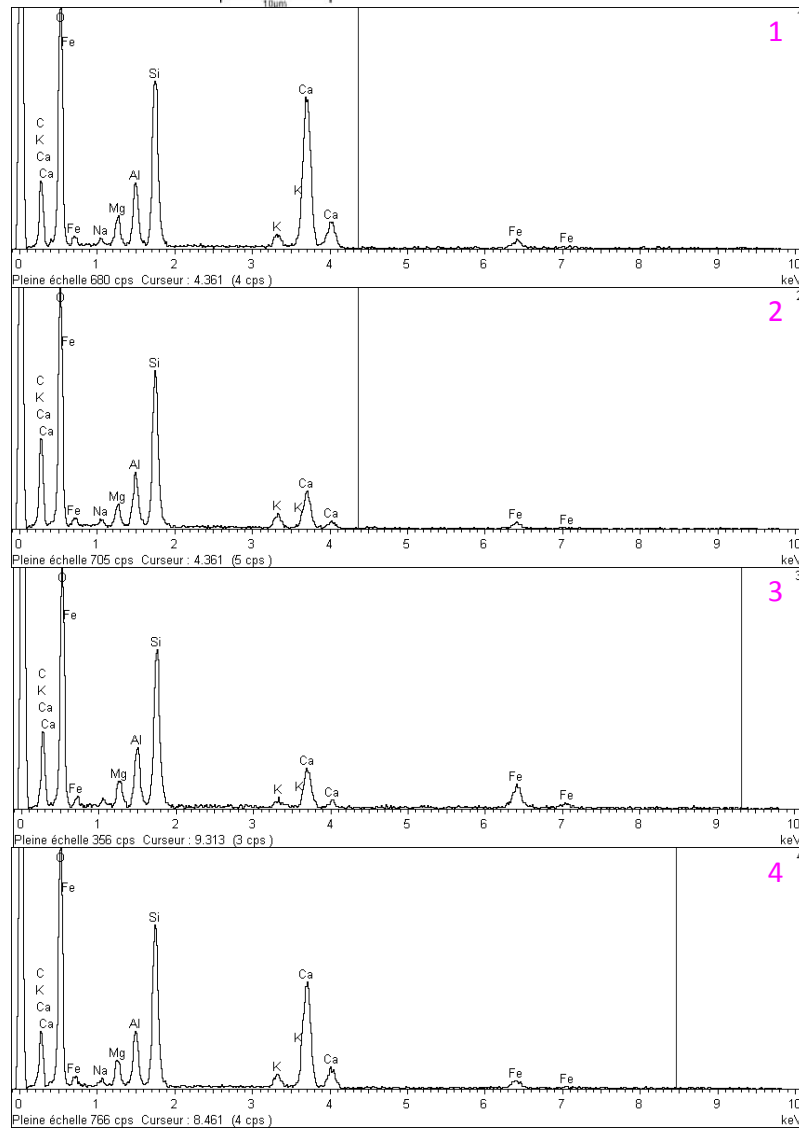
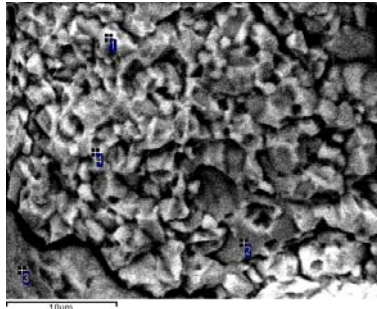


**Figure 4.80** SEM image of interior face of deteriorated sandstone piece (on top, and EDX analyses from points (1, 2, 3, 4) shown in image).

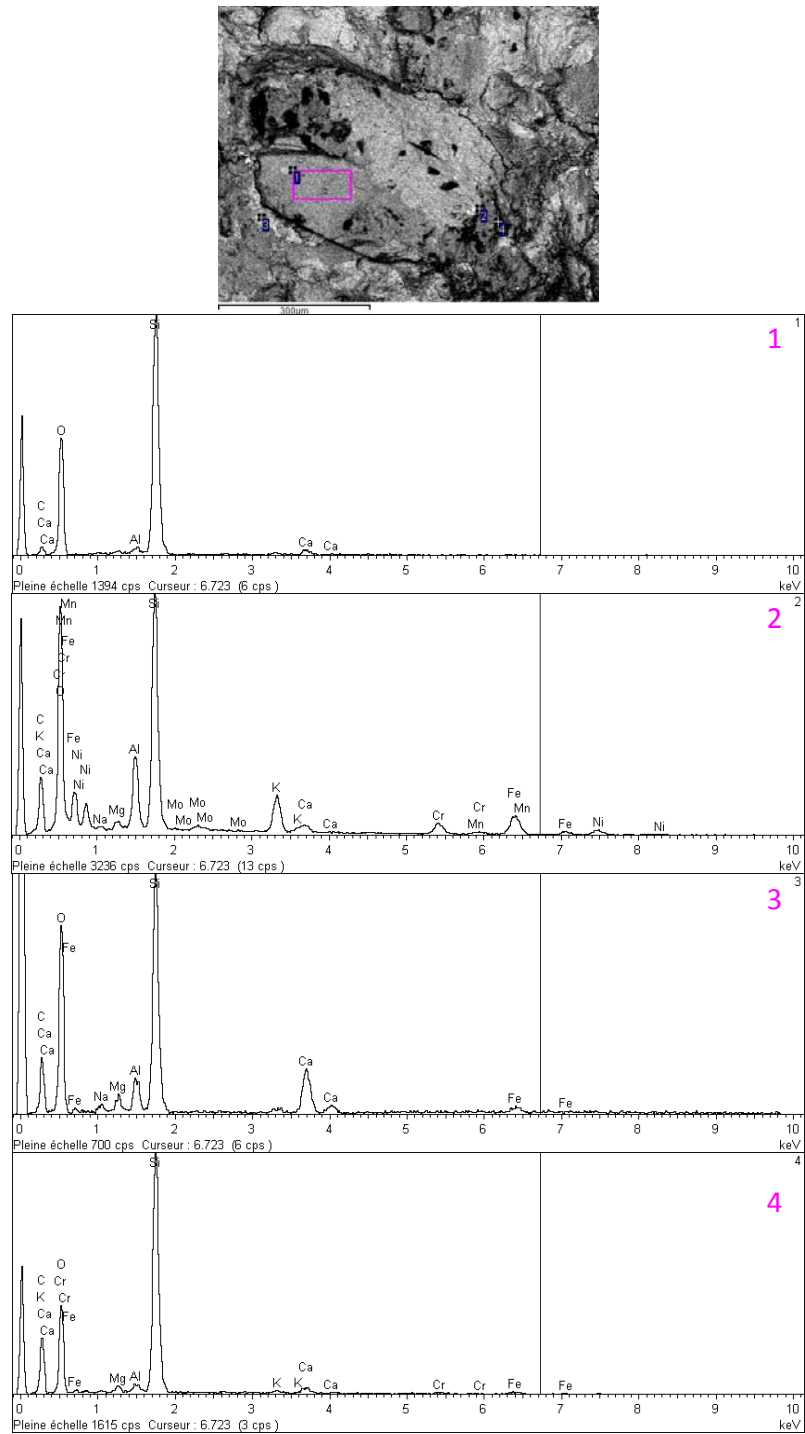


**Figure 4.81** SEM image of interior face of deteriorated sandstone piece on top, and EDX analyses from the points (1, 2, 3, 4) shown in image.

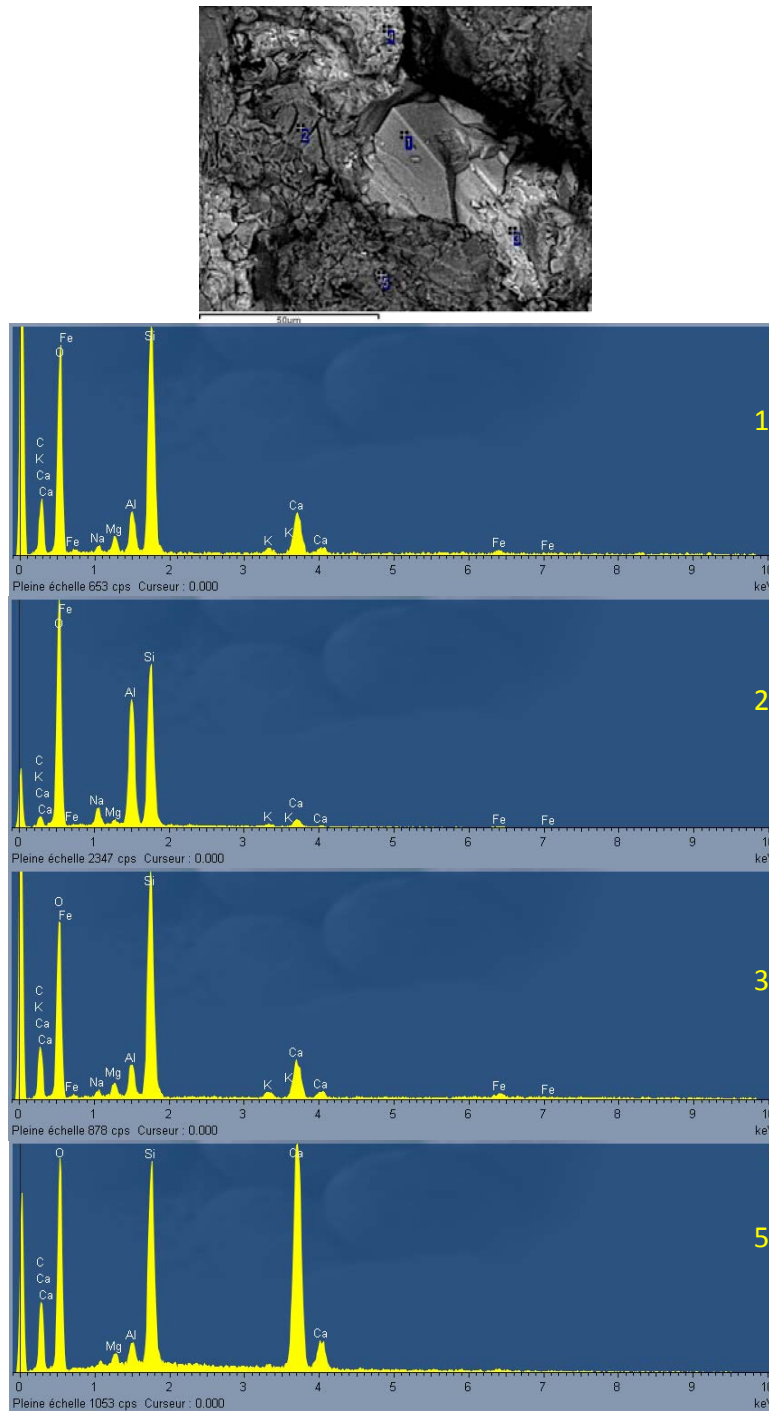


**Figure 4.82** SEM image of interior face of deteriorated sandstone piece on top, and EDX analyses from the points (1, 2, 3, 5) shown in image.

## **CHAPTER 5**

### **DISCUSSION**

In this chapter, experimental results of this study were evaluated and discussed under the titles “Characteristics of Nemrut Mount Sandstones”, “Factors Affecting the Deterioration of Nemrut Mount Sandstones” and “The Conservation Treatments Targeted to the Control of Deterioration”.

#### **5.1 Characteristics of Nemrut Mount Sandstones**

Nemrut Mount Monument sandstones were examined by using the representative samples from the site and from the quarry nearby. Results of analyses were used to describe microstructural characteristics of Nemrut Mount sandstones and their physicommechanical properties. As described before (see Chapter 1 Introduction, p.8) both the quarry samples and sandstones used in the site belong to “Lice Formation” and they show similar weathering forms, e.g. separation by layering was widespread both in the quarry and at the site.

##### **5.1.1 Micro-Structural Characteristics of Nemrut Mount Sandstones**

The sandstones of Nemrut consisted of considerable range of rock fragments and minerals such as limestones, granite, quartzite and minerals as feldspars, quartz, biotite and clay minerals (Figures 4.47, 4.48). Chlorite (Figures 4.47, 4.60) and opaque

minerals were observed in the thin sections (Figures 4.47-4.60). Those fragments of rocks and minerals were in a fine grained carbonatic-clayey matrix. The fabrics of sandstones were generally matrix supported, in addition, grain supported matrix and point contacts were also observed. Sandstones of Nemrut had parallel/flat bedding. They were classified as fine and medium grained sandstones. Medium grained sandstones had average grain size as 333 $\mu$ m with a range of 1300 to 60 $\mu$ m (Figures 4.61, 4.62). Fine grained sandstones had average grain size as 176 $\mu$ m in the range of 40-450 $\mu$ m (Figures 4.63, 4.64). Both fine and medium grained sandstones were poorly sorted sandstones (Figures 4.62, 4.64).

In their study, Heinrichs and Fitzner (2007) classified the Nemrut sandstones as “lithic greywacke” or “feldspathic greywacke”, since the characteristics of the greywacke is the fine grained matrix with intergrowth of chlorite and silt-sized (0.063-0.04mm) grains of quartz and feldspars (Tucker, 2001). In this study, since the samples having grain supported matrix and point contacts were also observed, the samples studied were defined as sandstones.

The main components of sandstones were verified through the XRD analyses as being quartz, feldspar, calcite and some clay minerals (Figures 4.65-4.67). There were no compositional differences in the main components of medium and fine grained sandstones (Figures 4.65, 4.66). The XRD analyses of the clays extracted showed the presence of chlorite and halloysite in sandstones (Figures 4.70, 4.71).

Chlorites and halloysites are known to be non-swelling clay minerals (Moore and Reynolds, 1997; Carroll, 1970). It should also be mentioned that the chlorites have been shown to gain some swelling layers upon weathering (Wangler et al., 2008).

Opaque minerals in the Nemrut sandstones were analyzed by XRD using magnetic separation (Section 4.3.2). The existence of magnetite/maghemite, goethite and

hematite minerals were verified in the composition of Nemrut Mount sandstones (Figure 4.68).

### **5.1.2 Physical and Physicomechanical Properties of Nemrut Sandstones**

The sandstone cubes of the Nemrut quarry had colors brownish, greenish and greyish color as observed by naked eye however and they fell into the same group of CIEL\*ab colors (Figure 4.22, Table 4.7).

Sandstones of Nemrut Mount Monument had high bulk density and low effective porosity values with good physicomechanical properties (Figure 4.4, Table 4.1, Figure 4.31, Table 4.8). Bulk density of the sandstone cubes from the quarry were found to be between 2.48 g/cm<sup>3</sup> and 2.66 g/cm<sup>3</sup>, with an average value of 2.58 g/cm<sup>3</sup>. Their effective porosities were found to be between 0.43% and 6.05% with an average value of 3.57% (Table 4.8).

The ultrasonic velocity measurements of sandstone cubes showed directional differences. Generally, one of the UPV values was smaller than the other two, that could be linked to the bedding direction of the sandstones since the UPV values are smaller for the measurements perpendicular to the bedding planes when they were clearly observed (Figure 4.4, 4.8, 4.9). That aspect, UPV values being smaller in one direction than the other two, was in accordance with the all UPV measurements at the site and in the laboratory (Figure 4.8, 4.9, Table 4.2, 4.3).

The pore size distribution characteristics of Nemrut Sandstones were studied by Mercury Porosimetry and their distribution were followed in the range of 100-0.01 μm.

The medium grained sandstones were found to have lower effective porosity (~0.8%-1.5%) than the fine grained ones (~ 5.2%) (Figure 4.32). In the medium grained sandstones the effective porosity was formed mainly by the pores having diameters of 100 $\mu$ m (Figure 4.32). In the fine grained sandstones majority of the pores had diameters in the range of 0.5  $\mu$ m (Figure 4.32).

In this study hydric, thermal and hygric dilatation properties of Nemrut Sandstones were followed in the laboratory for the cyclic wetting-drying conditions, thermal changes between 0 - 45°C and relative humidity changes between 15 – 95% respectively.

Hydric dilatation of medium and fine grained sandstones perpendicular to the bedding plane was about 0.32 $\mu$ m per millimeter (Figure 4.40). While the maximum expansion during wetting was reached in a few hours the contraction through drying takes longer time being around 30 hours in laboratory conditions (Figure 4.40). It has to be taken into consideration that, in the site conditions, drying takes shorter time. It was observed that the saturated sandstone cubes of 5cm size dried out in 6 hours (Figure 4.45) in a September day at 23°C and 30% RH with a windspeed of ~3.6 km/h.

The thermal dilatation of medium and fine grained sandstones perpendicular to bedding plane was around 0.35 $\mu$ m per millimeter between 0 - 45°C (Figure 4.39).

The dilatation perpendicular to bedding at 95 % RH was 0.01 $\mu$ m per millimeter for fine grained sandstones and 0.06 $\mu$ m per millimeter for medium grained sandstones (Figure 4.38). There is limited data on hydric, hygric and thermal dilatation characteristics of sandstones used in the historic monuments. The sandstones used in the construction of Strasbourg Cathedrale had the hydric dilatation values between 0.14-0.18  $\mu$ m/mm (Mertz et al., 2004). When compared with the sandstones of Strasbourg Cathedrale hydric dilatation value of Nemrut Sandstones (0.32 $\mu$ m/mm) can be considered rather high.

Nemrut Sandstones contained clay minerals chlorite and halloysite. Although they are non-swelling type of clay minerals, estimation of their amount and their cation exchange capacity was of importance for the understanding of their weathering behavior. Clay minerals were estimated to be around 4% by gravimetric analyses of clay minerals separated by extraction from finely powdered sandstone.

Clay mineral amount of sandstones was also tried to be estimated by the measurement of their Cation Exchange Capacity (CEC) with methylene blue adsorption using UV-Vis Spectrometry (Potgieter and Strydom, 1999; Ramasamy and Anandalakshmi, 2008; Shooneydt and Heughebaert, 1991). Using the CEC  $\sim 0.47$  meq/100g for non-deteriorated sandstone powders, the amount of clay in 100g of sandstone was calculated to be  $\sim 4.7\%$  by weight. That value seemed to be in accordance with the clay mineral amount found by gravimetric method (Section 4.3.2). Those clay minerals were homogeneously distributed in the clay matrix as determined in thin section analyses (Figure 4.47, 4.48, 4.53 – 4.55).

## **5.2 Factors Affecting the Deterioration of Nemrut Mount Sandstones**

The changes in Nemrut Sandstones during two thousand years of exposure to atmospheric conditions and the most important weathering factors which contribute to those changes were tried to be derived through analyses at the site and in the laboratory. In the site investigations, mapping of visual weathering forms, UPV measurements and QIRT analyses were carried out. In the laboratory investigations the changes in physical and physicommechanical properties and the changes in microstructural characteristics of sandstones were studied. The results of those investigations were discussed in the following titles.

### 5.2.1 Weathering forms and state of deterioration

The site of Nemrut Mount Monument possesses the weathering forms mainly as separation by layering especially along the bedding planes, back weathering due to loss

of scales, cracking, granular disintegration, rounding/notching and discoloration/biological deposition (Figure 4.1, 4.2). The most important weathering forms of Nemrut Sandstones were material loss due to i) loss of scales and ii) granular disintegration (Figure 4.1, 4.2).

The weathering had an effect on the color of the sandstones, discoloration of the sandstones could be observed in all over the site. The color change in sandstones was studied in the laboratory during the artificial weathering of sandstone cubes by salt crystallization (Figure 4.23-4.27). The color measurements of artificially weathered sandstone cubes after 10<sup>th</sup> and 15<sup>th</sup> cycles of salt crystallization were carried out (Figure 4.23-4.27). The color changes of sandstones were visible to eye even after the 5<sup>th</sup> cycle of salt crystallization (Figure 4.23). Main difference was in “b” –yellow-blue– component of the color which indicates a yellowing; a slight change is also existed in “a” –red-blue component– thus a browning of the sandstones is observed through weathering (Figures 4.23, 4.25, 4.27). The results of those measurements may indicate that wetting and drying cycles at the site could be responsible from those color changes. Deterioration by salt crystallization was not observed at the site, but salt crystallization cycles in the laboratory were obviously accompanied by wetting and drying phenomena.

The state of deterioration in sandstones were estimated in situ, by using nondestructive methods namely UPV. In situ UPV measurement could only be done by indirect measurements. Reference data for the evaluation of UPV measurements

were established in the laboratory by direct and indirect modes, UPV values of sandstones at different degree of deterioration were obtained by using the deteriorated sandstone samples subjected to salt crystallization cycles. The changes in UPV values of sandstones were also determined in water saturated state (Figures 4.7-4.10; Tables 4.2-4.4).

Increase in degree of deterioration resulted in decrease in UPV values in dry state, while wetting had further decreased the UPV measurements (Figures 4.4-4.6). Water saturation affected UPV values of deteriorated sandstones there was considerable drop in their indirect UPV measurements. In fresh sandstone, water saturation did not have considerable effect on UPV measurements only a small decrease in their indirect UPV measurements was observed. Indirect measurements were always a little lower than the direct ones (Figure 4.7-4.10; Tables 4.2-4.4). It was quite impossible to make in situ direct UPV measurements at any part of the sandstones (Figures 4.11-4.14). Therefore indirect UPV measurements were done at the site.

Reference data produced in the laboratory (Figures 4.3-4.10; Tables 4.1 – 4.4) showed that the indirect UPV values of sandstones  $UPV_{INDIRECT} < 1000\text{m/s}$  could indicate very deteriorated areas, whereas,  $UPV_{INDIRECT} 1000\text{m/s} - 2000\text{ m/s}$  could indicate the deteriorated areas and  $UPV_{INDIRECT} > 2000\text{ m/s}$  could indicate quite sound areas.

The sandstones with granular disintegration had UPV values generally below 1000 m/s indicating lower physicochemical properties (Figures 4.11, 4.12). On the other hand, the detaching scales themselves had  $UPV_{INDIRECT}$  values between 1000-2500 m/s indicating sufficient physicochemical properties (Figures 4.14, 4.17). Thus, it could be said that sandstones showing granular disintegration as deterioration type had poorer physicochemical properties than the detaching scales.

QIRT analyses of very deteriorated areas and deteriorated areas with granular disintegration showing low  $UPV_{INDIRECT}$  values, have indicated that their thermal inertia

was lower: detaching scales were detectable in the differential IR images and their thermal inertia characteristics were better than the areas showing granular disintegration (Figures 4.18-4.20). Another observation gathered by QIRT analyses was the effect of direct sunlight on the sandstones surfaces, i.e., when the atmospheric temperature was about 22.8°C the surface temperature of the sandstone could reach to about 40.4°C.

The changes in bulk density and effective porosity of the sandstones at different degree of deterioration were estimated by the data obtained in the laboratory with salt crystallization cycles (Figures 4.31-4.32, Tables 4.9 - 4.11). The effective porosity has increased gradually while the bulk density decreased during the artificial weathering by salt crystallization (Figures 4.31, 4.32; Tables 4.9 - 4.11).

The pore size distribution of weathered surface of the sandstones and relatively nonweathered interiors were studied by Mercury Porosimetry. It was seen that the total porosity of the weathered surface of the sandstones that exhibited granular disintegration was about 6% whereas its relatively unweathered deeper part had 4.5% of effective porosity. Pore size distribution of the weathered part has shown that while the fine pore percentage stayed the same, medium size pores increased when compared with deeper part of the stone, and the average pore diameter have slightly shifted to a higher value (Figures 4.32, 4.33). That was in accordance with the findings of Heinrich & Fitzner (2007) although they have found higher total porosity (11%) of surfaces with granular disintegration. In the detaching scales, total porosity of the weathered exterior surface was about 4.5%, whereas the detaching surface having clayey accumulation was 3.3% (Figures 4.34, 4.35). On the other hand, pore size distribution of detaching scale at the weathered exterior surface showed an increase in both fine and medium pore sizes. Most of the pores being in the fine pore sizes at the interior surface of the scale could be explained by the accumulation of clays on those surfaces (Mertz, 1991).

Pore size distributions of the artificially weathered sandstones from 10<sup>th</sup> (Figure 4.36) and 18<sup>th</sup> (Figure 4.37) showed that, as the salt crystallization cycles were repeated the total porosity has increased, the pores of sizes 0.9 to 5  $\mu\text{m}$  have shifted to 10 to 50  $\mu\text{m}$ .

However, there was no change in the percentage of finest pores. This type of enlargement of the pores was attributed to the weathering by salt crystallization cycles.

In summary, the average porosity of sandstones considerably increased in the deteriorated areas showing granular disintegration. Whereas in the areas showing material loss and detachment of scales, the change in average porosity of the scales were limited. That may signify the relative soundness of the scales in comparison to the granular disintegration surfaces.

### **5.2.2 The change in the microstructure of sandstones by weathering**

In the thin section analyses of deteriorated sandstones, the micro crack formations parallel to each other were observed which indicated the increase in the porosity (Figures 4.50-4.52, 4.56-4.59). Those micro cracks were the regions for the accumulation of clay minerals together with the iron oxides (Figure 4.49 4.51, 4.55). However, during the examination of micro cracks in thin sections their location and/or formation could not be associated with any mineralogical and petrographical characteristics of Nemrut sandstone. Chlorite (Figures 4.50 – 4.53) and opaque minerals were observed in the thin sections of weathered sandstones as well as non-weathered ones (Figure 4.49 - 4.60). More detailed analyses of clay mineral components and iron oxides seen as opaque minerals in thin sections were of

importance for the assessment of the major factors contributing to the deterioration of sandstones.

In the XRD traces, no difference in the composition of major components was observed between the deteriorated surface layers and relatively interiors of sandstones. Observed minerals were quartz, feldspar, calcite and some clay minerals (Figures 4.65, 4.66, 4.68).

Clay minerals were extracted and analyzed in more detail. The clay fraction of weathered sandstone showed the presence of chlorite and halloysite. Main chlorite peak at  $14^{\circ}A$  showed a minor shift (Figure 4.71) in deteriorated layer upon ethylene glycolation. That could be interpreted as formation of some swelling layers in chlorite structure through weathering. Accumulations between two detaching scales in the weathered sandstone did also showed chlorite, illite, kaolinite and mixed layers having swelling characteristics (Figure 4.72). That could be attributed to the accumulation of clay minerals in between the detaching scales carried by the wind from the site and geological formations around.

Swelling character of clay minerals between detaching scales was an important factor that may contribute to loss of scales. Estimation of their swelling nature were further done by CEC measurements. CEC measurements of weathered and nonweathered sandstone powders showed no difference in their CEC (Table 4.13) expressed that could be interpreted as the amount of clay minerals in weathered sandstone and non-weathered parts stayed the same in their microstructure. However, clay minerals that were accumulated in the cracks between the detaching scales from outside had much higher CEC (0.58 meq/100g) signifying their swelling nature and contribution to detachment and loss of scales (Table 4.13).

Ironoxides observed as opaque minerals in thin sections were further studied by their extraction from the powdered sandstone by magnetic separation. Existence of iron

oxides were verified as magnetite/maghemite, haemetite and goethite by XRD. The movement of iron oxides in the sandstone microstructure must have been possible during wetting and drying cycles of sandstones at the site. The iron oxides such as hematite are the well known accessory minerals in the sandstones (Tucker, 2001). Under certain conditions they undergo various phase transformations in aqueous media or in solid state, thus the different phases of iron oxides can be used also to understand the weathering environment of the sandstone. The stability of the iron oxides under different conditions was studied by different authors (Monnier *et al.*, 2008, Gotic, *et al.*, 2007, Dromgoole and Walter, 1989, Barnes *et al.*, 2009, Sun, *et al.*, 2004). Although a certain consensus was not reached about the activity of different phases under different conditions; magnetite, maghemite and goethite were accepted as the non-reactive phases whereas lepidocrocite, ferrihydrite and ferrioxyhite considered as reactive phases (Monnier *et al.*, 2008; Schwertmann and Taylor; 1989). Furthermore, different authors tried to define the ratio of stability by using the ratio of different phases of the iron oxides probably ferrihydrates (Monnier *et al.*, 2008; Schwertmann and Taylor; 1989). It is difficult to judge the reactivity of those phases of iron oxides found in XRD traces such as magnetite/maghemite, goethite and hematite which were known to be the non reactive phases. However, the not well crystallized forms of iron oxides, e.g., goethite, were known to be reactive. Abundance of colloidal iron oxides observed in the thin sections of Nemrut sandstones can be taken as an indicator of their movement in the sandstone during wetting and drying cycles (Figure 4.48-4.53). The clay minerals are expected to have an effect on the iron oxides' mobility and transformation of one phase to another since the high cation exchange and adsorption capacity of clay minerals have an effect on concentration, pH, ionic strength etc. (Caner, 1978). In summary, clay minerals contributed to the deterioration through their swelling nature, and their effect on the mobility and phase changes of iron oxides during wetting and drying cycles.

SEM images of the deteriorated sandstones further verified that existence of clay minerals and iron oxides in accumulations between two detaching scales in the weathered sandstone (Figures 4.74-4.81). The distribution of Si, Al, K, and Mg also indicated the existence of the clay minerals that were detected by XRD as chlorite, illite, kaolinite and swelling clay mineral (Figures 4.74, 4.75). The elemental point analyses showed the existence of the iron oxide rich areas on the same surface together with the clayey accumulation (Figures 4.77, 4.78).

The SEM images and the elemental mapping of the same piece's interior part of the scales also revealed the existence of iron oxides and clay minerals with the distribution of Si, Al and Na (Figure 4.79, 4.80). To sum up, the SEM analyses have further verified the existence of clay minerals and iron oxides in the composition of Nemrut Sandstones.

The color change on the exterior surfaces of the deteriorated sandstones could be due to the increased concentration of iron oxides in comparison to the interior of the stone as revealed by SEM-EDS analyses (Figures 4.74-4.82).

Hydric, hygric and thermal dilatation measurements of this study showed that the Nemrut sandstones had considerable dilatation during of wetting-drying cycles and temperature changes measured between 10 and 45°C. Thus the importance of wetting drying cycles and thermal changes on the deterioration of Nemrut sandstones were supported by those findings. On the other hand, the hygric dilatation was not found to be important in comparison to the hydric and thermal dilatation. Those points were important for the conservation strategy of Nemrut Sandstones.

Average thermal changes at the site during the year were studied for the last four years (Türer et al., 2010). It was seen that temperature generally did not drop below -10°C and the minimum temperature recorded was -15°C and the expected freezing-thawing cycles were around 70 in winter time. In summers average temperature was

around 18-25°C. Those freezing temperature could freeze the water in larger pores of the stone, however, temperatures lower than -20°C were necessary for water to freeze in fine capillaries of sandstone (Yurdakul, 1973). Rapid drying condition with strong winds was another factor to prevent complete saturation that decrease freezing - thawing damage. Therefore, importance of freezing – thawing in deterioration of Nemrut sandstones may be concluded to be less important in comparison to clay swelling by wetting – drying cycles.

### **5.3 The Conservation Treatments Targeted to the Control of Deterioration**

The main decay mechanisms of sandstones of Nemrut are related to the cyclic atmospheric conditions such as wetting-drying, heating-cooling and freezing thawing.

The clay minerals of sandstones of Nemrut namely, chlorite and halloysite, have non-swelling characteristics, though when they get wet they experience a swelling. This was followed by the dilatation measurements of the sandstones during wetting.

The water penetration can not be eliminated by the use of water repellent since they cause different problems in the course of time (Wendler and Snethlage, 1988; Wendler, 1995, Charola , 2001; Mertz et al., 2000).

The use of surfactants, designed for the swelling inhibition of clays were thought to be used before any consolidation treatment to avoid or slow down the further deterioration of the sandstones caused by the swelling of clays. Generally surfactants are used for the stones that have high dilatation characteristics (more then 4µm/mm) when that swelling was due to the clays in the structure of the stone. Hydric dilatation amount of Nemrut sandstones could be considered to be low; however, clays in the structure lead to a swelling and contraction during thousand years of wetting-drying cycles could not be ignored. In their study Mertz et al. (2002) found the total

dilatation of “grés a meules” (the sandstones used in Strasbourg Cathedral) as 0.14 to 0.18  $\mu\text{m}/\text{mm}$ . This amount was considered to be low for using the preventive surfactant treatment before consolidation treatments (Mertz et al., 2000). During their discussion for not to use water repellent for the sandstones of Strasbourg Cathedral, the authors have pointed out that the hygric dilatation of the parts treated with water repellent and the non treated parts were incompatible with each other (Mertz et al., 2000). That characteristics of the water repellent treatments was reported by other authors as well and considered to be a serious shortcoming of water-repellent treatments (Wendler and Snethlage, 1988; Wendler, 1995, Charola , 2001).

The surfactants are expected to reduce the swelling without affecting the overall water transport in the stone. Another advantage of using surfactants is that they could be targeted to clays without changing the pore structure of the stone itself contrary to many stone consolidation treatments (Von Plehwe-Leisen et al., 1996, Moropoulou et al., 1997, Storemyr et al., 2001). On the other hand, the clays contribute to the finest pores in the stone structure that are most harmful sites for decay when in contact with water. During the control of the clay swelling by surfactants water penetration to clay structure could be prevented that is filling of finest pores with water could be prevented.

In this study, the efficiency of surfactants on decrease of clay swelling was examined through hygric dilatation measurements of surfactant treated sandstones. Dilatation properties three surfactants, ethylenediaminedihydrochloride (DAA), hexadecilmethylammonium (HDTMA) and tetraethyleneammoniumchloride (Antihydro), were examined.

Hygric dilatation measurements of surfactant treated sandstones showed some decrease in swelling. For HDTMA treated sample that decrease was from 0.324 to 0.246 $\mu\text{m}/\text{mm}$  (Figure 4.42); for Antihydro from 0.32 to 0.257  $\mu\text{m}/\text{mm}$  (Figure 4.43)

and for DAA from 0.32 to 0.197  $\mu\text{m}/\text{mm}$  (Figure 4.43). Among those, DAA seemed to be the most successful surfactant for the inhibition of clay swelling (Wangler et al., 2008; Jimenez-Gonzalez et al., 2008; Wendler et al., 1997).

The use of surfactant e.g., DAA was considered to be an advantage for the control of dilatation due to clay swelling. The treatments with surfactants need to be done in a careful way in terms of its concentration and the amount of clay minerals in the stone. The importance of the use of surfactant in the proper amount and some danger of using excess amount of surfactant was explained in some other studies (Bildiren et al., 2009).

In this study the use of some nanosized consolidants which have silica in their structure were examined as consolidant to be used in the deteriorated sandstones especially the ones with granular disintegration, the consolidants used were SytonX30, FuncosilKSE500STE, KSE100 and KSE300.

The advantages of the use of silica and silicatic consolidants with nanosized particles for silicatic stones like sandstones were discussed in Chapter 4. In this study, the use of silica and silicatic consolidants with nanosized particles was thought to be an advantage due to their potential to form compatible network in the siliceous structure and improve the mechanical properties of the deteriorated Nemrut sandstones. Their compatibility with the siliceous network and improvement of mechanical properties were reported by different scholars (Von Plehwe-Leisen et al., 1996, Moropoulou et al., 1997, Storemyr et al., 2001, Milliani et al., 2007; Koblischek, 1995 ). On the other hand those siliceous nanosized particles were found not able to bridge the longer distances larger than 50-100 $\mu\text{m}$  (Storemyr et al., 2001). It may be an advantage for the consolidations studies since a network with an acceptable porosity is required in the treated stone. Another advantage of such a consolidant can be its success to penetrate deeply in the stone when they are used in very dilute solutions.

In this study the consolidation treatments were done using different types of silica and silicatic solutions in situ and in the laboratory. Diluted solution of Funcosil KSE500STE (10% by weight) in alcohol; diluted solution of SytonX30 (5% by weight) in water were used either by application on the surface as drop by drop in-situ or by soaking the stones in the solution in the lab. The FuncosilKSE100 and FuncosilKSE300 were used as they were, without any dilution. For both cases, the gel formations on the surfaces of the sandstones were eliminated by wiping out the excess amount of the consolidant solution on the sandstone surfaces.

The efficiency of the treatments were examined in terms of the changes in dilatation (by hydric dilatation measurements) and the improvement in physicommechanical and physical properties by UPV measurements together with QIRT analyses also the color changes by the treatments were measured by spectrophotometer.

The hydric dilatation of the sandstones treated with SytonX30 decreased from 0.33 $\mu\text{m}/\text{mm}$  to 0.28 $\mu\text{m}/\text{mm}$  for fine grained sandstones and 0.41 $\mu\text{m}/\text{mm}$  to 0.37 $\mu\text{m}/\text{mm}$  for medium grained sandstones (Figure 4.44). The hydric dilatation of sandstones treated with FuncosilKSE500STE decreased from 0.32  $\mu\text{m}/\text{mm}$  to 0.27  $\mu\text{m}/\text{mm}$  for medium grained sandstones and 0.32  $\mu\text{m}/\text{mm}$  to 0.25  $\mu\text{m}/\text{mm}$  for fine grained sandstones (Figure 4.46). Thus a decrease in hydric dilatation was observed for both Funcosil KSE500STE and SytonX30 treated sandstones.

The UPV values of the treated sandstones showed no increase for both Funcosil KSE500STE and Syton X30 for medium grained sandstones, however, an increase was observed for the fine grained sandstone (Figure 4.16, Table 4.5). Both KSE300 and KSE100 treatments have increased the UPV values of the stones. That was more evident for FuncosilKSE300 (Figure 4.17, Table 4.6).

Funcosil KSE500STE and Syton X30 were the consolidants that were also applied in-situ, the in-situ evaluation of consolidation efficiency by UPV, showed very slight

increase in the measurements (Figure 4.18). QIRT analyses showed a homogeneous thermal behavior of the stone surface and improved thermal inertia characteristics after the application of consolidants (Figure 4.21).

The color changes caused by the application of the consolidants were evaluated by colorimetric measurements of the surface. Color values were measured before and after consolidation treatments. Only a slight color change ( $\Delta E \leq 5$ ), and no darkening or gloss was required for a good consolidant (Sasse and Snethlage, 1997). Syton X30 (Figure 4.28, 4.29) and KSE 100 (Figure 30) were found to be the most successful treatments resulting in minimum color change having values  $\Delta E=4.98$  and  $\Delta E=3.51$  respectively (Figure 4.29, 4.90).

The consolidation treatments used in the study had promising results e.g. they improved the physicochemical properties. On the other hand, the long term behaviour of the treatments should be investigated by non-destructive analyses at the site as well as microstructural analyses in the laboratory on the equivalent samples at least for the next two years using the experimental methods described in this study and comparisons should be made with data presented here.

## CHAPTER 6

### CONCLUSIONS

In this study it was aimed to develop conservation methods for the sandstone statues and stele of Nemrut Mount Monument by the control of their deterioration mechanisms to help their survival in open air condition. The main conservation approach of this study was holistic as well as aiming at minimum intervention targeted to the problem areas.

As described before (see Chapter 1 Introduction p.8) both the quarry samples and sandstones used in the site belong to "Lice Formation" and they show similar weathering forms, e.g. separation by layering was widespread both in the quarry and at the site.

The sandstones of Nemrut Mount Monument consist of considerable range of rock fragments and minerals such as limestones, igneous rock fragments such as granite, quartzite and minerals as feldspars, quartz, biotite and clay minerals. Chlorite and opaque minerals were observed in the thin sections. Those fragments of rocks and minerals were in a fine grained carbonatic-clayey matrix.

Sandstones of Nemrut Mount Monument were classified as fine and medium grained sandstones. Medium grained sandstones had average grain size as  $333\mu\text{m}$  with a range of  $1300$  to  $60\mu\text{m}$ . Fine grained sandstones had average grain size as  $176\mu\text{m}$  in the range of  $40$ - $450\mu\text{m}$ . Both fine and medium grained sandstones were poorly sorted sandstones.

They were found to have high bulk density and low effective porosity values with good physicommechanical properties. Bulk density of the quarry sandstones were found to be between  $2.48\pm 1.3\text{ g/m}^3$  -  $2.66\pm 1.3\text{ g/m}^3$ , with an average value of  $2.58\pm 1.3\text{ g/m}^3$ . Their

effective porosity were found to be between  $0.4\pm 0.4\%$ - $6.1 \pm 0.4\%$  with an average value of  $3.6\pm 0.4\%$ .

The pore size distribution characteristics of Nemrut Sandstones were studied by Mercury Porosimetry. The medium grained sandstones were found to have lower effective porosity ( $\sim 0.8\%$ - $1.5\%$ ) than the fine grained ones ( $\sim 5.2\%$ ). In the medium grained sandstones the effective porosity was formed mainly by the pores having diameters of  $100\mu\text{m}$ . In the fine grained sandstones majority of the pores had diameters in the range of  $0.5 \mu\text{m}$ .

Hydric dilatation of medium and fine grained sandstones perpendicular to the bedding plane was about  $0.32\mu\text{m}$  per millimeter. The thermal dilatation of medium and fine grained sandstones perpendicular to bedding plane was around  $0.35\mu\text{m}$  per millimeter between  $0 - 45^\circ\text{C}$ . The dilatation perpendicular to bedding at  $95\%$  RH was  $0.01\mu\text{m}$  per millimeter for fine grained sandstones and  $0.06\mu\text{m}$  per millimeter for medium grained sandstones. When compared with hydric dilatation of the sandstones of Strasbourg Cathedrale ( $0.14$ - $0.18\mu\text{m}/\text{mm}$ ) (Mertz et al., 2004) the hydric dilatation of Nemrut Sandstones ( $0.32\mu\text{m}/\text{mm}$ ) were considered to be rather high. Hydric dilatation of Nemrut Sandstones were found to be negligible when compared to their hydric and thermal dilatation.

Clay mineral content of Nemrut Sandstones were estimated to be around  $4\%$  as determined by gravimetric analyses of clay minerals separated by extracts. Clay minerals content was also observed by CEC determinations of sandstone powders and found to be around  $4.7\%$  by weight.

Sandstones in the site of Nemrut Mount Monument possess the weathering forms mainly as separation by layering especially along the bedding planes, back weathering due to loss of scales, cracking, granular disintegration, rounding/notching and

discoloration/biological deposition. The most important weathering forms of Nemrut Sandstones are material loss due to i) loss of scales and ii) granular disintegration.

The sandstones with granular disintegration had UPV values are generally below 1000 m/s indicating lower physicochemical properties. The detaching scales themselves had  $UPV_{INDIRECT}$  values between 1000-2500 m/s indicating sufficient physicochemical properties.

QIRT analyses for deteriorated areas with granular disintegration and detached scales showing low  $UPV_{INDIRECT}$  values, have indicated that their thermal inertia was low meaning their deteriorated state.

The average porosity of sandstones considerably increased in the deteriorated areas showing granular disintegration. In some areas showing material loss and detachment of scales, the change in average porosity of the scales were less. That has signified the relative soundness of the scales in comparison to the granular disintegration surfaces.

Clay minerals caused the deterioration of sandstones through their swelling nature, and possibly through their effect on the mobility and phase changes of iron oxides during wetting and drying cycles.

Hydric, hygric and thermal dilatation measurements of this study showed that the Nemrut sandstones had considerable dilatation during wetting-drying cycles and temperature changes measured between 10-45°C. Thus, the importance of wetting drying cycles and thermal changes on the deterioration of Nemrut sandstones were shown by those findings. On the other hand, the hygric dilatation was not found to be important in comparison to the hydric and thermal dilatation. The importance of freezing – thawing in deterioration of Nemrut sandstones were concluded to be less important in comparison to clay swelling by wetting – drying cycles. Those points were important for the conservation strategy of Nemrut Sandstones.

During the control of the clay swelling by surfactants water penetration to clay structure could be prevented.

In this study surfactants were decided to be used targeted to the clay minerals of the sandstones. Hydric dilatation measurements of surfactant treated sandstones showed some decrease in swelling. DAA seemed to be most successful surfactant for the inhibition of clay swelling, which was in accordance with the previous studies (Wangler et al., 2008; Jimenez-Gonzalez et al., 2008; Wendler et al., 1997). In this study hydric dilatation was decreased by 40% with the use of DAA.

A decrease in hydric dilatation was observed for both Funcosil KSE500STE and SytonX30 treated sandstones. The UPV values of the treated sandstones showed no increase for both Funcosil KSE500STE and Syton X30 for medium grained sandstones, however, an increase was observed for the fine grained sandstone. Both KSE300 and KSE100 treatments have increased the UPV values of the stones. That was more evident for FuncosilKSE300.

Syton X30 and KSE 100 were found to be the most successful treatments resulting in minimum color change having values  $\Delta E=4.98$  and  $\Delta E=3.51$  respectively.

The success of the conservation interventions should be followed for color change ( $\Delta E$  values) indicating the difference after the treatments and UPV measurements. The sandstones should have UPV values not less than 1500 m/s if they need to be moved or transported.

#### *Further Studies*

Further studies may include the detailed studies on the control of clay minerals swelling in treated sandstones.

Presence of iron oxide centers in the stone and their movement mostly as colloidal accumulations were detected in sandstones, they were thought to be related with the

c browning during weathering. The contribution of iron oxides in the sandstone decay and their relationships with the presence of clay minerals need to be further studied.

In this study a few surfactants were examined and the promising results were obtained. On the other hand, different types of the surfactants with new properties are being developed in the market. Their properties and the expectations from those to be used in the field of historic stone conservation should be well defined and their long term behaviour with the stone needs to be well studied.

The performance of consolidation treatments with silica and silicate dispersions should be investigated for longer periods in more detail both in laboratory and at site for longer periods.

Most of the sandstone stele and pedestals on the East and North Terraces are heavily weathered, and hence, are not suitable for transportation. For this reason they should first be consolidated. However the long term performance of consolidation applications should be confirmed. Before generalizing the use of nano-dispersive silicate solutions, their performance should be examined on site and in the laboratory for at least two years. The need for transportation for each piece should be considered afterwards.

Some additional studies should be done to stop the harmful effects of wrong conservation interventions that were done in the past by the previous teams. Among those wrong interventions repairs with cement mortars and epoxy resins could be observed at the site, moreover, some consolidation interventions with polyvinyl acetate (PVA) were also reported by Sanders (1996). In this study presence of old PVA detected in some breakout surfaces of lion horoscope in the temporary laboratory at the site. By using UV lamp, the old PVA applications got fluorescent and became visible. Such a survey needs to be done widely and the methods to clean PVA should also be well studied before their cleaning attempt.

## REFERENCES

- Akdeniz, A., 2003, Investigation of the Sismicity, Crustal and Upper Mantle Structure, and Sismic Risk of the South Eastern Turkey; Güneydoğu Anadolu Bölgesi'nin Deprem Riski, Kabuk ve Üst Manto Yapısı ve Deprem Riskinin İncelenmesi, unpublished, MSc. Thesis, Ankara University, pp.109
- Alberts, H.C., and Hazen, H.D., 2010, Maintaining Authenticity and Integrity at Cultural World Heritage Sites, *The Geographical Review* 100 (1), 56-73.
- Anderson, R.L, Ratcliffe, I., Williams, P,A., Cliffe, S., Coveney, P.V., 2010, Clay swelling – A challenge in the oilfield, *Earth-Science Reviews* 98 (2010), 201-216
- ASTM E308-90, 1993- Standard test method for computing the colors of objects by using the CIE system. Annual Book of ASTM Standards, Vol. 14.02.,1993
- ASTM D2244-89, 1993, standard Test Method for calculation color differences from instrumentally measured color coordinates. Annual Book of ASTM Standards, Vol. 6.01.,1993
- Barf, F.S., 1860, British Patent, 2608, Oct. 26, 1860.
- Baer, N.S., and Snethlage, R., Introduction, In: *Saving our Architectural Heritage: The Conservation of Historic Stone Structures*. N.S. Baer and R. Snethlage, Eds., John Wiley & Sons Ltd., Chichester, pp. 1-6.
- Barnes, A., Sapsford, D.,J., Dey, M., Williams, K.P., 2009, Heterogeneous Fe (II) oxidation and zetapotential, *Journal of Geochemical Exploration*, 100, (2009), 192-198.

Belcher, A. M., Hansma, P.K., Stucky, Morse, D.E., 1998, First Steps in Harnessing the potential of Biomineralization as a Route to New High Performance Composite Materials, *Acta Mater.*, 46(3), 733-736.

Benavente, D., Garcia del Cura, M.A., Garcia-Guinead, J., Sanchez-Morald, S., Ordonez, S., 2004, Role of pore structure in salt crystallisation in unsaturated porous stone *Journal of Crystal Growth* 260 (2004) 532–544

Bildiren M., Günal Türkmenoğlu, A., Tinçer, T., 2009, Preparation of Clay-Polymer Nanocomposite for the Retardation for the Waste Water Infiltration in Landfill Sites, *Proceedings of 14th National Clay Symposium*, 1-3 October 2009, 749-465.

Busigny, V., Dauphas, N., 2007, Tracing Paleofluid circulations using iron isotopes: A study of hematite and goethite concretions from the Navajo Sandstone (Utah, USA), *Earth and Planetary Science Letters* 254 (2007) 272-287.

Calcaterra D., Cappelletti P, Langella A., Colella A. , Gennaro M.de, 2004, The ornamental stones of *Caserta* province: the Campanian Ignimbrite in the medieval architecture of *Casertavecchia*, *Journal of Cultural Heritage* 5 (2004), 137–148.

Caner, E.N., 1978, Factors Affecting the Deterioration of Limestones from Historic Monuments in Anatolis, unpublished Ph.D. Thesis, in the Faculty of Arts of the University of London, Department of Archaeological Conservation and Materials Science, 131p, Advisor: Dr. N.J. Seeley.

Caner-Saltık E.N., Özgenoğlu, A., Topal, T., 2001, Stages of damage to Marble by Salt Crystallization, *Proceedings of the 11th Workshop, Eurocare euomarble*, EU496, 53-61.

Caner-Saltık, E.N., 2005, TÜBİTAK Research Project İçtag-I684/PIA Progress Report “Development of New Methods Using Biomineralization And Nanoparticle

Technologies in The Preservation and Conservation of Historical Marbles” Proje Yürütücüsü: Prof. Dr. Emine N. Caner-Saltık, p. 26.

Caner-Saltık, E.N., Oriol, G., Mertz, J., Demirci Ş., Hugon, P., Akoğlu, K.G. and Caner E., 2006, Characteristics of Deteriorated Surface Layers of Some Marbles in Comparison to Their Less Deteriorated Interiors, 8th Association for the Study of Marble and Other Stones used In Antiquity (ASMOSIA) Symposium Proceedings, 12-18 June, Aix-en-Provence, France

Caner-Saltık, E.N., Oriol, G., Mertz, J., Demirci Ş., Hugon, P., Akoğlu, K.G. and Caner E., 2007, Improvements in the Decayed Microstructure of Marble by Treatments with Nano Dispersive Solutions, 7<sup>th</sup> International Symposium on the Conservation of Monuments in the Mediterranean Basin, June 6-9 2007, Orleans-France (in press)

Charola, A. E., 2001, “Water Repellents and Other “Protective” Treatments: A Critical Review”, Eds: K.Littmann, A.E. Charola, Hydrophobe 3, 3<sup>rd</sup> International Conference on Surface Technology with Water Repellent Agents, Aedificatio Publishers, pp 3-20.

Church, A. H., 1862, British Patent, 220, Jan. 28, 1862.

Costa, D., and Delgado Rodrigues, J., 1996, Assessment of colour changes due to treatment products in heterochromatic stones, Degradation and Conservation of Granitic Rocks in Monuments, Protection and Conservation of European cultural Heritage, Research Report no 5, 325-330.

Dash, J.G., Rempel, A. W., Wettlaufer, J.S., 2006, The physics of premelted ice and its geophysical consequences, Reviews of Modern Physics, Volume 78, July–September 2006, 10.1103/RevModPhys.78.695

Drever, J.I., 1992, Durability of Stone: Mineralogical and Textural Perspectives, Environmental Sciences Research Report 15: Durability and Change, The Science,

Responsibility, and Cost of Sustaining Cultural Heritage, ed. W.E. Krumbein, P. Brimblecombe, D.E. Cosgrove, S. Staniforth pp.

Dromgoole, E.L., Walter, L.M., 1990, Iron and manganese incorporation into calcite: Effects of growth kinetics, temperature and solution chemistry, *Chemical Geology*, 81 (1990), 311-336.

Fitzner, B., Heinrichs, K., Kownatzki, R., 1997, Weathering Forms at Natural Stone Monuments - Classification, Mapping and Evaluation. *International Journal for Restoration of Buildings and monuments*, 3(2), 105-123.

Frukawa, Y., O'Reilly, S.E., 2007, Rapid Precipitation of Amorphous silica in experimental systems with nontronite (Nau-1) and *Shewanella oneidensis* MR-1, *Geochimica et Cosmochimica Acta* 71 (2007), 363-377.

Garcia-Talegon, J., Vicente, M.A., Vicente-Tavera, S., and Moline-Ballesteros, E., 1998, Assessment of Chromatic Changes Due to Artificial Ageing and/or Conservation Treatments of Sandstones, *Color research and application*, CCC 0361-2317/98/010046-06, 46-51.

Gautier, C., Lopez, P.J., Livage, J., Coradin, T., 2007, Influence of poly-L-lysine on the biomimetic growth of silica tubes in confined media, *Journal of Colloid and Interface Science*, 309 (2007), 44-48.

Grinzato E., Marinetti S., Bison P.G., Concas M., Fais S., 2004, Comparison of ultrasonic velocity and IR thermography for the characterisation of stones *Infrared Physics & Technology* 46 (2004) 63–68.

Grissom, A.C., Charola, A. E., Boulton, A. and Mecklenburg, M.F., 1999, Evaluation over time of an ethyl silicate consolidant applied to ancient lime plaster, *Studies in Conservation*, 44 (1999), 113-120.

- Hallet, B., 2006, Why Do Freezing Rocks Break, *Science* vol.314, 1092-1093.
- Heinrichs K., & Fitzner, B., 2007, Stone Monuments of the Nemrud Dag sanctuary/ Turkey - Petrographical investigation and diagnosis of weathering damage, in *Z. dt. Ges Geowiss*, 158/3 pp. 519-548, 32 figs. 11 tables, Stuttgart, September, 2007.
- Jain, A., Bhadauria, S., Kumar, S., Chauhan, R. S., 2009, Biodeterioration of sandstone under the influence of different humidity levels in laboratory conditions, *Building and Environment* 44 (2009) 1276-1284.
- Jimenez-Gonzalez, I., Rodriguez-Navarro, C., and Scherer, G.W., 2008, Role of Clay minerals in the physicochemical deterioration of sandstone, *Journal of Geophysical Research*, Vol., 113, F2021, doi: 10.1029/2007JF000845.
- Jimenez-Gonzalez, I. and Scherer, G.W., 2004, Effect of swelling inhibitors on the swelling and stress relaxation of clay bearing stones., *Environmental Geology* (2004), 46, 364-377, doi: 10.1007/s00254-004-1038-8.
- Kröger, N, Lorenz, S., Brunner, E, Sumper, M., 2002, Self-Assembly of Highly Phosphorylated Silaffins and Their Function in Biosilica Morphogenesis, *Science*, 298, 584-586.
- Lopez, P.J., Desclés, J., Allen, E.A., and Bowler, C., 2005, Prospects in Diatom Research, *Current Opinion in Biotechnology*, 2005, 16, 180-186.
- Kahraman, S., 2002, Estimating the direct P-wave Velocity Value of Intact Rock from Indirect Laboratory Measurements, *International Journal of Rock Mechanics & Mining Sciences*, (39), 101-104.
- Kandemir, A., 2010, Soundness Assessment of Historic Structural Timber by the Use of Non-Destructive Methods, unpublished PhD. Thesis, METU, pp.228.

Koblischek, P.J., 1995, Protection of Surfaces of Natural Stone and Concrete Through Polymers, In: Proceedings of the First International Symposium on Surface Treatment of Building Materials with Water Repellent Agents, 9-10th November, 1995, Surface Treatment of Building Materials with Water Repellent Agents, Edited by: Wittman, F.H., Siemes, Ton A.J.M., Werhoef, Leo, G.W. 1-12.

Koestler, R.J., Warscheid, T., and Nieto, F., 1997, Biodeterioration: Risk Factors and Their Management, Report of the Dahlem Workshop on Saving Our architectural Heritage: The Conservation of Historic Stone Structures, Eds: Baer, N.S. and Snethlage, R., 25-36.

McAlister, J. J., Bernard, J. S., Curran, J.A., 2003, The use of sequential extraction to examine iron and trace metal mobilization and the case-hardening of building sandstone: a preliminary investigation, *Microchemical Journal*, 74, (2003), 5-18.

Mertz, J.D., 1991, Structures de Porosité et propriétés de transport dans les gres, Ph.D. Theseis of l'Université Louis Pasteur, Strasbourg, 149 p.

Mertz, J.D., and Jeanette, D., 2004, Effect of Water Repellent Treatments on the Hydric Dilatation of Sandstone during water capillary absorption and drying stages, Proceedings of the 10th International Congress on Deterioration and Conservation of Stone, Stockholm, June 27- July 2, 2004, Stockholm, 355-362.

Miliani, C., Velo-Simpson, M. L., Scherer, G. W., 2007, Particle-Modified Consolidants: A study on the effect of particles on sol-gel properties and consolidation effectiveness, *Journal of Cultural Heritage* 8 (2007) 1-7.

Mohan, K.K., Ravimadhav, N.V., Reed, M.G., and Fogler, H.S., 1993, Water Resistivity of sandstones containing swelling and non-swelling clays, *Colloids and Surfaces a: Physicochemical and Engineering Aspects*, 73, (1993), 237-254.

Mol, L., Viles, H. A., 2010, Geoelectric investigations into sandstone moisture regimes: implications for rock weathering and the deterioration of San Rock Art in Golden Gate Reserve, South Africa, *Geomorphology* 118 (2010), 280-287, doi:10.1016/j.geomorph.2010.01.008

Monnier, J., Legrand, L., Berlot-Gurlet, L., Foy, E., Reguer, S., Rocca, E., Dillman, P., Neff, D., Mirambet, F., Perrin, S., Guillot, I., 2008, Study of archaeological artefacts to refine the model of iron long-term indoor atmospheric corrosion, *Journal of Nuclear Materials*, 379 (2008) 105-111.

Moore, M.D., and Reynolds, C.R., 1997, X Ray Diffraction and the identification and Analysis of Clay minerals.

Moropoulou, A., Tsiourva, Th., Michailidis, P., Biscontin, G., bakolas, A., Zendri, E., 1997, Evaluation of Consolidation Treatments of Porous Stones- Application on the Medieval City of Rhodes, *Proceedings of 4th international Symposium on The Conservation of Monuments in the Mediterranean*, Rhodes, 6-11 May 1997, eds: A. Moropoulou, F. Zezza, E. Kollias, I. Papachristodoulou, 239-256.

Murton, J.B., Peterson, R., Ozouf, J., 2006, Bedrock Fracture by Ice Segregation in Cold Regions, *Science*, vol. 314, 1127-1129.

Nara Document on Authenticity, 1994, The Nara Document on Authenticity was drafted by the 45 participants at the Nara Conference on Authenticity in Relation to the World Heritage Convention, Nara, Japan, from 1-6 November 1994, at the invitation of the Agency for Cultural Affairs (Government of Japan) and the Nara Prefecture in cooperation with UNESCO, ICCROM and ICOMOS. Eds. Mr. Raymond Lemaire and Mr. Herb Stovel.

O'Connor, J., 2000, The role of consolidants in the conservation of sydney sandstone buildings, 9th International Congress on Deterioration and Conservation of Stone, Venice, June 19-24, 2000, proceedings Vol.2. pp. 413-417.

Osmay, S., Ataöv, A., 2010, Nemrut Kommagene Kültürel Miras Alan Yönetim Planlama Projesi Toplumsal Değişim Süreç Değerlendirmesi: 1. Aşama, in proceedings of Güneşe Yürümek II. Ulusal Medeniyetler Kavşağı Adıyaman Sempozyumu, 10-12 Ekim 2008, Adıyaman, Turkey, 19-28.

Paradise, T. R., 2000, Sandstone Architectural Deterioration in Petra, Jordan, in Proceedings of 9<sup>th</sup> International Congress on Deterioration and Conservation of Stone, Venice 19-24 June 2000; 145-154.

Perinçek, D. ve Kozlu, H., 1983. Stratigraphy and structural relations of the units in the Afşin-Elbistan-Doğanşar region (Eastern Taurus) In Tekeli, O. And Göncüoğlu, M.C. (eds), Geology of the Taurus Belt. Ankara-Turkey, 181- 197.

Potgieter, J.H., Strydom, C.A., 1999, Determination of the clay index of limestone with methylene blue adsorption using a UV-VIS spectrophotometric method, Cement and Concrete Research 29 (1999), 1815–1817.

Ramasamy, V. , Anandalakshmi, K., 2008, The determination of kaolinite clay content in limestones of western Tamil Nadu by methylene blue adsorption using UV–vis spectroscopy, Spectrochimica Acta Part A 70 (2008), 25–29.

RILEM, 1980, Tentative Recommendations, Commission –25-PEM, Recommended Tests to Measure the Deterioration of Stone and to Assess the Effectiveness of Treatment Methods, *Materiaux and Construction*, Vol. 13, No. 73, pp. 173-253.

Rossi-Maneressi, R., and Tucci, A., 1991, Pore structure and the disruptive or cementing effect of salt crystallization. *Studies in Conservation*, 36, pp.344-347.

Sandoz, J.L., 1996, Ultrasonic Solid Wood Evaluation in Industrial Applications, NDTnet, December 1996, vol.1, no.12.

Sasse, H. R., and Snetlage, R., 1997, Methods for the Evaluation of Stone Conservation Treatments, In: Saving our Architectural Heritage: The Conservation of Historic Stone Structures. N.S. Baer and R. Snethlage, Eds., John Wiley & Sons Ltd., Chichester, pp. 223-243.

Schaffer, R.J., 1932, The weathering of Natural building stones, Department of Scientific and industrial research, Building Research, Special Report No.18; reprinted 1949 p.149.

Schoonheydt, R.A. and Heughebaert, L., 1992, Clay Adsorbed Dyes: Methylene Blue on Laponite, Clay Minerals (1992) 27, 91-100.

Scherer, G.W., 1997, Effect of drying on properties of silica gel, journal of Non-Crystalline Solids, 215 (1997), 155-168.

Scherer, G.W, 1999, Structure and Properties of Gels, Cement and Concrete Research 29 (1999), 1149-1157.

Scherer, G. W., 2000, Stress from Crystallization of salt in pores, in Proceedings of 9<sup>th</sup> International Congress on Deterioration and Conservation of Stone, Venice 19-24 June 2000; 187-194.

Scherer, G.W., and Jimenez-Gonzalez, I., 2005, Characterization of swelling in clay bearing stone, in: Stone decay in the Architectural Environment, ed.: Alice V. Turkington, The geological Society of America, Special Paper, 390; 51-61.

Sanchez-Martin, M.J., Dorado, M.C., del Hoyo, C., Rodrigues-Cruz, M.S., 2008; Influence of Clay mineral structure and surfactant nature on the adsorption capacity of surfactants by clay, *Journal of Hazardous Materials* 150 (2008) 115-123.

Sanders, D. H., 1996, "Nemrud Dağı The Hierothesion of Antiochos I of Commagene", Vol.I-II, Indiana Eisenbrauns, Winona Lake

Staniford, S. (Rapporteur); Ballard, M.W., Caner-Saltık, E.N.; Drewello, R.; Eckmann, I.L., Krumbein, W.E.; Padfield, T.; Reddy, M.M.; Schuller M.; Simmon, S., Slavoshevskaya, L., Tennent, N.H.; Wolters, W. (Moderator), 1992, Group Report: What Are Appropriate Strategies to Evaluate Change and Sustain Cultural Heritage, in Dahlem Workshop Reports, *Environmental Sciences Research Report 15: Durability and Change, The Science, Responsibility, and Cost of Sustaining Cultural Heritage*, ed. W.E. Krumbein, P. Brimblecombe, D.E. Cosgrove, S. Staniforth. 217-224.

Schwertmann, U; and Taylor, R.M., 1989, Chapter 8, Iron Oxides, Minerals in Soil Environment, *Soil Science Society of America, SSSA Book Series*no:1 p.404-405.

Simon, S., 2001, The four virtues of the Porta della Carta, Ducal Palace, Venice-Ultrasonic Velocity investigation of Gothic Marble Sculptures, *Proceedings of the 11th Workshop, Eurocare euromarble, EU496*, 5-16

Simon, S., 2011, Personal Communication during Final Workshop of MonumentsLab-206710 Workshop, 17-19 May 2011, Ankara, Turkey.

Smith, B.J., Turkington, A.V., and Curran, J.M., 2005, Urban stone decay: The great weathering experiment? In *Stone Decay in the Architectural Environment*, The Geological society of America, Special Paper 390, ed. Alice V. Turkington, 1-10.

Soe, A.K.K., Osada, M., Win, T.T.N., 2010, Drying induced deformation behaviour of Shirahama sandstone in no loading regime, *Engineering Geology* 114, (2010), 423-432.

Storemyr, P., Wendler, E., Zendher, K., 2001, Weathering and Conservation of Soapstone and Greenschist Used at Nidaros Cathedral (Norway), In: Report Raphael II Nidaros Cathedral Restoration Tromdheim Norway 2000. EC Raphael Programme – European Heritage Laboratory, Report No: 2/2001, The restoration Workshop of Nidaros Cathedral, Trondheim , Norway.

Sun, Q., Vrieling , E.G., van Santen, A.R., Sommerdijk, N.A.J.M., 2004, Bioinspired Synthesis of mesoporous silicas, *Current Opinion in Solid State and Materials Science*, 8 (2004), 111-120.

Sun, Y., Ma, M., Zhang, Y., Ning; G., 2004, Synthesis of nanometer-size maghemite particles from magnetite, *Colloids and Surfaces A: Physicochem. Eng. Aspects*, 245, (2004), 15-19.

Şahin Güçhan, N., 2011(a), “The Kommagene Nemrut Conservation and Development Program: An Approach to the Conservation Problem of Nemrut Dağ Tumulus”, in: E. Winter (ed.), *Von Kummuh nach Telouch. Archäologische und Historische Untersuchungen in Kommagene. Dolichener und Kommagenische Forschungen IV. Asia Minor Studien 64*, Bonn 2011, 309-339.

Şahin-Güçhan, N., 2011(b), Keynote speaker: “Conservation of relationship between place and context: Mount Nemrut Tumulus”, *BHCICOP-The 4th International Conference on Hazards and Modern Heritage: The Importance of Place*, 13 - 16 June, 2011, Sarajevo, 151-167.

Şahin-Güçhan, N., 2010, Adıyaman’daki Kültür Varlıklarının Nemrut Dağı Odaklı Değerlendirilmesi: Kommagene Nemrut Koruma Geliştirme Programı (KNKGP), in *proceedings of Güneşe Yürümek II. Ulusal Medeniyetler Kavşağı Adıyaman Sempozyumu*, 10-12 Ekim 2008, Adıyaman, Turkey, 29-62.

Tabasso M. L., 1993, Materials for stone conservation *Congres International sur la Conservation de la pierre et autres materiaux*, Paris, Unesco, 29 Juin – 1 er Juillet 1993, 54-58.

Taber, S., 1929, Frost Heaving, *J. Geology*, 37 (5), 428-461.

Tate, W., Murchison, R.I., Bonham-Carter, A., 1861, Report on the Committee on the Decay of the stone of the New palace Westminster. London, 1861,126 pp.

Teutonico, J.M., (Rapporteur), Charola, A.E., De Witte, E., Grassegger, G., Koestler, R.J., Tabasso, M.L., Sasse, H.R., Snethlage, R., 1997, Group Report: How can We Ensure the Responsible, and Effective Use of Treatments (Cleaning, Consolidation, Protection?), In: *Saving our Architectural Heritage: The Conservation of Historic Stone Structures*. N.S. Baer and R. Snethlage, Eds., John Wiley & Sons Ltd., Chichester, 293-313.

Theoulakis, P and Tzamalís A., 2000, Effectiveness of surface treatments for sedimentary limestone in Greece, 9th International Congress on Deterioration and Conservation of Stone, Venice, June 19-24, 2000, proceedings v.2.. 493-501.

Topal T., Ertaş, B.; , 2011, Jeolojik Araştırmalar, in: *Kommagene Nemrut Koruma ve Geliştirme Programı Nemrut Dağı ve Tümülüsü ve Anıtları Malzeme, Yapısal Durum, Jeolojik Araştırmalar ve Koruma Önerileri Geliştirme ve Yönetim Planı Hazırlanmasına İlişkin Protokol; Nemrut Dağı Tümülüsü ve Anıtları Malzeme, Yapısal Durum ve Jeolojik Araştırmalar ve Koruma Önerileri Geliştirme Projesi Malzeme Araştırmaları Sonuç Raporu*; pp.192.

Topal, T., 1996, The Use of Methylene Blue Adsorption Test to Assess the Clay Content of The Cappadocian Tuff, in *Proceedings of “International Congress on Deterioration and Conservation of Stone”*; Volume II, 791-799.

Toracca, G, 1982, Porous Building Materials: Materials Science for Architectural Conservation, ICCROM, pp.145.

Tucker, M. E., 2001, Sedimentary Petrology, An Introduction to the Origin of Sedimentary Rocks, 3<sup>rd</sup> Edition, Blackwell Publishing.

Tunçoku, S.S., Saltık-Caner, E.N., Hugon, P., 2004, Raw Materials Properties of some Medieval Mortars in Kubadabad palaces (Turkey), *Revue D'Archéométrie*, no: 28, 109-116.

Tunçoku, S, 2001, "Characterization of Masonry Mortars Used in Some Anatolian Seljuk Monuments in Konya, Beyşehir and Akşehir", Ph. D. Thesis, METU, 128p. Supervisor: E. N. Caner-Saltık, co-Supervisor: Ö. Bakırer.

Turer, A; Aktaş, D.Y., 2010, Nemrut Anıtları Yapısal Durum Değerlendirme Raporu, in: Kommagene Nemrut Koruma ve Geliştirme Programı Nemrut Dağı ve Tümülüsü ve Anıtları Malzeme, Yapısal Durum, Jeolojik Araştırmalar ve Koruma Önerileri Geliştirme ve Yönetim Planı Hazırlanmasına İlişkin Protokol; Nemrut Dağı Tümülüsü ve Anıtları Malzeme, Yapısal Durum ve Jeolojik Araştırmalar ve Koruma Önerileri Geliştirme Projesi Malzeme Araştırmaları 3. Ara Raporu; pp.135.

Turkington, A.V., Paradise, T.R., 2005, Sandstone Waethering: a century of research and innovation, *Geomorphology* 67 (2005), 229-253.

Viles, H.A. (Rapporteur), Camuffo, D., Fitz, S., Fitzner, B., Lindqvist, O., Livingstone, R.A., Marevelaki, P.-N.V., Sabbioni, C., Warscheid, T., 1996, Group Report: What is the State of Our Knowledge of the Mechanisms of deterioration and How Good are Our Estimates of Rates of Deterioration?, In: *Saving our Architectural Heritage: The Conservation of Historic Stone Structures*. N.S. Baer and R. Snethlage, Eds., John Wiley & Sons Ltd., Chichester, 95-112.

Von Plehwe-Leisen, E., Warscheid, T., Leisen, H., 1996, Studies of Long-Term Behaviour of conservation agents and microbiological contamination on Twenty Years Exposed Treated Sandstone Cubes, in 8<sup>th</sup> International Congress on Deterioration and Conservation of Stone, Berlin 30 Sept. 1996 – 4 Oct 1996, ed. Josef Riederer, Volume 2, 1029-1037

Wangler, T., Scherer, G.W, 2008, Clay swelling mechanism in clay-bearing sandstones, *Environmental Geology*, (2008) 56, 529-534.

Weiner, S., Addadi, L., Wagner, H.D., 2000, Materials Design in biology, *Materials Science & Engineering C*, 11 (2000), 1-8.

Weiss T., Siegesmund S., Kirchner D. and Sippel J., 2004, Insolation weathering and hygric dilatation: two competitive factors in stone degradation, *Environmental Geology*, Volume 46, no: 3-4, Aug. 2004, 402-413

Wendler, E., 1997, New Materials and Approaches for the Conservation of Stone, In: *Saving our Architectural Heritage: The Conservation of Historic Stone Structures*. N.S. Baer and R. Snethlage, Eds., John Wiley & Sons Ltd., Chichester, pp. 181-196.

Wendler, E and Snethlage, R., 1997, Moisture Cycles and Sandstone Degradation, In: *Saving our Architectural Heritage: The Conservation of Historic Stone Structures*. N.S. Baer and R. Snethlage, Eds., John Wiley & Sons Ltd., Chichester, pp. 7-24.

Wright, J.D. and Sommerdijk, N.A.J.M., 2001, *Sol-gel materials: chemistry and applications*. Amsterdam, The Netherlands: Gordon and Breach Science Publishers, 125p.

Xi, Y., Mallavarapu, M., Naidu, R., 2010, Preparation, characterization of surfactants modified clay minerals and nitrate adsorption, *Applied Clay Science*, 48 (2010) 92-96.

Yavuz, H., Altindag, R., Sarac, S., Ugur, I., Sengun, N., 2006, Estimating the index properties of deteriorated carbonate rocks due to freeze-thaw and thermal shock weathering, *International Journal of Rock Mechanics & Mining Sciences*, 43(5), 767-775.

Yurdakul, O., 1973, Freezing\_melting Behaviour of Water in H<sub>2</sub>SiF<sub>6</sub> Treated Vycor Glasses, M.Sc. Thesis, METU, Ankara.

Zendri, E., Biscontin, G., Nardini, I., Riato, S., 2006, Characterization and reactivity of silicatic consolidants, *Construction and Building Materials*, Volume 21, Issue 5, 1098-1106.

## CURRICULUM VITAE

### PERSONAL INFORMATION

Surname, Name : AKOĞLU, KIRAZ GÖZE

Date and Place of Birth : 25 APRIL 1978, Ankara

### EDUCATION:

MSc : **2003**, Archaeometry Program, Institute of Natural and Applied Sciences, METU, Ankara

BS : **1999**, Physics, Faculty of Arts and Science, METU, Ankara

High School : **1994**, Aksaray High School, Aksaray, Turkey.

**LANGUAGES:** English (Advanced)  
French (Fluent)  
Italian (Beginner)